

# Microstructure of styrene methyl methacrylate copolymers grafted onto polybutadiene seeds

**Citation for published version (APA):**

Aerdt, A. M. (1993). *Microstructure of styrene methyl methacrylate copolymers grafted onto polybutadiene seeds*. [Phd Thesis 1 (Research TU/e / Graduation TU/e), Chemical Engineering and Chemistry]. Technische Universiteit Eindhoven. <https://doi.org/10.6100/IR394704>

**DOI:**

[10.6100/IR394704](https://doi.org/10.6100/IR394704)

**Document status and date:**

Published: 01/01/1993

**Document Version:**

Publisher's PDF, also known as Version of Record (includes final page, issue and volume numbers)

**Please check the document version of this publication:**

- A submitted manuscript is the version of the article upon submission and before peer-review. There can be important differences between the submitted version and the official published version of record. People interested in the research are advised to contact the author for the final version of the publication, or visit the DOI to the publisher's website.
- The final author version and the galley proof are versions of the publication after peer review.
- The final published version features the final layout of the paper including the volume, issue and page numbers.

[Link to publication](#)

**General rights**

Copyright and moral rights for the publications made accessible in the public portal are retained by the authors and/or other copyright owners and it is a condition of accessing publications that users recognise and abide by the legal requirements associated with these rights.

- Users may download and print one copy of any publication from the public portal for the purpose of private study or research.
- You may not further distribute the material or use it for any profit-making activity or commercial gain
- You may freely distribute the URL identifying the publication in the public portal.

If the publication is distributed under the terms of Article 25fa of the Dutch Copyright Act, indicated by the "Taverne" license above, please follow below link for the End User Agreement:

[www.tue.nl/taverne](http://www.tue.nl/taverne)

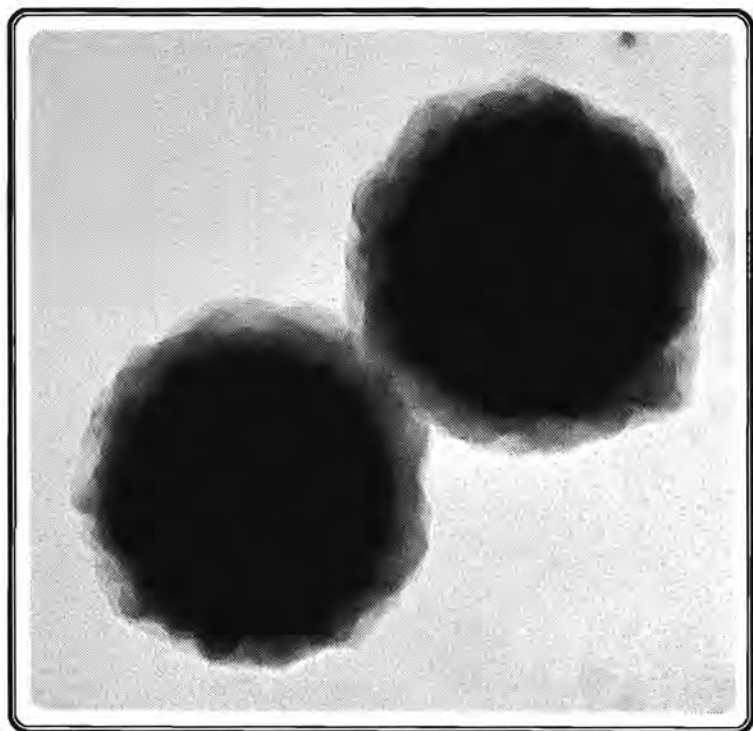
**Take down policy**

If you believe that this document breaches copyright please contact us at:

[openaccess@tue.nl](mailto:openaccess@tue.nl)

providing details and we will investigate your claim.

**MICROSTRUCTURE OF STYRENE  
METHYL METHACRYLATE  
COPOLYMERS GRAFTED ONTO  
POLYBUTADIENE SEEDS**



**ANNEMIEKE AERDTS**

MICROSTRUCTURE OF STYRENE METHYL METHACRYLATE  
COPOLYMERS GRAFTED ONTO POLYBUTADIENE SEEDS

# **MICROSTRUCTURE OF STYRENE METHYL METHACRYLATE COPOLYMERS GRAFTED ONTO POLYBUTADIENE SEEDS**

**PROEFSCHRIFT**

ter verkrijging van de graad van doctor aan de  
Technische Universiteit Eindhoven, op gezag van  
de Rector Magnificus, prof. dr. J.H. van Lint, voor  
een commissie aangewezen door het College  
van Dekanen in het openbaar te verdedigen op  
maandag 3 mei 1993 te 16.00 uur

door

**ANNA MARIA AERDTS**

geboren te Venlo

Dit proefschrift is goedgekeurd door

de promotoren: prof. dr. ir. A.L. German  
prof. drs. J. Bussink  
en de copromotor: dr. A.M. van Herk

*cover*

*Transmission electron micrograph of a MBS  
(methyl methacrylate/butadiene/styrene)  
graft copolymer prepared by emulsifier free  
semi-continuous emulsion polymerization*

The author is indebted to General Electric Plastics, for financially supporting this work.

*Een goede kok,  
is de beste dokter o/p*

*(oud spreekwoord)*

*aan mijn ouders,  
aan Rob*

## Contents

### Chapter 1 Introduction

1.1	Short historic overview	1
1.2	Aim of this investigation	3
1.3	Survey of this thesis	4
	References	6

### Chapter 2 Theoretical Backgrounds

2.1	Emulsion polymerization	9
2.2	Mechanism of graft polymerization	13
	References	18

### Chapter 3 Characterization of Intramolecular Microstructure of Styrene Methyl Methacrylate Copolymers by Means of Proton NMR

3.1	Introduction	19
3.2	Experimental section	22
3.3	Results and discussion; sequence distribution	23
3.4	Results and discussion; coisotacticity parameter	30
3.5	Results and discussion; 2D NOESY NMR	32
3.6	Conclusions	39
	References	40

<b>Chapter 4</b>	<b>Proton and Carbon NMR Spectra of Alternating and Statistical Styrene Methyl Methacrylate Copolymers Revisited</b>	
4.1	Introduction	43
4.2	Experimental section	45
4.3	Results and discussion; Alternating SMMA copolymers	47
4.3.1	Proton NMR	48
4.3.2	Carbon NMR	50
4.4	Results and discussion; Statistical SMMA copolymers	54
4.4.1	Proton NMR	55
4.4.2	Carbon NMR	55
4.5	Conclusions	60
	References	62
<b>Chapter 5</b>	<b>Free Radical Copolymerization: An NMR Investigation of Current Kinetic Models</b>	
5.1	Introduction	63
5.2	Theory	66
5.3	Results and discussion	71
5.4	Conclusions	88
	References	90
<b>Chapter 6</b>	<b>Partial and Saturation Swelling in Latex Particles of Polybutadiene, Styrene Methyl Methacrylate Copolymers and Composite Particles.</b>	
6.1	Introduction	91
6.2	Experimental section	93
6.3	Results and discussion; Partial swelling of latex particles by one monomer	96
6.4	Results and discussion; Saturation swelling of latex particles by two monomers	101
6.5	Conclusions	107
	References	108



## Contents

---

<b>Chapter 7</b>	<b>Emulsifier Free Grafting of Styrene and Methyl Methacrylate onto Polybutadiene and Determination of the Copolymer Microstructure</b>	
7.1	Introduction	109
7.2	Experimental	111
7.2.1	Procedures and analytical techniques used in emulsion homopolymerization of butadiene	111
7.2.2	Processes developed and analytical techniques used in emulsion graft copolymerization of styrene and methyl methacrylate onto polybutadiene seed particles	112
7.3	Results and Discussion	123
7.3.1	Grafting of styrene and methyl methacrylate onto polybutadiene	123
7.3.2	Grafting of styrene and methyl acrylate onto polybutadiene	132
7.4	Conclusions	136
	References	137
<b>Chapter 8</b>	<b>Grafting of Styrene and Methyl Methacrylate onto Polybutadiene in Semi-Continuous Emulsion Processes and Determination of Copolymer Microstructure.</b>	
8.1	Introduction	139
8.2	Experimental procedures and techniques used in emulsion graft copolymerization	141
8.3	Results and discussion	142
8.3.1	Batch emulsion graft copolymerization	142
8.3.2	Semi-continuous emulsion graft copolymerizations under starved conditions	146
8.3.3	Comparison of the morphology of the batch and semi-continuous graft copolymers	150
8.4	Conclusions	152
	References	154

Epilogue	155
Summary	159
Samenvatting	162
Dankwoord	165
Curriculum Vitae	166

## Chapter 1

### Introduction

#### 1.1 Short historic overview

High impact resistant polymers like ABS (acrylonitrile/butadiene/styrene) and MBS (methyl methacrylate/butadiene/styrene) are mostly prepared by emulsion polymerization of an acrylonitrile/styrene or a methyl methacrylate/styrene monomer mixture using a polybutadiene seed latex. The first attempts to make these high impact resistant polymers were accomplished during the 1940's by modifying existing polymers; the ABS polymers were simply mechanical mixtures of styrene-acrylonitrile (SAN) and acrylonitrile-butadiene copolymers, two distinct incompatible phases. In the 1950's ABS was made via the emulsion process which resulted in SAN grafted rubber particles and these grafts provided compatibility between the rubber particles and the SAN matrix. This greatly increased the impact strength of these materials compared with the early materials made via mechanical mixing. At present, such rubber modified (ABS) polymers are produced on a large scale and find many applications in coatings, elastomers, adhesives and impact modifiers. Because of the commercial importance, in industry attention has been paid to the synthesis, analysis, kinetics, morphology, mechanical properties and to the application as impact modifiers of ABS.

The production of MBS started about ten years later. One important difference from ABS is its transparency. MBS finds its application mainly as impact modifier for polyvinyl chloride (PVC). Transparency is more an exception than a rule in mixed polymer systems. Optical mixtures can be

achieved because the refractive index of a styrene methyl methacrylate copolymer of a certain composition may match the refractive index of polybutadiene.

Emulsion polymerization is a complex process due to its heterogeneous and colloidal nature. The advantage of emulsion polymerization include an easy control of the process due to the physical state of the colloidal system. Thermal and viscosity problems are much less severe than in bulk or solution polymerization. The molecular weights of the polymer formed in emulsion can easily be controlled by the initiator concentration or by chain transfer agents. In addition, an important advantage of the emulsion polymerization technique is that the molecular weight and reaction rate can be controlled independently. Over the last few decades much attention has been paid to the theory and kinetics of emulsion polymerization. Some excellent review articles were published<sup>4,6</sup>. Emulsion copolymerization is even more complex since here the heterogeneity of the emulsion system combines with the different behaviour of the monomers, e.g. in terms of water solubility, monomer reactivity and swellability of the latex particles by the monomers.

The industrial and scientific importance in homogeneous radical copolymerization in solution and bulk was recognized in the 1920's<sup>7,9</sup>. The interest in copolymerization is still growing because copolymerization offers the possibility of modifying the properties of homopolymers and thus of designing tailor made polymer products.

Graft (co)polymers became important with the demand for high impact resistant polymers. The graft polymers improved the dispersion and compatibility of the rubbery domains in the continuous glassy phase. These graft (co)polymers are synthesized by grafting the monomer(s) (second stage of the process) onto separately prepared rubber seed particles (first stage). The second stage monomer(s) will not only graft onto the polybutadiene seed particles, but also form (co)polymer that is not chemically bonded to the polybutadiene core, the so-called free (co)polymer. During the emulsion graft copolymerizations, the presence of the polybutadiene seed latex particles will, in principle influence the partitioning behaviour of the monomers due to the specific interactions between the monomers and the different polymers. Locally

different monomer concentrations will lead to differences between the compositions of the grafted copolymer onto polybutadiene and that of the free copolymer. Differences in copolymer composition and increasing heterogeneity between grafted and free copolymer can affect phase separation<sup>10</sup> between the different copolymers. The properties and behaviour of the graft polymers depend on the degree of grafting<sup>11-14</sup>, particle morphology, the number and length of the grafts, molecular weights and, in case of copolymers, also on copolymer composition and chemical compositional distribution. Despite the great industrial interest in graft copolymerization, the process parameters, the copolymer characteristics in terms of graft and free copolymer microstructure and the resulting properties are not well understood and fundamental insight is missing. These considerations have formed the main motive for the research work described in the present thesis.

## 1.2 Aim of this investigation

The investigation described in this thesis aims at a better understanding of the emulsion copolymerization of styrene and methyl methacrylate onto polybutadiene seed particles. In a number of studies the main emphasis has been on the type of polymerization process, the degree of grafting, the molecular weight,<sup>15-29</sup> the analysis of the graft polymers<sup>25,30-37</sup>, mechanical properties<sup>11-14</sup>, kinetics<sup>20,38-45</sup>, the morphology<sup>46-51</sup>, the polymer swelling in bulk<sup>52-56</sup>.

In this study, however, not only the graft polymer characteristics mentioned above were investigated, but also the chemical composition and molecular weight distributions and the intramolecular microstructure, *i.e.* the sequence distribution and tacticity. Heterogeneous copolymers are often obtained from emulsion copolymerization as a result of the composition drift that occurs during the (batch) reaction, sometimes limiting the practical application of the resultant polymers in commercial products. Thus a better understanding of the effect of process parameters on the chemical microstructure of both the grafted and free polymer is required and various analytical methods were used to achieve this end. The intramolecular

microstructure (sequence distribution and tacticity) can be determined by Nuclear Magnetic Resonance (NMR) Spectroscopy. The average copolymer composition and molecular weight distribution are determined by NMR spectroscopy and by Size Exclusion Chromatography (SEC), respectively. The information can be coupled with results from Thin Layer Chromatography/Flame Ionisation Detection (TLC/FID)<sup>57,58</sup>, or by High Performance Liquid Chromatography (HPLC)<sup>59,60</sup>.

It has been shown that the copolymer microstructure directly reflects the molecular reactions occurring in the reaction loci<sup>61,62</sup>, and that this copolymer microstructure controls polymer properties<sup>63-69</sup>. In order to optimise the polymer properties, experimental verification of the copolymer microstructure is a prerequisite for model development of graft polymerization. The monomer partitioning between the organic and aqueous phases was studied so that the process conditions, swelling behaviour and microstructure could be correlated and understood. Since the peak assignments available from literature for the interpretation of the proton and carbon NMR spectra of styrene methyl methacrylate copolymers turned out to be unreliable, considerable effort was made to develop improved and unambiguous peak assignments for the NMR analysis of the intramolecular microstructure.

Also, the use of free radical copolymerization models has to be reconsidered; more experimental information about the sequence distribution of styrene-methyl methacrylate copolymers using carbon-13 NMR is necessary to allow discrimination between copolymerization models.

### 1.3 Survey of this thesis

In Chapter 2 the major theoretical aspects of emulsion graft copolymerization relevant to this investigation are briefly discussed.

In Chapter 3 the determination of the intramolecular microstructure by proton NMR is described. The new peak assignment of the methoxy protons of styrene methyl methacrylate copolymers developed in this chapter is confirmed by 2D NOESY NMR measurements.

Due to the limited application of proton NMR to determine the intramolecular microstructure of styrene methyl methacrylate copolymers, the assignments of the carbon-13 NMR spectra are discussed and revisited in Chapter 4.

In Chapter 5 the free radical copolymerization models are critically examined and verified by measuring triad sequences by carbon-13 NMR.

In Chapter 6 the experimental results and theoretical verification of the monomer partitioning experiments are discussed.

In Chapter 7 the composition drift of grafted and free copolymer is studied in batch polymerizations. The copolymer composition, copolymer compositional distribution, the molecular weight, the degree of grafting, and grafting efficiency are obtained in this investigation.

Finally, in Chapter 8 the batch and semi-continuous graft polymerizations are investigated. The results comprise crucial information in terms of the degree of grafting, copolymer composition and compositional distribution and morphology, as a function of variation in the process conditions.

Parts of this work have been presented at the Rolduc Polymer Meeting-4 (Kerkrade, The Netherlands, April 1989), 10th European Experimental NMR Conference (Veldhoven, The Netherlands, May 1990), CNRS-IUPAC-CFP Conference (Paris, France, September 1990), the 9th European Symposium on Polymer Spectroscopy (Cologne, Germany, September 1990), and the Gordon Research Conference on Polymer Colloids (Irsee, Germany, September 1992).

Parts of this thesis have been published or will be published soon: the proton NMR work of Chapter 3<sup>70</sup>, the carbon NMR work of Chapter 4<sup>71</sup>, the copolymerization model verification in Chapter 5<sup>72</sup>, the monomer partitioning investigation of Chapter 6<sup>73</sup> and the graft copolymerization study in Chapters 7 and 8<sup>74-75</sup>.

## References

1. Odian G.V., "Principles of Polymerization", 2nd Ed., John Wiley & Sons, Inc., New York, 1981.
2. Blackley D.C., "Emulsion Polymerization", Applied Science Publishers LTD, London 1975.
3. Gerrens H., Adv. Polym. Sci., 1, 234, 1959.
4. Hoff van der B.M.E., "The mechanism of emulsion polymerization", in "Vinyl Polymerization", 1, Part II, Ed. Ham G.E., Marcel Dekker Inc., New York, 1969.
5. Ugelstad J. and Hansen F.K., Rubber Chem. Tech., 49, 536, 1976.
6. Poehlein G.W., Schork F.J., Polym. News, 13, 231, 1988.
7. Alfrey T., Bohrer J.J., and Mark H., "Copolymerization" Interscience Publishers, New York, 1952.
8. Ham G.E., Ed., "Copolymerization", Interscience Publishers, New York, 1964.
9. Ham G.E., in "Kinetics and Mechanisms of Polymerization", Vol. I., "Vinyl Polymerization", Part I, Ed. G.E. Ham, Marcel Dekker Inc., New York, 1967.
10. Molau G.E., J. Polym. Sci., A3, 4235, 1965.; Kollinsky F, Markert G., Macromol. Chem., 121, 117, 1969.
11. Baum B., Holley W.H., Stiskin H., White R.A., Willis P.B., Wilde A.F., (Debell and Richardson, Inc, Enfield, Conn.), Adv. Chem. Ser., 154 (toughness and Brittleness Plast., Symp., 1974), 263, 1976.
12. Arakawa K., Nagai H., Kobunshi Robunshu, Eng Ed., 5(2), 95, 1976.
13. Purcell Jr. T.O., J. Vinyl Techn., 1 (3), 127, 1979.
14. Kim H., Keskhula, Paul D.R., Polymer, 32(8),1447, 1991.
15. Minoura Y., Mori Y., Imoto M., Makromol. Chem., 24, 205, 1957.
16. Mori Y., Minoura Y., Imoto M., Makromol. Chem., 25, 1, 1958.
17. Ghosh P., Sengupta P.K., J Appl. Polym. Sci., 11, 1603, 1967.
18. Moore L.D., Moyer W.W., Frazer W.J., Appl. Polym. Symposia, 7, 67, 1968.
19. Ide F., Sasaki I., Deguchi S., J. Appl. Polym. Sci, 15, 1791, 1971.
20. Locatelli J.L., Riess G., Angew. Makromol. Chem., 28, 161, 1973.
21. Locatelli J.L., Riess G., Angew. Makromol. Chem., 32, 101, 1973.
22. Locatelli J.L., Riess G., Angew. Makromol. Chem., 32, 117, 1973.
23. Ludwico W.A., Rosen S.L., J. Polym. Sci. Polym. Chem. Ed., 14, 2121, 1976.
24. Burfield D.R., Ng S.C., Eur. Polym. J., 14, 799, 1978.
25. Yoshida K., Ishigure K., Garreau H., Stannett V., J. Macromol. Sci.-Chem., A14(5), 739, 1980.



26. Shevchuk L.M., Batuyeva L.I., Kuvarina N.M., Duiko N.V., Kulikova A.Ye., *Pol. Sci. U.S.S.R.*, 23(4), 1022, 1981.
27. Mariamma George K., Claramma N.M., Thomas E.V., *Radiat. Phys. Chem.*, 30, 189, 1987.
28. Merkel M.P., Dimonie V.L., El-Aasser M.S., Vanderhoff J.W., *J. Appl. Polym. Sci.*, 41, 2463, 1990.
29. Barnard D., *J. Polym. Sci.*, 22, 213, 1956.
30. Schuster H., Hoffmann, M., Dinges K., *Angew. Makromol. Chem.*, 9, 35, 1966.
31. Locatelli J.L., Riess G., *Angew. Makromol. Chem.*, 26, 117, 1972.
32. Llauro-Daricades M.F., Banderet A., Riess G., *Makromol. Chem.*, 174, 105, 1973.
33. Llauro-Daricades M.F., Banderet A., Riess G., *Makromol. Chem.*, 174, 117, 1973.
34. Locatelli J.L., Riess G., *Eur. Polym. J.*, 10, 545, 1974.
35. Ide F, Mukadige Y., Kanchunk Y., *Kobunshi Robunshu, Eng. Ed.*, 4(7), 567, 1975.
36. Kranz D., Dinges K., Wendling P., *Angew. Makromol., Chem.*, 51, 25, 1976.
37. Jelinski L.W., Dumais Pl., Watnick Bass S.V., Shepherd, *J. Polym. Sci. Polym. Chem. Ed.*, 20, 3285, 1982.
38. Allen A., Merret F.M., *J. Polym. Sci.*, 22, 193, 1956.
39. Ayrey G., Moore C.G., *J. Polym. Sci.*, 36, 41, 1959.
40. Allen F.W., Ayrey G., Moore C.G., *J. Polym. Sci.*, 36, 55, 1959.
41. Dinges K., Schuster H., *Makromol. Chem.*, 101, 200, 1967.
42. Brydon A., Burnett G.M., Cameron G.G., *J. Polym. Sci. Polym. Chem. Ed.*, 11, 3255, 1973.
43. Brydon A., Burnett G.M., Cameron G.G., *J. Polym. Sci. Polym. Chem. Ed.*, 12, 1011, 1974.
44. Locatelli J.L., Riess G., *Angew. Makromol. Chem.*, 35, 47, 1974.
45. Ludwico W.A., Rosen S.L., *J. Appl. Polym. Sci.*, 19, 757, 1975.
46. Okubo M., Katsuta Y., Matsumoto T., *J. Polym. Sci. Polym. Lett. Ed.*, 18, 481, 1980.
47. Daniel J.C., *Makromol. Chem., Suppl.*, 10/11, 359, 1985.
48. Hergeth W.D., Schmutzler K., *Acta Polym.*, 36(9), 472, 1985
49. Merkel M.P., Dimonie V.L., El-Aasser M.S., Vanderhoff J.W., *J. Polym. Sci. Polym. Chem. Ed.*, 25, 1219, 1987.
50. Merkel M.P., Dimonie V.L., El-Aasser M.S., Vanderhoff J.W., *Polym. Preprints*,
51. Hergeth W.D., Bittrich H.J., Eichhorn F, Schlenker S., Schmutzler K., Steinau U.J., *Polymer*, 60, 1913, 1989.

52. Locatelli J.L., Riess G., *Angew. Makromol. Chem.*, 27, 201, 1972
53. Locatelli J.L., Riess G., *J. Polym. Sci. Polym. Lett. Ed.*, 11, 257, 1973.
54. Locatelli J.L., Riess G., *Makromol. Chem.*, 175, 3523, 1974.
55. Shaffer K., Dimonie V.L., El-Aasser M.S., Vanderhoff J.W., *J. Polym. Sci. Polym. Chem. Ed.*, 25, 2595, 1987.
56. Mathey P., Guillot J., *Polymer*, 32(5), 934, 1991.
57. Tacx J.C.J.F., Ammerdorffer J.L., German A.L., *Polymer* 29, 2087, 1988.
58. Tacx J.C.J.F., German A.L., *J. Polym. Sci. Polym. Chem. Ed.*, 27, 817, 1989.
59. Sparidans R.W., Claessens H.A., Doremaele van G.H.J., Herk van A.M., *J. Chromatogr.* 508, 319, 1990.
60. Doremaele van G.H.J., Kurja J., Claessens H.A., German A.L., *J. Chromatogr.*, 31(9/10), 493, 1991.
61. Stockmayer W.H., *J. Chem. Phys.*, 13, 199, 1945.
62. Koenig J.L. 'Chemical Microstructure of Polymer Chains', John Wiley and Sons, New York, 1980.
63. Kollinsky F., Markert G., *Makromol. Chem.*, 121, 117, 1969.
64. Barton J.M., *J. Polym. Sci., Part C*, 30, 573, 1970.
65. Johnston N.W., *Appl. Polym. Symp.*, 25, 19, 1974.
66. Schmitt B.J., *Angew. Chem.*, 91, 286, 1979.
67. Rodriguez ER., 'Principles of Polymer Systems', McGraw Hill, Japan, 1983.
68. ten Brinke G., Karasz FE., MacKnight W.J., *Macromolecules*, 16, 1827, 1983.
69. Balasz A.C., Karasz FE., MacKnight W.J., Ueda H., Sanchez I.C., *Macromolecules*, 18, 2786, 1985.
70. Aerdts A.M., Haan de J.W., German A.L., Velden v.d. G.P.M., *Macromolecules*, 24, 1473, 1991.
71. Aerdts A.M., de Haan J.W., German A.L., *Macromolecules*, in press.
72. Maxwell I.A., Aerdts A.M., German A.L., *Macromolecules*, in press.
73. Aerdts A.M., Boei M.M.W.A., German A.L., *Polymer*, in press.
74. Aerdts A.M., Kreij de J.E.D., Kurja J., German A.L., in preparation.
75. Aerdts A.M., Theelen S.J.C., Smit T.M.C., German A.L., in preparation.

## Chapter 2

### Theoretical Backgrounds

**ABSTRACT:** Most methods of synthesizing graft copolymers involve the use of radical polymerization, although ionic graft polymerizations are receiving increasing attention. Graft polymerizations are carried out in either homogeneous or heterogeneous systems depending on whether the polymer substrate is soluble or insoluble in the monomer. For preparing ABS or MBS all types of processes available are used, *i.e.* bulk-, solution-, and emulsion polymerizations. In this thesis MBS is prepared via the emulsion route. Therefore, different types of emulsion polymerization processes and the mechanism of the graft copolymerization will be briefly discussed.

#### 2.1 Emulsion polymerization

Radical emulsion polymerization involves the dispersion of monomer in a continuous aqueous phase and stabilization of this system by an emulsifier. Usually, a water soluble initiator is used to start the free radical polymerization. This results in a reaction medium consisting of submicron polymer particles swollen with monomer and dispersed in an aqueous phase. The final product is called a latex and consists of a colloidal dispersion of polymer particles in water.

According to the Harkins-Smith-Ewart theory<sup>1,2</sup> the process can be divided into three distinct intervals. During interval I, water monomer and surfactant are initially present. Free radicals are generated in the aqueous phase by adding a water soluble initiator. These free radicals can then add on monomer units until they become insoluble, whereupon particle nucleation takes place. If particle nucleation is ceased, the number of particles and the

rate of reaction is constant, and the system is said to be in interval II. During interval II the polymerization takes place within the latex particles in which the monomer concentration remains constant by continual diffusion of monomer, through the aqueous phase, from the monomer droplets to the particles. These monomer droplets, however, will have been completely consumed at the end of interval II. The monomer remaining in the particles and possibly in the water phase is polymerized during interval III, so the rate of reaction also decreases.

The advantage of emulsion polymerization includes an efficient heat transfer as a result of the aqueous medium. This usually means a good control of the process temperature. Toxic and flammable organic solvents are not required and the reaction can proceed till high conversion. Molecular weight can easily be controlled by the use of chain transfer agents.

#### *Surfactant-free emulsion polymerization*

The presence of a surfactant is a disadvantage in certain applications of emulsion polymers. For example, during film formation in coatings, surfactants may lead to poor color and color stability and reduction of gloss. Removal of the surfactant, on the other hand, can lead to coagulation or flocculation of the destabilized latex. Surfactant free emulsion polymerization, involving the omission of surfactant in the recipe, is a useful approach to solve this problem. The technique requires the use of an initiator yielding initiating species that after some propagation impart surface active properties to the polymer particles. Persulfate is a most useful initiator for this purpose. Latices prepared by the surfactant-free technique thus are stabilized by chemically bond charged surface active groups such as ion containing oligomeric species. The latices can then be purified without loss of stability<sup>3</sup>.

#### *Emulsion copolymerization*

Emulsion copolymerizations can be carried out using batch, semi-continuous or continuous processes. The chemical microstructure of the copolymer formed depends upon the type of process used, the reactivity ratios of the monomers, the monomer polarity and the partitioning behaviour

between the various phases in the emulsion system<sup>4</sup>.

Heterogeneous copolymers with a two peaked or very broad distribution of copolymer composition usually result from batch processes and are caused by composition drift (when there are differences in reactivity and polarity of the two monomers used). More homogeneous copolymers can be made by semi-continuous processes (*i.e.* through addition of monomer during polymerization, see Chapter 8).

Two models are used to describe the copolymerization kinetics, the sequence distribution and the chemical composition of copolymers prepared in homogeneous systems such as bulk and solution copolymerization. The ultimate model<sup>5,6</sup>, also known as terminal model is the most frequently used. In this model the monomer addition rate only depends on the nature of the terminal group and therefore obeys first order Markov statistics<sup>7</sup>. The penultimate model is used in systems where the nature of the penultimate unit has a significant effect on the rate constants in copolymerization. This means that eight different reactions have to be considered<sup>8</sup>. The different schemes of the two models are given in Table 2.1 and 2.2. The proper model choice will be discussed in Chapter 5<sup>9</sup>.

*Table 2.1: Copolymerization scheme according to the ultimate model.*

terminal group	added monomer	rate	final
-S*	[S]	$k_{ss}[S^*][S]$	-SS*
-S*	[M]	$k_{sm}[S^*][M]$	-SM*
-M*	[S]	$k_{ms}[M^*][S]$	-MS*
-M*	[M]	$k_{mm}[M^*][M]$	-MM*

The two reactivity ratios of monomer S and M are defined by:

$$r_s = k_{ss}/k_{sm} \text{ and } r_m = k_{mm}/k_{ms}$$

Table 2.2: Copolymerization scheme according to the penultimate model.

penultimate group	added monomer	rate	final
-SS*	[S]	$k_{ss}[SS^*][S]$	-SSS*
-SS*	[M]	$k_{sm}[SS^*][M]$	-SSM*
-MS*	[S]	$k_{ms}[MS^*][S]$	-MSS*
-MS*	[M]	$k_{mm}[MS^*][M]$	-MSM*
-SM*	[S]	$k_{ss}[SM^*][S]$	-SMS*
-SM*	[M]	$k_{sm}[SM^*][M]$	-SMM*
-MM*	[S]	$k_{ms}[MM^*][S]$	-MMS*
-MM*	[M]	$k_{mm}[MM^*][M]$	-MMM*

The six reactivity ratios of monomer  $i$  and  $j$  are defined by:

$$r_i = k_{ii}/k_{ij}, r^j = k_{ji}/k_{jj} \text{ and } s_j = k_{ji}/k_{ij}$$

(with  $i = s, m$  and  $j = m, s$ , successively)

### Seeded emulsion copolymerization

Seeded emulsion polymerization starts in interval II or III, in presence and absence of monomer droplets, respectively, *i.e.* in the presence of preformed polymer latex particles. The polymerization will start in the polymer particles, which will grow further. Hence, it is a very good method of obtaining very large particles. Ideally, the number of particles will remain constant but sometimes a second crop of particles will be formed (secondary nucleation). These polymerizations can also be carried out using batch, semi-continuous or continuous processes.

The monomers are distributed between the particles, the aqueous phase and, if present, the monomer droplets. As a result of the monomer partitioning during emulsion copolymerization the local monomer ratio inside the particles can be quite different from the overall monomer ratio. The particles can be of different chemical types (presence of secondary nucleation or domains in latex particles) if monomers other than those whereof the seed is prepared are employed. An important factor determining the chemical microstructure of the copolymers formed is the monomer concentration in the different loci. In seeded emulsion copolymerization of two monomers onto polybutadiene seed particles, the monomer partitioning can be influenced by the two different

types of polymers, *i.e.* the seed polymer and the secondary polymer, by the polarities of the monomers, and by the monomer to water ratio. The monomer to polymer ratio will also play an important role. At low monomer to water ratios, more composition drift may occur because of the relatively higher concentrations of the more polar monomer in the water phase. One of the key questions in the present study is, whether or not the graft copolymerization and the copolymerization leading to free copolymer, will exhibit different copolymerization characteristics. This question will be dealt with in Chapters 7 and 8.

## 2.2 Mechanism of graft polymerization

The free radical seeded emulsion polymerization of a monomer using an oil soluble initiator or a water soluble initiator can result in grafting due to radical formation on the polymer backbone. An example of the former initiator is cumene hydroperoxide (CHP). Potassium persulfate (KPS) is a typical example of the latter type. There are a number of possible mechanisms for the initiation of a polymer chain grafted upon the backbone of the seed polymer. The first stage polymer, in this case polybutadiene, is prepared by emulsion polymerization and consists of three different structural units, *cis*-1,4, *trans*-1,4, and vinyl-1,2, with concentrations typically of 20%, 62% and 18%, respectively. These ratios can only be varied in emulsion polymerization when the temperature is changed.<sup>10</sup>

Graft polymers result from the polymer radical formation either by chain transfer between a propagating radical (*i.e.* initiator radical or polymeric radical) and the polymer (where we must discriminate between the 1,4 units and the 1,2 units), or by addition to the double bonds in the 1,4 units and in the 1,2 units. These processes of radical formation and the subsequent propagations are summarized by the following equations :

transfer by proton abstraction followed by propagation:



or

direct radical addition to the double bond followed by propagation:



where  $X^{\bullet}$  is either an initiator radical or a polymeric radical, RH denotes an  $\alpha$ -methyleneic hydrogen atom on a polybutadiene chain, and R indicates the polymer backbone, the polybutadiene chain;  $R^{\bullet}$  is a polybutadiene radical; M is a monomer;  $RM_{n+1}^{\bullet}$  and  $XRM_n^{\bullet}$  are radicals comprising a polymer side chain grafted onto polybutadiene and  $XR^{\bullet}$  is a polybutadiene radical arising from a direct addition attack to the double bond of the polybutadiene.

There are some conflicting views concerning several important details of initiation of the polymer backbone. Most studies were performed in solution or in the bulk on a natural rubber (polyisoprene) seed latex. Some investigators aver that AIBN would not produce any grafting<sup>11-17</sup> due to the fact that its radical (the resonance stabilized-2-cyano-2-propyl radical) which has weak capabilities for hydrogen-abstraction.

Others maintain that AIBN produces a small number of grafts<sup>14</sup>, less graft sites, but the grafts have higher molecular weights. Brydon *et al.*<sup>17</sup> stated that the radical grafting reaction can be carried out under widely varying conditions which might significantly alter the mechanisms of the polymerization and the polymer characteristics. One of the important polymerization conditions is the type of the polymer backbone. This is shown by Locatelli *et al.*<sup>18</sup> who increased the vinyl content of the polybutadiene. The same level of degree of grafting at high vinyl contents in the PB was obtained



with both AIBN and BPO. Dinges *et al.*<sup>14</sup> reported that no grafting with AIBN occurs when the monomer to polymer ratio is too high. The competitive initiation reaction of either the monomer and the free polymer chain or the polymer backbone by AIBN resulting in a free polymer chain.

On the other hand, Allen *et al.*<sup>13</sup>, who also studied graft polymerization in solution, concluded that 55-65 % of the initiation of the polymer backbone occurs via the double bond, and 35-45% proceeds by abstracting an allylic hydrogen atom. Furthermore, it has been found that with all types of initiators, both the degree of grafting and the reaction rate are higher for increasing vinyl contents of the rubber<sup>18</sup>. This is caused by the hybridisation state in the radical stabilisation phase, or by the greater ease of abstracting an  $\alpha$ -H atom of the vinyl-1,2 unit which compared with that of the cis-1,4 and trans-1,4 units in polybutadiene.

Additional confusion arises from the work of Chern and Poehlein<sup>19</sup>, who claimed that the direct attack of the initiator on the residual carbon-carbon double bond of the polybutadiene backbone is the most important initiation mechanism during grafting in solution. On the other hand, when the same authors carried out modelling studies on grafting in emulsion polymerization systems, they found that the grafted polymer chain is initiated by chain transfer of a growing polymeric free radical to the rubber core by allylic proton abstraction<sup>20</sup>.

Sundberg *et al.*<sup>21</sup> studied the grafting of styrene onto polybutadiene in emulsion and considered that incoming free radicals may initiate both grafted and free second stage polymer chains in the monomer swollen rubber phase, with the probability of each chain formation being related to a specific initiation rate constant. The chain length of the polymer formed in the second stage is controlled by the transfer processes rather than of by the cross-termination of free and grafted polymer chains.

Most published studies of grafting in emulsion polymerization systems do not describe the mechanisms of initiation of the rubber seed polymer, but rather show the effects of varying the process parameters on some characteristics in graft polymerization like polymerization rate, degree of grafting and grafting efficiency.

Summarizing, most conclusions about the nature of the polymer backbone initiation arise from modelling experimental polymerization rates invoking many assumptions. It must be concluded that initiation in grafting processes is very complicated and still partly understood. Grafting certainly depends on the applied process and also on the process parameters such as the type of the rubber and the monomer.

As already mentioned above, not only the polymer formed in the first step is initiated, but the initiator radical can also start monomer, leading to free radical (homo)polymerization:

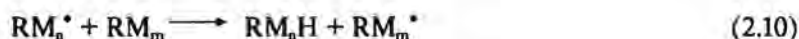


followed by propagation:

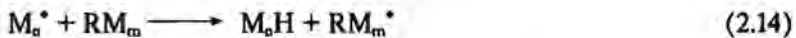


Reaction 2.6 competes with reactions 2.1 and 2.4. The probabilities of occurrence of reaction 2.1 and 2.4 will increase when the monomer concentration decreases.

Further, beside the initiation and propagation processes, important chain transfer reactions involving seed polymer anchored radicals proceed as follows:

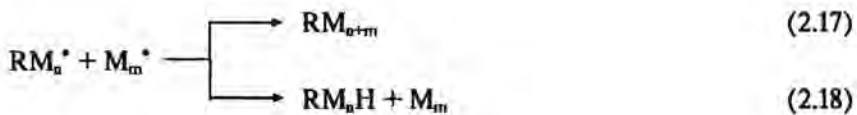
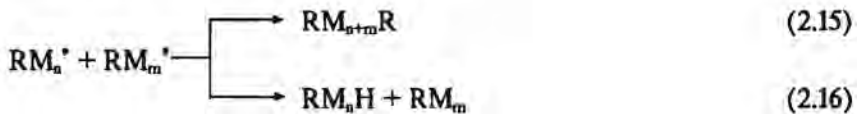


Analogously, for transfer reactions involving free polymeric radicals:



Reactions 2.9, 2.10, 2.13 and 2.14 (re-)initiate the PB.

The termination processes can be outlined as follows: a grafted polymer radical ( $RM_n^*$ ) can terminate either through reaction with another grafted polymer radical ( $RM_m^*$ ) or through cross-termination with a free polymer radical ( $M_m^*$ ). In each case termination may occur by combination or by disproportionation:



In addition to the above termination reactions, also free polymer chain radicals  $M_n^*$  will undergo bimolecular self termination, either by combination or by disproportionation.

The large variety of reactions occurring during graft polymerization, together with all the appropriate rate constants combined with the complexities of heterogeneous emulsion polymerization results in an extremely complicated system. The results of the present investigation, aiming at the microstructural characterization of grafted and free copolymer formed under different conditions, will contribute to more qualitative and semi-quantitative insight in this complicated process.

## References

1. Harkins W.D., *J. Am. Chem. Soc.*, 69, 1428, 1947.
2. Smith W.V., Ewart R.H., *J. Chem. Phys.*, 16, 592, 1948.
3. Verdurmen E.M., Albers J.G., Dohmen E.H., Zirkzee H., Maxwell I.A., German A.L., in preparation.
4. Doremaele van G.H.J., Ph. D. thesis, "Model Prediction, Experimental Determination, and Control of Copolymer Microstructure", Eindhoven University of Technology, the Netherlands, 1990.
5. Alfrey T., Goldfinger G., *J. Chem Phys.*, 12, 205, 1944.
6. Mayo F.R., Lewis F.M., *J. Am. Chem. Soc.*, 66, 1594, 1944.
7. Koenig J.L., "Chemical Microstructure of Polymer Chains", John Wiley and Sons, New York, 1980.
8. Merz E., Alfrey T., Goldfinger G., *J. Polym. Sci.*, 1, 75, 1946.
9. Chapter 5; this thesis
10. Hampton R.R., *Anal. Chem.*, 21, 323, 1949.
11. Allen F.W., Merret F.M., *J. Polym. Sci.*, 22, 193, 1956.
12. Minoura Y., Mori Y., Imoto M., *Makromol. Chem.*, 24, 205, 1957.
13. Allen F.W., Ayrey G., Moore C.G., *J. Polym. Sci.*, 36, 55, 1959.
14. Dinges K., Schuster H., *Die Makromol. Chem.*, 101, 200, 1967.
15. Ghosh P., Sengupta P.K., *J. Appl. Polym. Sci.*, 11, 1603, 1967.
16. Brydon A., Burnett G.M., Cameron G.G., *J. Polym. Sci. Polym. Chem. Ed.*, 11, 3255, 1973.
17. Brydon A., Burnett G.M., Cameron G.G., *J. Polym. Sci. Polym. Chem. Ed.*, 12, 1011, 1974.
18. Locatelli J.L., Riess G., *Angew. Makromol. Chem.*, 32, 117, 1973.
19. Chern C.S., Poehlein G.W., *Chem. Eng. Comm.*, 60, 101, 1987.
20. Chern C.S., Poehlein G.W., *J. Polym. Sci. Polym. Chem. Ed.*, 25, 617, 1987.
21. Sundberg D.C., Arndt J., Tang M.Y., *J. Dispersion Sci. Techn.*, 5, 433, 1984.

## Chapter 3

# Characterization of Intramolecular Microstructure of Styrene Methyl Methacrylate Copolymers by Means of Proton NMR

**ABSTRACT:** The methoxy  $^1\text{H}$  NMR signals in the 2.10-3.70  $\delta$  region for statistical styrene-methyl methacrylate copolymers have been reassigned for several methyl methacrylate centered triad/pentad resonances. Former literature assignments for statistical copolymers were inconsistent with experimental results. New peak assignments are completely based on pentad sequence distributions. Supporting evidence for these reassignments is twofold: comparison of theoretically calculated and experimentally observed peak areas, and the use of various independent procedures for the determination of the coisotacticity parameter  $\sigma$ , yields consistent results ( $\sigma=0.44$ ). Secondly, 2D NOESY (Nuclear Overhauser Effect Spectroscopy) NMR experiments were carried out for alternating as well as for statistical copolymers. The results supported the proposed reassignments.

### 3.1 Introduction

High resolution Nuclear Magnetic Resonance (NMR) spectroscopy has been particularly effective in the determination of the intramolecular chain structure of polymers. The intramolecular (sequence distribution and tacticity) and intermolecular (chemical composition molar mass distribution) copolymer microstructure is important, because it may supply information about the monomer addition process, e.g. about the preference of monomers to add in

(co)iso- or cosyndiotactic configuration<sup>13</sup>. Moreover, knowledge about the inter- and intramolecular structure is of paramount importance for the understanding of relations between molecular structure and polymer properties<sup>4</sup>.

In our laboratories much attention has been paid to low and high conversion solution and high conversion emulsion SEMA<sup>5</sup> (styrene-ethyl methacrylate) and SMA<sup>6</sup> (styrene-methyl acrylate) copolymers. Modelling of high conversion solution and emulsion copolymers requires experimental data on sequences and sometimes tacticities to confirm the correctness of the model. Also, for SMMA (styrene-methyl methacrylate copolymers) an unambiguous assignment of proton NMR spectra is a prerequisite for comparing the experimental results with our kinetic model, used in the modelling of several polymerization processes.

Several groups have (re-)investigated the <sup>1</sup>H NMR spectra of statistical SMMA copolymers, *i.e.* the groups of Ito/Yamashita<sup>7-10</sup>, Bovey<sup>11</sup> and Harwood/Ritchey<sup>3,12</sup>, San Roman *et al.*<sup>13</sup> and the Eastman Kodak group (Uebel/Dinan)<sup>14,15</sup>. Alternating SMMA copolymers have been recently analysed by the groups of Hirai/Koinuma/Tanabe<sup>16,17</sup>, Niknam/Harwood<sup>18</sup> and Heffner/Bovey<sup>19</sup>. In early studies<sup>3,7-12</sup>, the 40-60 MHz proton NMR spectra of statistical copolymers were found to exhibit a multiplicity in the 2.1-3.7  $\delta$  region characteristic of methoxy protons. The methoxy region was broken into three composite peak groupings, designated X, Y, and Z, respectively. The improved resolution of the methoxy region in <sup>1</sup>H NMR spectra recorded at higher magnetic fields<sup>13-15</sup> leads to significantly more observable fine structure. The complex peak envelopes has been reinterpreted in terms of six major peak groupings (contrary to the earlier observed three peak groupings), each of which is attributed to an individual M-centered triad or to groups of M-centered triads. Subsequently, San Roman *et al.*<sup>13</sup> and Uebel<sup>14</sup> have partly reassigned resonances (270 MHz) in the oxymethylene region of the M-centered triads and pentads. Unfortunately, the improvements of Uebel, valid for SMMA copolymers, appeared to be inapplicable to SEMA copolymers<sup>5</sup>, and a new set of peak triad/pentad assignments was proposed, confirmed by data from <sup>13</sup>C-NMR. A reinvestigation of the SMMA proton NMR spectra of Uebel<sup>14</sup> at 400 MHz has been performed by a joined effort of the groups of Kale/O'Driscoll and Uebel/Dinan<sup>15</sup>. The

spectra of the previous series of statistical nondeuterated copolymers<sup>14</sup> and a series of deuterated copolymers of styrene-d<sub>8</sub> and MMA were analysed quantitatively<sup>15</sup>. In the Z peak region (Ito notation) a methine-methoxy overlap has been proven to exist (already pointed out by Harwood<sup>3</sup>). As a result the peak areas, reported earlier by Uebel<sup>14</sup> have been remeasured<sup>15</sup>. Kale *et al.*<sup>15</sup> have also suggested a minor correction in the assignments, moreover a different method has been used to estimate the coisotacticity parameter  $\sigma$  in comparison to the method put forward in ref. 14. This leads to a value different from Uebel's earlier proposal ( $\sigma = 0.63$ <sup>14</sup> and  $\sigma = 0.44$ <sup>15</sup>).

The theoretical triads and pentads have been calculated using the ultimate model (*i.e.* Alfrey-Mayo kinetics)<sup>1</sup>. The copolymer composition could be described successfully with the ultimate model. However, Fukuda<sup>20</sup> and O'Driscoll<sup>21</sup> have shown that, quite to the contrary, this model is apparently incapable of describing the kinetic process (*i.e.* the propagation rate  $k_p$ ). From this we conclude that beside the copolymer composition also the sequences can be readily described by the ultimate model. This will be further discussed in Chapter 5, where several models were verified with the copolymer composition and sequence distribution. This shows that the ultimate model is good enough to describe the copolymer composition and sequence distribution.

Although Kale *et al.*<sup>15</sup> have achieved a better agreement between the experimentally observed peak areas and those predicted by theory, an inconsistency remains in some part of their assignments. Different estimation procedures for the coisotacticity parameter  $\sigma$  lead to widely differing  $\sigma_{SM}$  values, as will be shown in paragraph 3.4. This coisotacticity parameter  $\sigma_{SM}$  ( $=\sigma$ ) is defined as a measure of the probability that alternating S and MMA centered triads adopt a coisotactic configuration. In order to explain these discrepancies in peak areas and  $\sigma$  values, we propose a new M-centered mixed configurational triad, compositional pentad sequence assignment, based on a comparison of experimentally observed and theoretically predicted peak areas for a series of low conversion solution copolymers and supported by 2D NOESY NMR data on both statistical and alternating SMMA copolymers. 2D NOESY is an NMR technique, specifically tailored to detect spatial relations over short distances (generally  $< 5 \text{ \AA}$ ). By this technique, the close proximity of

styrene units to the methoxy group can directly be shown through nuclear Overhauser effects. A recent 2D NOESY study on an alternating SMMA copolymer has been published by Heffner *et al.*<sup>19</sup>. Up to now the NOESY spectra of statistical copolymers have not been published to the best of our knowledge, possibly due to the complexity in the OCH<sub>3</sub> region. The present paper shows that, in spite of the complex grouping, additional information can be obtained. More cross peaks were observed than would be possible according to the earlier proposed assignments of iso- and heterotactic SMMA triads, which justifies a reassignment in pentads.

### 3.2 Experimental section

#### *Chemicals and samples*

The monomers styrene and methyl methacrylate (Merck) were distilled at reduced pressure under nitrogen. The middle fraction of the distillate was collected and used. The free radical initiator AIBN (2,2'-Azobis(isobutyronitrile), Fluka p.a.) was recrystallized once from methanol. The solution synthesized copolymers were prepared in a 100 ml glass vessel, thermostated at 323 K. The total monomer concentration was 3 mol/l in toluene. The total conversion was determined by means of solid weight, and amounted to 5 wt%. The initiator concentration was 8 mmol/l. To isolate and purify the copolymer, the reaction mixture was poured out in a tenfold excess of cold hexane. The final product was dried out at 328 K in a vacuum stove for at least 16 h at 10<sup>-5</sup> T.

The alternating copolymer was prepared as published by Tanabe<sup>22</sup>, employing zinc chloride initiator, in the dark at 278 K. The alternating structure is confirmed by proton NMR.

#### *<sup>1</sup>H NMR measurements*

<sup>1</sup>H NMR spectra were recorded with a 400 MHz (Bruker AM 400) spectrometer at 298 K, using CDCl<sub>3</sub> as a solvent and locking agent. Generally, the spectra were obtained using a spectral width of 6024 Hz, an acquisition



time of 2.7 sec, a flip angle of  $45^\circ$  and a pulse delay of 5 sec. Spectra were obtained after accumulating 64 scans, using a sample concentration of 1% (w/v). The digital resolution amounted to 0.38 Hz, corresponding to a data length of 32 K. In performing quantitative NMR measurements via compositional sequence placements, one must take into account differences in spin lattice relaxation times ( $T_1$ ). The  $T_1$ 's were measured by inversion recovery.

### 2D NOESY NMR

The phase sensitive 2D NOESY<sup>23</sup> experiment employed a  $\pi/2 - t_1 - \pi/2 - \tau_m - \pi/2 - t_2$  pulse sequence<sup>24,25</sup>, and has been used for the observation of dipole-dipole interactions between neighbouring S and MMA units. The 2D NOESY experiments were recorded on a Bruker 600 AM spectrometer. The polymer solutions were prepared in hexachlorobutadiene with 10% benzene-d<sub>6</sub> as lock. The concentrations were 2% (w/v). The spectra were recorded at a temperature of 353 K. The process data matrix consisted of 512 \* 512 points covering 5882 Hz in both dimensions. The repetition time was 2 s with 16 scans collected for each of the 256 spectra. Repetition times of up to 5 s did not lead to different cross peak patterns. The phase sensitive spectra were processed with window multiplication of sine bell squared with a shift of 2 in F2 direction and a shift of 4 in F1 direction.

### 3.3 Results and discussion; sequence distribution

Figure 3.1 depicts a typical 400 MHz <sup>1</sup>H NMR spectrum of a statistical SMMA copolymer, whereas in Figure 3.2 expanded 400 MHz spectra are presented, showing only the methoxy region for a series of low conversion solution copolymers with various S/MMA feed ratios. At a higher magnetic field strength, i.e. 600 MHz no more additional resolution enhancement can be achieved in the methoxy region (Figure 3.3b). The impurities at  $\delta=5.3$  and  $\delta=4.1$  ppm are resonances of unknown compounds. In Figure 3.2 the peak areas are designated I - VI, these are due to combined compositional (=sequence) and configurational (=tacticity) effects. The areas are assigned to specific M-

Table 3.2, the molar feed ratio  $x$ , the experimentally corrected observed peak areas, and the peak calculated areas according to intrinsically related peak assignments, are given. Overlapping of the  $\text{OCH}_3$  (Z) peak with the methine proton of styrene can be seen in Figure 3.1. To circumvent this problem in an attempt to measure quantitatively the peak areas I-VI, Gotoh<sup>17</sup> *et al.* have suggested the use of equations 3.1-3.4:

$$\text{Area OCH}_3 = 3/8 (\text{Area } A_2 - 3/5 \text{ Area } A_1) \quad (3.1)$$

$$\text{Peak X} = \text{I} + \text{II} + \text{III} \quad f_X = X / \text{Area OCH}_3 \quad (3.2)$$

$$\text{Peak Y} = \text{IV} + \text{V} \quad f_Y = Y / \text{Area OCH}_3 \quad (3.3)$$

$$\text{Peak Z} = \text{VI} \quad f_Z = 1 - f_X - f_Y \quad (3.4)$$

where  $A_1$  and  $A_2$  represent the total peak areas of the aromatic and aliphatic proton resonances, respectively. The theoretical relative methoxy peak areas have been calculated using the theoretical triads and pentads and a coisotacticity parameter  $\sigma = 0.63$  (Uebel<sup>14</sup>) and  $\sigma = 0.44$  (Kale<sup>15</sup>). The triads and pentads can be calculated using Alfrey-Mayo (AM) kinetics or ultimate model (= 1<sup>st</sup> order Markov statistics)<sup>1</sup>, assuming this model to be valid at any moment of the

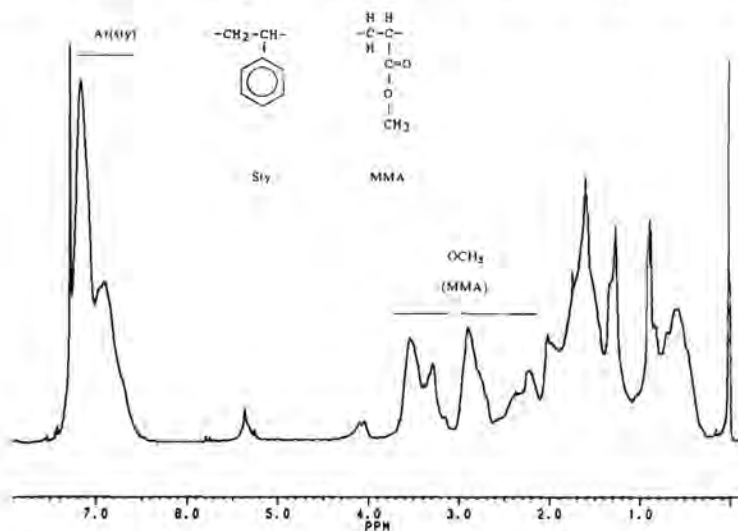


Figure 3.1: 400 MHz  $^1\text{H}$  NMR spectrum of a low conversion solution styrene-methyl methacrylate copolymer ( $f_m=0.47$ ) in  $\text{CDCl}_3$  at 298 K.

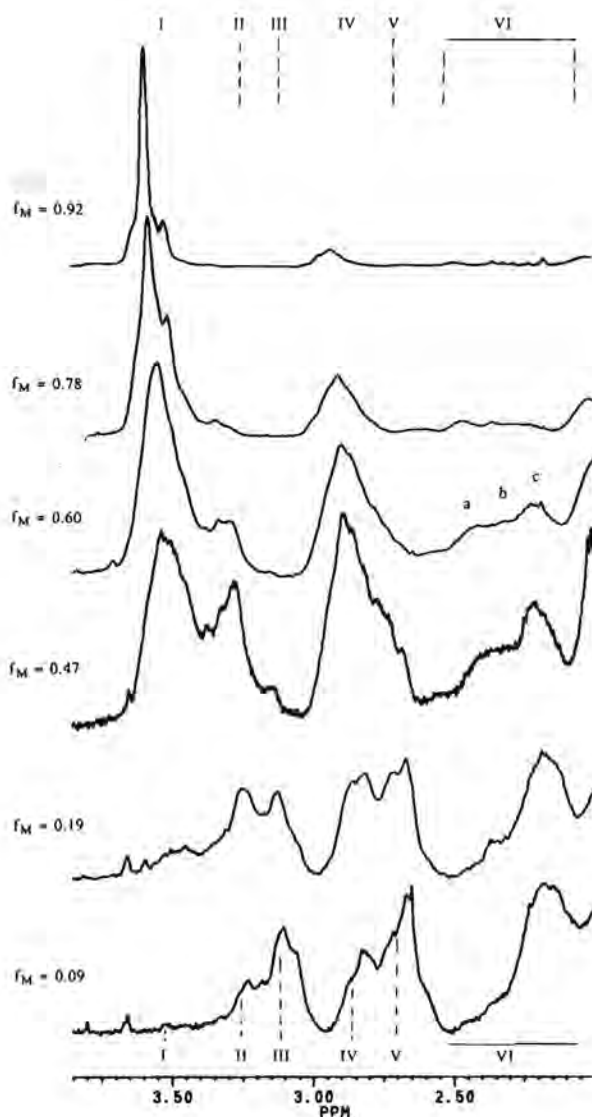


Figure 3.2: Expanded 400 MHz  $^1\text{H}$  NMR spectra of low conversion solution SMMA copolymers, showing the methoxy region only. Spectra were recorded in  $\text{CDCl}_3$  at 298 K. Molar feed compositions ( $f_M$ ) are indicated for each copolymer on the left hand side.

Table 3.1: Literature and new assignment of methoxy resonances for statistical SMMA copolymers.

Peak chemical shift region (ppm)	I	II	III	IV	V	VI
	3.70-3.40	3.40-3.17	3.17-2.95	2.95-2.78	2.78-2.50	2.50- 2.10
Ito-Bovey <sup>10,11</sup> (60-100 MHz)	MMM	(1- $\sigma$ )MMS (1- $\sigma$ ) <sup>2</sup> SMS		$\sigma$ MMS	2 $\sigma$ (1- $\sigma$ )SMS	$\sigma^2$ SMS
Uebel-Dinan <sup>14</sup> (270 MHz)	MMM (1- $\sigma$ )MMS	(1- $\sigma$ ) <sup>2</sup> MSMSM (1- $\sigma$ ) <sup>2</sup> SSMSM	(1- $\sigma$ ) <sup>2</sup> SSMSS	$\sigma$ MMS	2 $\sigma$ (1- $\sigma$ )SMS	$\sigma^2$ SMS
Kale-O'Driscoll <sup>15</sup> (400 MHz)	MMM (1- $\sigma$ )MMS	(1- $\sigma$ ) <sup>2</sup> MSMSM (1- $\sigma$ ) <sup>2</sup> SSMSM	(1- $\sigma$ ) <sup>2</sup> SSMSS	$\sigma$ MMS + 2 $\sigma$ (1- $\sigma$ )MSMSM	2 $\sigma$ (1- $\sigma$ )SMS - 2 $\sigma$ (1- $\sigma$ )MSMSM	$\sigma^2$ SMS
This work (400 MHz)	MMMMM 2MMMMS SMMMS (1- $\sigma$ )MSMMM (1- $\sigma$ )MSMMS (1- $\sigma$ ) <sup>2</sup> MSMSM	$\sigma$ SSMMM $\sigma$ SSMMS (1- $\sigma$ )SSMMM (1- $\sigma$ ) <sup>2</sup> SSMSM	(1- $\sigma$ ) <sup>2</sup> SSMSS	$\sigma$ MSMMM $\sigma$ MSMMS 2 $\sigma$ (1- $\sigma$ )MSMSM 2 $\sigma$ (1- $\sigma$ )SSMSM	(1- $\sigma$ )SSMMS 2 $\sigma$ (1- $\sigma$ )SSMSS	$\sigma^2$ MSMSM 2 $\sigma^2$ SSMSM $\sigma^2$ SSMSS

reaction for low conversion solution copolymers with reactivity ratios  $r_M = 0.45$  and  $r_S = 0.50$  (Kelen-Tüdös<sup>26</sup>). The following equations apply to M-centered triads or pentads:

$$\begin{aligned}
 F_{MMMM} &= (1-P(S/M))^2 \\
 F_{MMS} &= 2 P(S/M) (1-P(S/M)) \\
 F_{SMS} &= P(S/M)^2 \\
 F_{MMMMM} &= F_{MMMM} P(M/M)^2 \\
 F_{SMMMM} &= F_{MMMM} 2 P(S/M) P(M/M) \\
 F_{SMMM} &= F_{MMMM} P(S/M)^2 \\
 F_{MSMMM} &= F_{SMMM} P(M/S) P(M/M) \\
 F_{SSMMM} &= F_{SMMM} P(S/S) P(M/M) \\
 F_{MSMMS} &= F_{SMMM} P(M/S) P(S/M) \\
 F_{SSMMS} &= F_{SMMM} P(S/S) P(S/M) \\
 F_{MSMSM} &= F_{SMS} P(M/S)^2 \\
 F_{SSMSM} &= F_{SMS} 2 P(S/S) P(M/S) \\
 F_{SSMSS} &= F_{SMS} P(S/S)^2
 \end{aligned} \tag{3.5}$$

where  $F$  represents the number fraction of triads and pentads normalized to unity,  $P(M_1/M_2)$  is the probability of an  $M_2$  type growing chain end to react with monomer  $M_1$ . In addition,  $P(M/M) = (r_M/x)/(1+(r_M/x))$ ,  $P(S/M) = 1/(1+(r_M/x))$ ,  $P(S/S) = (r_S x)/(1+(r_S x))$ ,  $P(M/S) = 1/(1+(r_S x))$ , and  $x = S/MMA$ , the molar feed ratio. The numerical values of the theoretical number fractions of M-centered triads and pentads are summarized in Table 3.3.

If we compare the experimental results with the theoretical relative peak areas calculated according to the various assignments, none of the earlier published assignments yields a satisfactory agreement (Table 3.2). The results of Uebel's assignment and  $\sigma = 0.63$  yield widely differing relative peak areas for all copolymer compositions. The improvements made by Kale *et al.*<sup>15</sup> are clearly observable. However, still some discrepancies remain. For the copolymer feed compositions  $f_M = 0.47 - 0.09$  the predicted peak areas of peak II have too small values, and at higher styrene content of the copolymer, peak I is too high. For the same copolymers the predicted peak areas of peak IV are much too small and of peak V too high<sup>15</sup>.

Table 3.2: Normalized peak areas of the methoxy resonances of SMMA copolymers obtained by low conversion batch solution processes. Predicted relative areas calculated using the model valid for low conversion polymers, and  $r_S=0.50$ ,  $r_M=0.45$ ,  $\sigma_{SM}=0.63$  (Uebel<sup>16</sup>),  $\sigma_{SM}=0.44$  (Kale<sup>15</sup>) and the appropriate assignment with  $\sigma_{SM}=0.44$  for various initial feed ratios  $x_0 = [S]/[MMA]$ .

$x_0$	$f_M$	Relative peak areas						Assignment
		I	II	III	IV	V	VI	
0.09	0.92	0.84	0.01	0.00	0.14	0.00	0.01	Observed
		0.80	0.00	0.00	0.18	0.00	0.01	Uebel
		0.85	0.01	0.00	0.13	0.00	0.01	Kale
		0.86	0.01	0.00	0.13	0.00	0.01	This work
0.29	0.78	0.66	0.05	0.01	0.20	0.03	0.06	Observed
		0.55	0.02	0.00	0.35	0.02	0.06	Uebel
		0.64	0.05	0.00	0.27	0.02	0.03	Kale
		0.65	0.06	0.00	0.25	0.01	0.03	This work
0.66	0.60	0.43	0.13	0.01	0.30	0.06	0.08	Observed
		0.34	0.05	0.00	0.30	0.17	0.14	Uebel
		0.43	0.11	0.01	0.31	0.08	0.07	Kale
		0.42	0.12	0.01	0.32	0.05	0.07	This work
1.15	0.47	0.30	0.17	0.02	0.33	0.09	0.09	Observed
		0.23	0.06	0.01	0.35	0.14	0.20	Uebel
		0.31	0.14	0.02	0.28	0.15	0.10	Kale
		0.30	0.16	0.02	0.33	0.09	0.10	This work
4.26	0.19	0.07	0.20	0.12	0.21	0.21	0.18	Observed
		0.07	0.06	0.04	0.15	0.34	0.33	Uebel
		0.11	0.14	0.12	0.13	0.36	0.16	Kale
		0.07	0.17	0.12	0.24	0.25	0.16	This work
9.72	0.09	0.02	0.13	0.21	0.16	0.32	0.16	Observed
		0.03	0.04	0.07	0.06	0.42	0.36	Uebel
		0.09	0.05	0.20	0.05	0.43	0.18	Kale
		0.02	0.11	0.20	0.14	0.35	0.18	This work

Table 3.3: Predicted number fraction of MMA-centered triads and pentads, using initial feed ratios  $x_0$ ,  $r_S=0.50$ ,  $r_M=0.45$ , and Alfrey-Mayo kinetics.

$x_0$	$f_M$	$F_{MMM}$	$F_{MMS}$	$F_{SMS}$	$F_{MMMMS} +$								$F_{MSMSS} +$	
					$F_{MMMMM}$	$F_{SMMMM}$	$F_{SMMSM}$	$F_{MSMMM}$	$F_{SSMMM}$	$F_{MSMMS}$	$F_{SSMMS}$	$F_{MSMSM}$	$F_{SSMSM}$	$F_{SSMSS}$
0.09	0.92	0.70	0.27	0.03	0.49	0.19	0.02	0.22	0.01	0.04	0.00	0.02	0.00	0.00
0.29	0.78	0.38	0.47	0.15	0.14	0.18	0.06	0.26	0.04	0.16	0.02	0.11	0.03	0.00
0.66	0.60	0.16	0.48	0.36	0.03	0.08	0.06	0.15	0.05	0.21	0.07	0.20	0.14	0.02
1.15	0.47	0.08	0.41	0.51	0.01	0.03	0.04	0.07	0.04	0.19	0.11	0.21	0.24	0.07
4.26	0.19	0.01	0.17	0.82	0.00	0.00	0.01	0.01	0.01	0.05	0.11	0.08	0.36	0.38
9.72	0.09	0.00	0.08	0.92	0.00	0.00	0.00	0.00	0.00	0.01	0.07	0.03	0.25	0.64

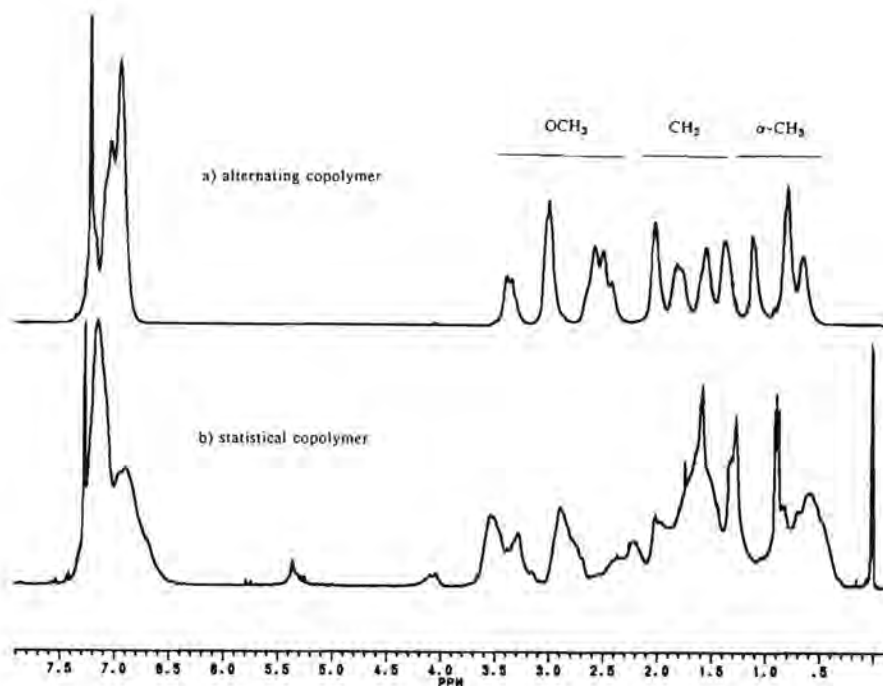


Figure 3.3: a) 600 MHz  $^1\text{H}$  NMR spectrum of an alternating SMMA copolymer in hexachlorobutadiene at 298 K. b) 600 MHz  $^1\text{H}$  NMR spectrum of a low conversion statistical SMMA copolymer in  $\text{CDCl}_3$  at 298 K.

### 3.4 Results and discussion; coisotacticity parameter

A disagreement also occurs in the calculation of the coisotacticity parameter  $\sigma$  from experimental results (Table 3.4), using different sets of equations (see later this section). Uebel<sup>14</sup> has suggested to calculate  $\sigma(=\sigma(a))$  from the ratio of the areas (1- $\sigma$ ) MMS and  $\sigma$  MMS. According to Uebel's assignment, peak I is assumed to consist of approximately coinciding twin resonances of MMM and heterotactic MMS triads, and peak IV is exclusively attributed to the resonance of isotactic MMS. Using the calculated number fraction of MMM triads and the experimentally observed peak areas I and IV the coisotacticity parameter  $\sigma$  according to Uebel<sup>14</sup> can be calculated:

$$f_s = \text{area I} - F_{\text{MMM}} = (1-\sigma) F_{\text{MMS}} \quad (3.6)$$

$$f_{\text{IV}} = \text{area IV} = \sigma F_{\text{MMS}} \quad (3.7)$$

$$\sigma(a) = f_{\text{IV}}/(f_s + f_{\text{IV}}) \quad (3.8)$$

*Table 3A: Various calculated  $\sigma_{SM}$ ;  $\sigma(a)$  calculated from equation 8,  $\sigma(b)$ ,  $\sigma(c)$  and  $\sigma(d)$  from equations 3.12-3.14 respectively, according to Uebel's assignment<sup>14</sup>;  $\sigma(d)$ ,  $\sigma(e)$ ,  $\sigma(f)$  and  $\sigma(g)$  were calculated from equations 3.14, 3.15, 3.16 and 3.18 respectively, according to the assignment of Kale<sup>15</sup>;  $\sigma(h)$  was calculated using a nonlinear least squares procedure based on current assignment.*

$x_0$	$f_M$	Assignment Uebel				Assignment Kale				New assignment
		$\sigma(a)$	$\sigma(b)$	$\sigma(c)$	$\sigma(d)$	$\sigma(e)$	$\sigma(f)$	$\sigma(g)$	$\sigma(h)$	
0.09	0.92	0.50	----	----	----	0.74	0.26	0.46	0.45	
0.29	0.78	0.42	0.80	0.23	0.52	0.76	0.28	0.35	0.41	
0.66	0.60	0.44	0.67	0.19	0.41	0.52	0.35	0.40	0.44	
1.15	0.47	0.53	0.63	0.25	0.43	0.54	0.32	0.42	0.45	
4.26	0.19	0.77	0.63	0.32	0.43	0.54	0.32	0.39	0.44	
9.72	0.09	0.88	0.50	0.24	0.41	0.43	0.38	0.42	0.42	



The results of  $\sigma(a)$  are collected in Table 3.4 for the series of copolymers. The average  $\sigma(a)$  value, considering all the copolymer compositions, except the  $\sigma(a)$  value for  $x_0 = 4.26$  and  $x_0 = 9.72$ , is  $0.47 \pm 0.06$ . The average  $\sigma$  value of the uncorrected peak areas as published in ref. 14 is  $\sigma = 0.63$ , which is also somewhat higher than the values published by other groups<sup>15,18,27</sup>. Using other peak combinations, for example using the SMS triad resonances (Table 3.1), one arrives at:

$$\text{area (II+III)} = (1-\sigma)^2 F_{\text{SMS}} \quad (3.9)$$

$$\text{area V} = 2\sigma(1-\sigma) F_{\text{SMS}} \quad (3.10)$$

$$\text{area VI} = \sigma^2 F_{\text{SMS}} \quad (3.11)$$

in which  $F_{\text{SMS}}$  is the normalized number fraction of SMS triads, and the areas (II+III), V and VI are experimentally observed. The following set of equations is valid:

$$\text{area VI} / \text{area V} = \sigma^2 / 2\sigma(1-\sigma) \longrightarrow \sigma(b) \quad (3.12)$$

$$\text{area (II+III)/area V} = (1-\sigma)^2 / 2\sigma(1-\sigma) \longrightarrow \sigma(c) \quad (3.13)$$

$$\text{area (II+III)} / \text{area VI} = (1-\sigma)^2 / \sigma^2 \longrightarrow \sigma(d) \quad (3.14)$$

All  $\sigma$  values are summarized in Table 3.4. Actually  $\sigma$  should be constant over one copolymer using several calculation procedures. It is obvious from Table 3.4 that the four estimated  $\sigma$  values vary largely over the entire series of copolymers. This cannot only be due to the low accuracy of measuring the very small peak areas (error < 5%). Using the slightly modified assignments of Kale et al.<sup>15</sup>, it can be shown, that the set of equations 3.12-3.14 passes into:

$$\frac{\text{area VI}}{\text{area(IV+V)-MMS+f}} = \frac{\sigma^2}{2\sigma(1-\sigma)} \longrightarrow \sigma(e) \quad (3.15)$$

$$\frac{\text{area (II+III)}}{\text{area(IV+V)-MMS + f}} = \frac{(1-\sigma)^2}{2\sigma(1-\sigma)} \longrightarrow \sigma(f) \quad (3.16)$$

$$\frac{\text{area (II+III)}}{\text{area VI}} = \frac{(1-\sigma)^2}{\sigma^2} \longrightarrow \sigma(d) \quad (3.17)$$

Equation 3.17 is identical to equation 3.14 and therefore also designated as  $\sigma(d)$  and tabulated in Table 3.4 together with  $\sigma(e)$  and  $\sigma(f)$ . Kale et al.<sup>15</sup> have also introduced an alternative method for the calculation of the coisotacticity parameter  $\sigma$ :

$$\begin{aligned} \frac{\text{Area peak X}}{\text{Area peak Y}} &= \frac{(1-\sigma P(S/M))^2}{(2P(S/M)\sigma(1-\sigma P(S/M)))} \\ &= (1/2\sigma P(S/M)) - 1/2 \end{aligned} \quad (3.18)$$

wherein  $P(S/M) = 1/(1+(r_M/x))$ . The series averaged  $\sigma$  value ( $\sigma = \sigma(g) = 0.41$ ). From Table 3.2 and Table 3.4 ( $\sigma(a)-\sigma(d)$ ) and ( $\sigma(d)-\sigma(g)$ ) we may conclude that both, the assignments made by Uebel/Dinan<sup>14</sup> and by Kale/O'Driscoll<sup>15</sup> are not completely correct.

### 3.5 Results and discussion; 2D NOESY NMR

Apparently, the assignments of the resonances in the methoxy region are more complicated than suggested by the above results, possibly as a consequence of the influence of the next neighbour styrene unit on the MMA in the center of the sequence. Therefore, we have performed 2D-NOESY NMR on statistical copolymers to analyse in greater detail, the pentad sequences assuming coisotacticity being present on a triad level.

In the literature<sup>7-15</sup> several assumptions have been made about the assignments in the methoxy region. In order of decreasing importance we mention:

1) Chemical shift differences are due to directly neighbouring styrene units ( $= \alpha$ ) in an M centered sequence. Styrene rings at larger distance (*i.e.* next neighbour) ( $= \beta$ ) contribute considerably less. The coisotactic phenyl rings are assumed to have a greater shielding effect than non-coisotactic rings.

2) Styrene rings with different conformations with respect to the backbone may induce shielding differences.

The first assumption was confirmed by Heffner *et al.*<sup>19</sup> for an alternating S-MMA copolymer. From 2D-NOESY experiments it has been shown that the assignments made for the 1D spectrum were consistent with the cross peaks observed between aliphatic and aromatic parts of the spectrum. In the methoxy region, the upfield resonances ( $\delta=2.2-2.7$  ppm), which are assigned to co-iso SMS triads, indeed give strong cross peaks. The central resonance ( $\delta=2.8-3.10$  ppm), assigned to co-hetero SMS triads give weak cross peaks and the low field resonances ( $\delta=3.2-3.5$  ppm) have no cross peaks at all and therefore these are assigned to co-syndio configuration of the SMS triads.

According the second assumption, Heffner *et al.*<sup>19</sup> invoked non-complete staggering of the backbone to explain their results with dihedral angles of  $-20^\circ$  and  $100^\circ$ . According to the assignment of Kale *et al.*<sup>15</sup>, in a 2D-NOESY spectrum of a statistical SMMA copolymer one would expect three cross peaks between the styrene and the methoxy regions:

2.10-2.50	—————>	co-isotactic SMS triad	(strong)
2.50-2.78	—————>	co-hetero SMS triad	(weak)
2.78-2.95	—————>	co-isotactic SMM triad	(weak)

Prior to recording the 600 MHz 2D NOESY spectrum of the statistical SMMA copolymer, we reproduced the 2D NOESY spectrum of alt-SMMA as published by Heffner<sup>19</sup>, to make sure that the differences in recording conditions between our spectra and those of Heffner *et al.*<sup>19</sup> do not interfere with the interpretation of the results of the statistical copolymer.

The spectra were recorded under the same conditions as in ref. 19 apart from the field strength and sample concentration (see experimental section). Lower sample concentrations were used in order to diminish the intermolecular interactions which could lead to too many cross peaks in the NOESY spectrum. But sample concentrations of 10% and 2% give identical results. As expected, the spectra of the alternating copolymer recorded with a mixing time of  $\tau_m=300$  ms do not show all of the NOE interactions (Fig. 3.4a). This could be due to

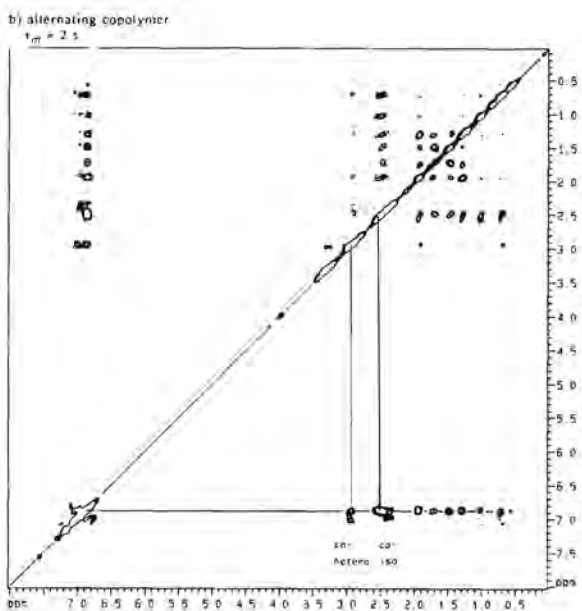
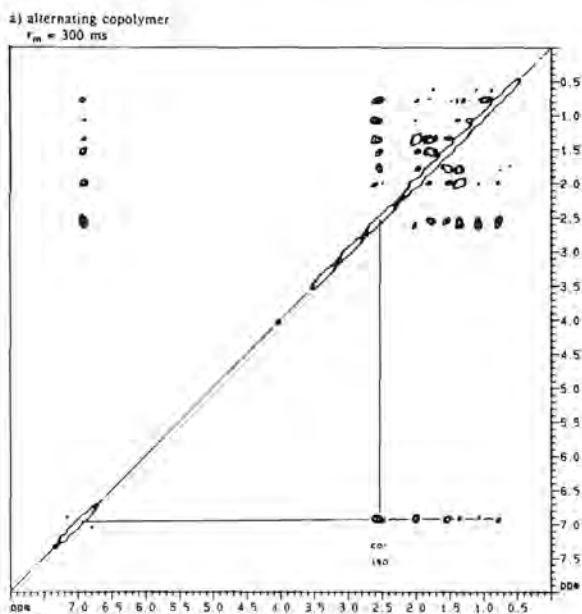


Figure 34: Contour plot of two NOESY experiments (600 MHz), of the alternating SMMA copolymer using mixing times of a) 300 ms, and b) 2 s.

differences in  $T_1$  between our sample and Heffner's. Also different contour levels show no more cross peaks. The  $T_1$  values of several peak groupings were measured and are tabulated in Table 3.5. From this table it appears that with a mixing time of 300 ms only the aliphatic  $\text{CH}_3$  and  $\text{CH}_2$  protons could have optimal NOE contacts (Fig. 3.4a). For the methoxy region, with  $T_1$ 's of about 800-900 ms, a mixing time of at least 1 s is necessary. This can be seen in Figure 3.4b, where the NOE contacts of the methoxy protons with the aromatic protons are optimal and those of the  $\text{CH}_3$  and  $\text{CH}_2$  protons are losing intensity. The diagonal of the 2D spectrum corresponds with the 1D spectrum as shown in Figure 3.3a.

For the statistical SMMA copolymer almost the same  $T_1$  values are observed (Table 3.5). At present, it is not completely clear what causes the difference in relaxation behaviour between our samples and that of Heffner. An explanation could be that our polymers have larger molecular weights. This would result in a decreased overall mobility for a given concentration and thus in larger  $T_1$ -values. With our polymers we have to perform at least two experiments with different mixing times to see all NOE contacts for one copolymer. Figures 3.5a and 3.5b show the phase sensitive NOESY spectra of a statistical SMMA ( $f_M = 0.47$ ) copolymer with mixing times of 300 ms and 2 s, respectively. Instead of the expected three cross peaks between the  $\text{OCH}_3$  and styrene resonances, we now observe five cross peaks:

- |    |               |             |   |
|----|---------------|-------------|---|
| 5) | 2.20-2.45 ppm | → strong    | ( $\sigma^2$ SMS)   |
| 4) | 2.70-2.78 ppm | → weak      | ( $2\sigma(1-\sigma)$ SSMSS)  |
| 3) | 2.78-2.95 ppm | → medium    | ( $\sigma(\text{MSMMM} + \text{MSMMS}) +$<br>$2\sigma(1-\sigma)(\text{MSMSM} + \text{SSMSM})$ ) |
| 2) | 3.15-3.25 ppm | → very weak | ( $\sigma$ SSMMM)   |
| 1) | 3.30-3.40 ppm | → very weak | ( $\sigma$ SSMSM)   |

This is only compatible with several pentads rather than triads having different chemical shifts induced by phenyl rings in next neighbour position (B).

Table 3.5: Spin lattice relaxation time  $T_1$  in ms measured by inversion recovery of alternating and statistical ( $f_M=0.47$ ) copolymers, for several proton regions. The 600 MHz  $^1\text{H}$  NMR spectra were recorded at 353 K and sample concentration was 2% (w/v) in hexachlorobutadiene.

Region (ppm)	$T_1$ alt SMMA (ms)	$T_1$ statis. SMMA (ms)
Aromatic protons (ca.7)	ca.900	900 - 1100
$\text{OCH}_3$		
X (2.95-3.70)	700	800-900
Y (2.50-2.95)	700	900
Z (2.10-2.50)	600	600
$\text{CH}_2$ (1.20-2.10)	325	325
$\text{CH}_3$ (0.50-1.20)	350	300

Along these lines we can conclude that several pentad resonances have to be reassigned. The new mixed assignment of compositional pentad sequences and configurational sequence placement (on a triad level) tacticity is given in Table 3.1. This new assignment is based on several observations:

- MMM resonates at  $\delta=3.6$  ppm and depicts no tacticity splitting. Pentads such as SMMMM or SMMMS may resonate slightly upfield with regard to MMM because of shielding by aromatic rings but these sequences are still assumed to resonate at peak I.

- Alternating pentads will resonate at the same position as the alternating copolymer; *i.e.* syndiotactic MSMSM coincides with peak I, similarly, heterotactic MSMSM (crosspeak 3 Fig. 3.5) with peak IV, and isotactic MSMSM with peak VI.

- Phenyl rings in next neighbour position ( $\beta$ ) give significant shielding effects, syndio- and heterotactic SSMSM and SSMSS sequences will resonate at higher field in this order. For example peak II is assigned to syndiotactic MSMSM and SSMSM sequences, and peak III to the syndiotactic SSMSS

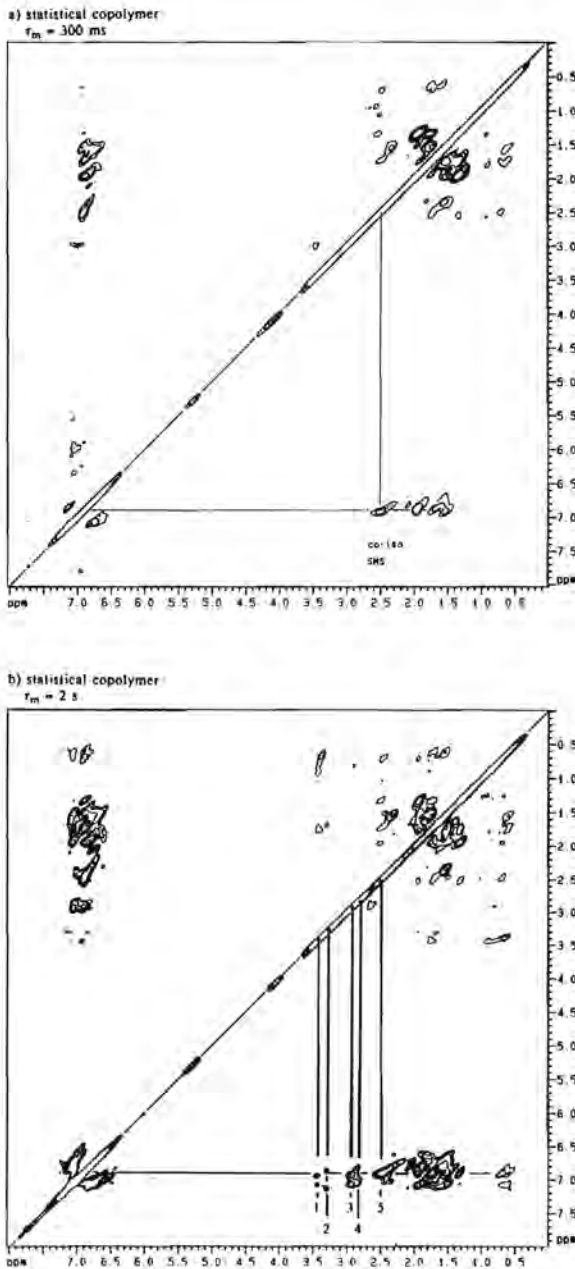


Figure 3.5: Contour plot of two NOESY experiments (600 MHz), of a statistical low conversion solution SMMA copolymer ( $f_M=0.47$ ), using mixing times of a) 300 ms, and b) 2 s; (1)= $\sigma$ SSMMS, (2)= $\sigma$ SSMMM, (3)= $\sigma$ (MSMMM + MSMMMS) +  $2\sigma(1-\sigma)$ (MSMSM + SSMSM), (4)= $2\sigma(1-\sigma)$ SSMSS, and (5)=  $\sigma^2$ SMS.

pentad, according to the assignment of Uebel<sup>14</sup>.

Heterotactic SSMSM and MSMSM are assigned to peak IV (cross peak 3 Fig. 3.5), and heterotactic SSMSS to peak V (cross peak 4 Fig. 3.5).

- The shift effects are not significant for isotactic SSMSM and SSMSS, but in peak VI we can distinguish three parts of isotactic pentads (a) MSMSM, (b) SSMSM, and (c) SSMSS (Figure 3.2 and cross peak 5 Fig 3.5).

- Only the two cross peaks at lower field must be due to a coisotactic configuration which has a deshielding effect; possible triads are isotactic MMS and heterotactic SMS. We assume that isotactic SSMMM and isotactic SSMMS with deshielding effects resonate at  $\delta=3.20$  ppm and  $\delta=3.35$  ppm (crosspeak 2 and 1 Fig. 3.5), respectively. These resonances both appear in peak II.

- The remaining pentads have been assigned in the same way following the two assumptions as mentioned earlier, but the concentrations of some of the pentads are very low thus somewhat complicating the assignments. Assignments based solely on the agreement between the observed and predicted distributions should be considered tentative because they are not unique. The results of assigning these pentads are given in Table 3.1. From Table 3.2 it can be seen that over the whole range of copolymers all relative peak areas agree satisfactorily with the experimentally observed peak areas. Even for copolymers with higher styrene contents no discrepancies are observed in peak I, II, IV, and V.

In order to estimate  $\sigma$  in a reliable manner, the coisotactic tacticity parameter was fitted to the six equations corresponding to the six peak areas, using a non-linear least squares procedure, where  $\sum((a_{\text{calc}} - a_{\text{meas}})/a_{\text{meas}})$  was minimized for each copolymer. In the latter expression  $a_{\text{meas}}$  is the experimentally observed peak area (Table 3.4), and  $a_{\text{calc}}$  is the calculated peak area using the theoretically calculated pentads (Table 3.3) and the current peak assignments. The resulting value,  $\sigma(h) = 0.44 \pm 0.03$  predicts all six peak areas based on theoretical pentads within 5% error. The inaccuracy determining the peak areas from the NMR spectra is about 8%. The present results should enable us to analyse <sup>1</sup>H NMR spectra of higher conversion solution and emulsion copolymers of styrene and methyl methacrylate.



### 3.6 Conclusion

The 2D NOESY spectrum of a statistical SMMA copolymer ( $f_M=0.47$ ) enables us to draw a number of conclusions regarding the methoxy proton assignments. It shows that the complex peak grouping in the methoxy region is sensitive to pentad sequences rather than triads. The new peak assignments proposed in this paper show a satisfying agreement between experimental and theoretical peak areas over a wide range of copolymer compositions, based on the ultimate copolymerization model and a constant, best-fitting average coisotacticity parameter  $\sigma=0.44$ .

## References

1. Koenig J.L., "Chemical Microstructure of Polymer Chains", Wiley, New York, 1980.
2. Frisch H.L., Mallows G.L., Heathly E, Bovey EA. *Macromolecules*, 1, 553, 1968.
3. Harwood H.J., "Problems in Aromatic Copolymer Structure in Natural and Synthetic High Polymers", Vol. 4, 'NMR' (Ed. P. Diehl), Springer-Verlag, Berlin, 1970.
4. Pichot C.H., Llauro M., Pham Q., *J. Polym. Sci. Polym. Chem. Ed.*, 19, 2619, 1981.
5. Tacx J.C.J.F., Velden v.d. G.P.M., and German A.L., *J. Polym. Sci., Polym. Chem. Ed.*, 26, 1439, 1988.
6. Doremaele v. G., German A.L., Vries de N.K., Velden v.d. G.P.M., *Macromolecules*, 23, 4206, 1990.
7. Ito K. and Yamashita Y., *J. Polym. Sci., Part B*, 3, 625, 1965.
8. Ito K., Iwase S., Umehara K., and Yamashita Y., *J. Macromol. Sci.*, A1, 891, 1967.
9. Yamashita Y., Ito K., *Appl. Polym. Symp.*, 8, 245, 1969.
10. Ito K., Yamashita Y., *J. Polym. Sci., Part B*, 6, 22, 1968.
11. Bovey EA., *J. Polym. Sci.*, 62, 197, 1962.
12. Harwood H. J. and Ritchey W. M., *J. Polym. Sci., Part B*, 3, 419, 1965.
13. San Roman J., Madruga E.L., Del Puerto M.A., *Angew. Makromol. Chem.*, 78, 1293, 1978.
14. Uebel J.J. and Dinan E.J., *J. Polym. Sci., Polym. Chem. Ed.*, 21, 2427, 1983.
15. Kale L.T., O'Driscoll K.F., Dinan E.J., Uebel J.J., *J. Polym. Sci., Part A.*, 24, 3145, 1986.
16. Hirai H., Tanabe T., Koinuma H., *J. Polym. Sci., Polym. Chem. Ed.*, 17, 843, 1979.
17. Gotoh Y., Hirai H., "Current Topics in Polymer Science", Vol. I, (Ed. Ottenbrite R. M., Utrachi D.L., Inoue S.), Hauser Publishers, 151- 167, 1978
18. Niknam M.K., Univ. of Akron, Akron, Ohio, USA (1985), *Diss. Abstr. Int. B.*, 1985, 46 (4) 1196. Avail. Univ. Microfilms, Int. Order No. DA 85 13339
19. Heffner S.A., Bovey EA., Verge L.A., Mirau P.A., Tonelli A.E., *Macromolecules*, 19, 1628, 1986.
20. Fukuda T., Ma Y-D., Inagaki H., *Macromolecules*, 18, 17, 1985
21. O'Driscoll K.F. and Davis T.P., *J. Polym. Sci., Part C: Polym. Letters*, 27, 417, 1989.
22. Tanabe T., Koinuma H., Hirai H., *J. Polym. Sci. Polym. Chem. Ed.*, 19, 3293, 1981.
23. States D.J., Haberkorn R.A., Ruben D.J., *J. Magn. Res.*, 48, 286, 1982.

24. Jeener J., Meier B.H., Bachmann P, Ernst R.R., *J. Chem. Phys.*, 71, 4546, 1979.
25. Macura S., Ernst R.R., *Mol. Phys.*, 41, 95, 1980.
26. Kelen T. and Tüdös F, *J. Macromol. Sci.*, 9, 1, 1975.
27. Jenkins A.D. and Rayner M.G., *Eur. Polym. J.*, 8, 221, 1972.



## Chapter 4

# Proton and Carbon NMR Spectra of Alternating and Statistical Styrene Methyl Methacrylate Copolymers Revisited

**ABSTRACT:** The  $\alpha$ -methyl proton NMR resonances of the three different configurational methyl methacrylate centered triad sequences of the alternating styrene-methyl methacrylate (SMMA) copolymers have been reassigned. Literature assignments are inconsistent with data and each other. Selective decoupling experiments were carried out in the present study to assign the carbon NMR resonances of the  $\alpha$ -methyl groups of alternating styrene-methyl methacrylate copolymers. Subsequently, the carbon resonances of the aromatic C1 and  $\alpha$ -methyl literature assignments of the statistical SMMA copolymers have been reconsidered and reassigned in terms of configurational triad sequences.

### 4.1 Introduction

As already mentioned in Chapter 3, the determination of the intramolecular (sequence distribution and tacticity) and intermolecular (chemical composition molar mass distribution) chain structure of copolymers is of great importance because it supplies information regarding the polymerization processes.<sup>1,2,3</sup> Further, the molecular microstructure may supply information about the monomer addition process, *e.g.* about the preference of monomers to add in coiso- or cosyndiotactic configurations. One of the techniques which has been very effective in the determination of the average copolymer composition and of the intramolecular microstructure of

copolymers is high-resolution Nuclear Magnetic Resonance (NMR). One of the most important systems of interest in copolymerization studies is the Styrene-Methyl Methacrylate (SMMA) copolymer. These copolymers have been extensively studied by proton NMR (see reference 3 and references cited therein). The result of these studies is that the analysis of sequence distribution is possible, although rather complicated due to sensitivity towards pentad sequences in the methoxy region.

Another possibility for analysing sequence distributions is carbon-13 NMR. The carbon NMR spectra of statistical copolymers of Styrene-Methyl Methacrylate have been investigated by Katritzky *et al.*<sup>4</sup> in 1974 and by Kato *et al.*<sup>5</sup> in 1975. It was shown that in carbon NMR not only a splitting in the carbonyl, quaternary, methoxy and  $\alpha$ -methyl carbons in the MMA-centered unit occurs, but also in the aromatic C1 and methine carbons in the S-centered unit. Therefore, carbon NMR made it possible to determine simultaneously MMA centered and S centered stereosequences.<sup>4,5,6</sup>

Katritzky and Kato independently developed an assignment for the aromatic C1 resonance and the  $\alpha$ -methyl main chain carbon resonance.<sup>4,5</sup> The assignments of the aromatic C1 and  $\alpha$ -methyl carbon resonance by Katritzky<sup>4</sup> and Kato<sup>5</sup> are, however, reversed. Hirai *et al.*<sup>7</sup> pointed out this problem, and confirmed that the Kato assignment (*e.g.* of the aromatic C1) is the correct one, and showed that the assignments pertaining to the alternating structural parts in the carbon NMR spectra of the statistical SMMA copolymers are in agreement with the carbon NMR spectra of fully alternating SMMA copolymers. The triplet peaks in the NMR spectra of the alternating copolymer of the SMS (methoxy protons) or MSM (C1 carbon) triads were assigned as cosyndiotactic, coheterotactic and coisotactic configuration in order of increasing shielding. This assignment was substantiated by comparison of the NMR peak areas of several carbons with the peak areas of the methoxy proton NMR signals of several alternating copolymers made with different kinds of Lewis acids,<sup>7,8</sup> and by the combined use of partly relaxed NMR signals and selective decoupling NMR techniques. Another ambiguity also exists in the literature: the tacticity splitting of the SMS triad of the  $\alpha$ -methyl carbon resonance in the alternating SMMA copolymer seems to have the same order

of shielding as the aromatic C1,<sup>9</sup> but in the proton NMR assignment the reverse situation has been suggested.<sup>10</sup> Although these assignments in the proton NMR spectra are seemingly confirmed by calculations,<sup>10</sup> the 2D NOESY (two dimensional Nuclear Overhauser Effect Spectroscopy) experiments of Heffner<sup>11</sup> showed that this is impossible: a cross peak exists between  $\alpha$ -methyl and the aromatic proton signals at lower field. Notwithstanding these contradictions in the assignments, up to now the assignments and the conclusions of Katritzky *et al.*<sup>4</sup> and of Hirai *et al.*<sup>7</sup> are both used in literature indiscriminately.<sup>9,12</sup>

In this chapter the following topics are discussed. First, the  $\alpha$ -methyl resonances in both the proton and carbon NMR spectra of the alternating copolymers will be discussed, and secondly, the carbon resonances of the aromatic C1 and  $\alpha$ -methyl carbon of the statistical copolymers.

## 4.2 Experimental section

### *Materials*

The monomers styrene (S) and methyl methacrylate (MMA) (Merck) were distilled at reduced pressure under nitrogen. The middle fraction of the distillate was collected and used. 2,2'-Azobis(isobutyronitrile) (AIBN) p.a. purchased from Fluka was recrystallized once from methanol.

### *Alternating copolymer.*

The preparation of the alternating copolymer has been described in reference 3

### *Statistical copolymers*

The SMMA copolymers were synthesized in bulk at 313 K in a 100 ml glass vessel. The solution was degassed and the polymerization took place under nitrogen atmosphere. The initiator (AIBN) concentration was approximately  $2 \times 10^{-2}$  mol/l. To isolate and purify the copolymer, the reaction mixture was poured into a 10-fold excess of cold heptane. The total conversion was determined by means of solid weight and was always less than 3 %.

## NMR

Proton NMR spectra were recorded with a 400 MHz (Bruker AM 400) spectrometer at 298 K, using  $\text{CDCl}_3$  as solvent and locking agent. The spectra were obtained using a spectral width of 6024 Hz, an acquisition time of 2.7 s, a flip angle of  $45^\circ$  and a pulse delay of 5 s. Spectra were obtained after accumulating 32 scans. The digital resolution amounted to 0.38 Hz, corresponding to a data length of 32 K.

The carbon NMR spectra were recorded at 100 MHz with the same spectrometer. The sample concentration was 10% (w/v) in  $\text{CDCl}_3$ . The spectra were obtained accumulating 8000 scans with a digital resolution of 1.526 Hz/point, corresponding to a spectral width of 25000 Hz and a data length of 32 K. The flip angle and the pulse delay were  $45^\circ$  and 4 s respectively. Monomer sequence placements were determined by comparing the relative peak areas of the carbon atoms involved. In performing quantitative NMR measurements via compositional or configurational sequence placements one must take into account difference in nuclear Overhauser effects (NOE) and spin-lattice relaxation times ( $T_1$ ). No NOE or  $T_1$  values have initially been determined, but an additional  $^{13}\text{C}$  NMR experiment was performed on one sample with a much longer delay (15s) and gating off the decoupler to remove the NOE. The results were identical with those obtained via  $^{13}\text{C}$  NMR with the standard method. Within these limits relative peak areas are proportional to the numbers of carbon atoms involved. Peak areas were determined via planimeter methods.

The alternating copolymer was dissolved in hexachloro-1,3-butadiene and benzene- $d_6$  as lock at 353 K. With this solvent a better resolution was achieved in the proton NMR spectra, in contrast to the carbon NMR spectra. (Figure 4.1 and *cf.* Figure 4.4a and 4.5a).

Selective proton decoupling was used to correlate the proton NMR signals of the  $\alpha$ -methyl groups with the corresponding carbon NMR signals. Typical spectra are shown in Figure 4.4. Typically, 15000 scans were accumulated (pulse interval time 4 s) for three different values of the proton irradiation frequencies (with reduced power by a factor of ca. 3 with respect to the broadband case). The irradiation frequencies are given in the text (par.4.3.2.b).



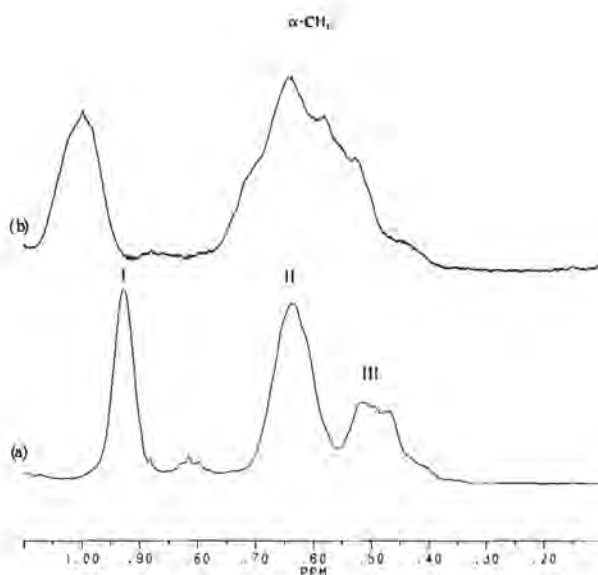


Figure 4.1: Expanded proton NMR spectra of the  $\alpha$ -methyl resonances of the alternating copolymer (a) in hexachloro-1,3-butadiene and (b) in  $CDCl_3$ .

### 4.3 Results and discussion; Alternating SMMA copolymers

In the next paragraphs we discuss first the proton NMR spectra of the alternating copolymers (methoxy protons and  $\alpha$ -methyl protons) and subsequently their carbon NMR spectra. Only the aromatic C1 and the  $\alpha$ -methyl carbon resonances are described because these resonances are the most interesting ones in the statistical SMMA copolymers, since they can be analysed as a combination of comonomer sequence distributions and different configurational situations. Note that the terminologies (between brackets) of the peak signals are mostly taken from literature and where in some cases the terminologies were slightly adapted ( $X'$  for  $X$ ) in order to avoid the use of one symbol for more than one purpose, and are as follows. For the methoxy protons ( $X$ ,  $Y$ ,  $Z$ ), the  $\alpha$ -methyl protons (I, II, III), the C1 carbon ( $X'$ ,  $Y'$ ,  $Z'$ ), and the  $\alpha$ -methyl carbon (I', II', III').

### 4.3.1 Proton NMR

The proton NMR spectra of alternating copolymers have been investigated by several groups,<sup>7,9,10,11</sup> in particular with respect to the methoxy protons (summarized in paragraph 4.3.1.a) and the  $\alpha$ -methyl protons (discussed in paragraph 4.3.1.b).

#### a) methoxy protons

It is clearly shown in the literature that the methoxy proton NMR signals are split into three peaks ( $\delta = 3.5 - 2.2$  ppm), designated X, Y, and Z, where X corresponds to the syndiotactic, Y to the heterotactic and Z to the isotactic configuration<sup>7,9,10,11</sup> (Figure 3.3a and Table 4.1). That this assignment is correct, is clearly demonstrated by Heffner *et al.*<sup>11</sup> by 2D-NOESY NMR spectra where dipole-dipole interactions between methoxy protons and phenyl protons result in a cross peak. Peak Y yields a weak cross peak (heterotactic) and peak Z yields a strong cross peak (isotactic). In Figure 4.2, the three different configurations of the SMS triad are shown. Because of the shielding effects by the aromatic ring, the methoxy protons in the meso configuration are shifted to higher field.

Table 4.1: Proton methoxy and  $\alpha$ -methyl assignments of alternating SMMA copolymers, and where  $\sigma = \sigma_{\text{m}}$  coisotacticity parameter.

	OCH <sub>3</sub>		
	X (3.5-3.2 ppm)	Y (3.0-2.8 ppm)	Z (2.7-2.2 ppm)
literature <sup>11</sup>	$(1-\sigma)^2$ SMS	$2\sigma(1-\sigma)$ SMS	$\sigma^2$ SMS
	$\alpha$ -CH <sub>3</sub>		
	I (1.0-0.85 ppm)	II (0.8-0.65 ppm)	III (0.6-0.5 ppm)
literature <sup>11</sup>	$\sigma^2$ SMS	$2\sigma(1-\sigma)$ SMS	$(1-\sigma)^2$ SMS
this work	$(1-\sigma)^2$ SMS	$2\sigma(1-\sigma)$ SMS	$\sigma^2$ SMS

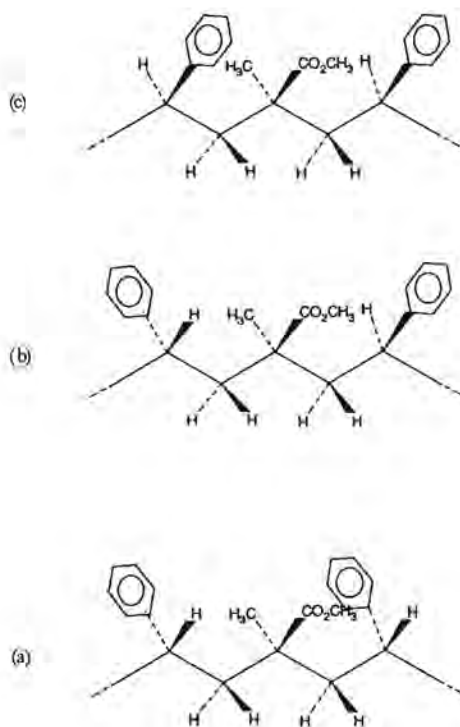


Figure 4.2: Various configurations of the SMS triad, (a) syndiotactic, (b) heterotactic, and (c) isotactic.

#### b) $\alpha$ -methyl protons

The assignments of the  $\alpha$ -methyl proton resonances are also given in the literature<sup>7,10,11</sup>; the three peaks, in order of increasing shielding are assigned to isotactic, heterotactic and syndiotactic (I ( $\delta=0.95$ ), II ( $\delta=0.65$ ), and III ( $\delta=0.5$ ) respectively, Table 4.1). The assignments are based on the assumption that if styrene rings are in meso conformation with respect to the  $\alpha$ -methyl protons (Figure 4.2, syndiotactic), then the latter group consequently resonates at higher field. The assignment of Koinuma *et al.*<sup>10</sup> results from a theoretical concept, based on simple ring current calculations. However, this assignment has never

been proved by experiment. On the other hand, the 2D NOESY experiment published by Heffner *et al.*<sup>11</sup> (used for assigning the methoxy and methylene protons) can also be used for assigning the  $\alpha$ -methyl protons. In the racemic configuration (denoted as isotactic) of the styrene rings and the  $\alpha$ -methyl protons (Figure 4.2) no cross peaks can occur because there are no measurable dipole-dipole interactions between the protons of the respective groups. A weak and a strong cross peak is expected in the heterotactic and syndiotactic configuration, respectively. As mentioned before the  $\alpha$ -methyl group is split into three peaks ( $\delta=0.95$ , 0.65 and 0.5 ppm). According to the assignments of Koinuma<sup>10</sup> and Hirai,<sup>7</sup> one would expect cross peaks at higher fields ( $\delta=0.7$  and  $\delta=0.5$  ppm) but not at low field ( $\delta=0.95$  ppm), which is clearly in contrast with the observations in Figure 3 of reference 11. Therefore, the assignments of the alternating SMS triad in the existing literature<sup>10</sup> are incorrect. This means that the assignment of the  $\alpha$ -methyl protons should be in the reversed order as published in the literature (Table 4.1). The reason for this deshielding effect is already mentioned in the text of Heffner *et al.*,<sup>11</sup> a given proton may be very close to the ring but on the periphery of the shielding cone or actually in the deshielding region. It can be correctly deduced<sup>11</sup> from the deshielding that the three  $\alpha$ -methyl peaks should be assigned as cosyndiotactic, coheterotactic, and coisotactic in order of increasing shielding. Hence, the new assignments are given (Table 4.1).

### 4.3.2 Carbon NMR

The carbon NMR spectra of alternating copolymers have previously been studied.<sup>7,9,11,13</sup> Several carbon NMR resonances of the styrene-centered and of the MMA-centered triads are split due to tacticity effects.<sup>7</sup> Figure 4.3 shows a 100 MHz carbon NMR spectrum of an alternating copolymer. The carbonyl, quarternary, methoxy,  $\alpha$ -methyl carbons in MMA and the aromatic C1 and the methine carbons in S show induced splitting because of different tacticities. Here, only the aromatic C1 resonances are summarized and the  $\alpha$ -methyl carbon resonances are discussed.

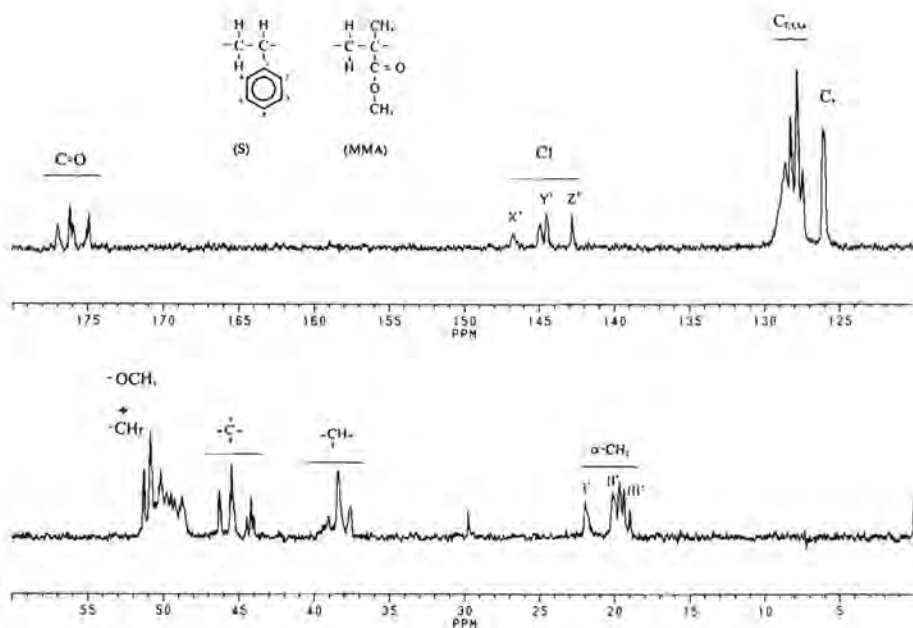
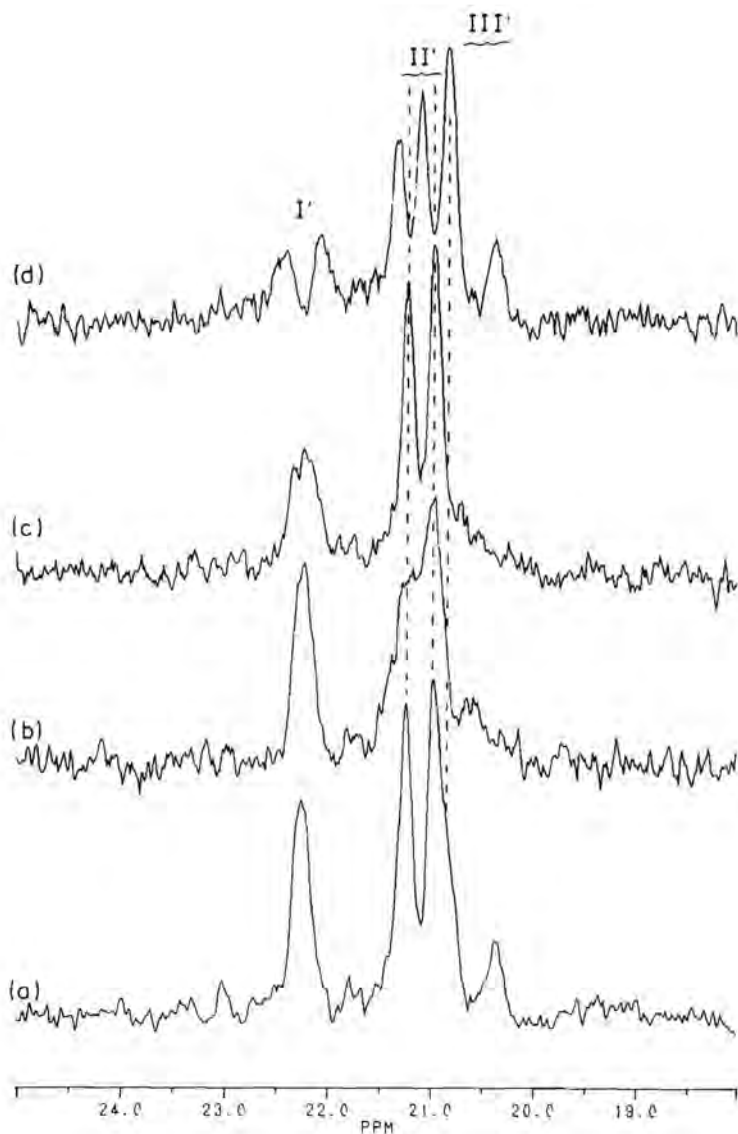


Figure 4.3: 100 MHz carbon-13 NMR spectrum of an alternating SMMA copolymer in  $\text{CDCl}_3$  at 298 K.

#### a) C1 carbon

The three groups of signals of the C1 carbon in the alternating copolymer are designated X', Y' and Z' ( $\delta = 148 - 143$  ppm, Figure 4.3). These peaks are assigned to cosyndiotactic, coheterotactic and cosyndiotactic configurations, respectively (Table 4.2). Hirai *et al.*<sup>7</sup> analysed several alternating copolymers made by using various metal halides as catalysts. The relative signal areas of the three different configurations varied with the metal halides used (see also '4.1 Introduction'). The assignments of the C1 and other carbons (except  $\alpha$ -methyl) are based on comparisons of the relative NMR peak intensities of the C1 carbon with the relative NMR peak intensities of the methoxy protons. These assignments of the methoxy carbon NMR signals were justified by the combined use of partly relaxed NMR signals and selective decoupling experiments.<sup>7</sup>



**Figure 44:** Expanded 100 MHz carbon-13 NMR spectra of an alternating SMMA copolymer in hexachloro-1,3-butadiene at 353 K (a) broadband decoupled, (b) selective decoupling of peak III (Figure 4.1), (c) selective decoupling of peak II (Figure 4.1), and (d) selective decoupling of peak I (Figure 4.1).

b)  $\alpha$ -methyl carbon

In contrast to the carbonyl, quaternary, methoxyl carbons in MMA and the aromatic C1 and methine carbons in styrene, no obvious assignments of the  $\alpha$ -methyl carbons exist, although a clear peak splitting can be observed at stronger magnetic fields (Figure 4.3 and 4.5a, peak I', II' and III'). There exists an assignment for the  $\alpha$ -methyl group originating from the thesis of Niknam<sup>9</sup> albeit without any justification, (see Table 4.2). As is apparent from previous paragraph 4.3.1.b, containing the correct assignment for the  $\alpha$ -methyl protons, justification of the assignments of the  $\alpha$ -methyl carbon can be achieved by selective decoupling experiments. These experiments were carried out in the present investigation and are shown in Figure 4.4. Figure 4.4a is a broadband decoupled carbon NMR spectrum of an alternating SMMA copolymer in hexachloro-1,3-butadiene at 353 K. A comparison of Figures 4.4a and 4.5a, shows that there exists a strong solvent effect: the induced splitting in hexachloro-1,3-butadiene is not as clear as in chloroform. We assume that the order of the peaks is the same for both solvents. The solvent hexachloro-1,3-butadiene is preferred because a better splitting in the  $\alpha$ -methyl proton NMR

Table 4.2: Carbon C1 and  $\alpha$ -methyl assignments of alternating SMMA copolymers, and where  $\sigma = \sigma_{sm}$  = coisotacticity parameter.

	X' (148.0-147.0 ppm)	C1 Y' (145.5-144.5 ppm)	Z' (144.0-143.0 ppm)
Hirai <sup>7</sup>	$(1-\sigma)^2$ MSM	$2\sigma(1-\sigma)$ MSM	$\sigma^2$ MSM
Niknam <sup>9</sup>	$(1-\sigma)^2$ MSM	$2\sigma(1-\sigma)$ MSM	$\sigma^2$ MSM

	I' (22.8-22.0 ppm)	$\alpha$ -CH <sub>3</sub> II' (21.0-20.2 ppm)	III' (20.2-19.8 ppm)
Hirai <sup>7</sup>	-	-	-
Niknam <sup>9</sup>	$(1-\sigma)^2$ SMS	$2\sigma(1-\sigma)$ SMS	$\sigma^2$ SMS
This work	$\sigma^2$ SMS	$2\sigma(1-\sigma)$ SMS	$(1-\sigma)^2$ SMS

signals is obtained (Figure 4.1). In experiment 4.4d (Figure 4.4) the protons of peak I ( $\delta = 0.95$  ppm) are irradiated resulting in a narrowing of the carbon-13 NMR shoulder at  $\delta = 20.8$  ppm and the signal peak at  $\delta = 20.4$  ppm.

In experiment 4.4c the protons of peak II ( $\delta = 0.65$  ppm) and in experiment 4.4b the protons of peak III ( $\delta = 0.5$  ppm) are irradiated. Summarizing, the experiments in Figure 4.4 showed that the order in which the carbon-13 NMR signals appear is the converse of that for the proton NMR signals (Table 4.2).

At this stage we know the assignments of the carbon NMR resonances of the aromatic Cl (MSM triads) and of the  $\alpha$ -methyl (SMS triads) of the alternating copolymers, which is a prerequisite for assigning the carbon resonances of the statistical SMMA copolymers.

#### 4.4 Results and discussion; Statistical SMMA copolymers

In the alternating SMMA copolymers, there exist only three different configurations of the SMS triad and three different configurations of the MSM triad. The number of sequences in statistical SMMA copolymers clearly exceeds that in alternating copolymers. For this reason and because of the indiscriminate use of contradicting assignments (see paragraph 4.1 Introduction), the following discussion is necessary rather than elaborate.

In statistical copolymers a total of twenty configurational sequences occur, *i.e.* for the MMA-centered triads the ten following tacticity coefficients and sequences are possible:

$\sigma_{mm}^2$  MMM,  $2\sigma_{mm}(1-\sigma_{mm})$  MMM, and  $(1-\sigma_{mm})^2$  MMM for the MMM sequence,  $\sigma_{mm}\sigma_{ms}$  MMS,  $(1-\sigma_{mm})\sigma_{ms}$  MMS,  $\sigma_{mm}(1-\sigma_{ms})$  MMS, and  $(1-\sigma_{mm})(1-\sigma_{ms})$  MMS for the MMS or SMM sequences and,  $\sigma_{ms}^2$  SMS,  $2\sigma_{ms}(1-\sigma_{ms})$  SMS,  $(1-\sigma_{ms})^2$  SMS for the SMS sequences.

Here  $\sigma$  is the probability that two adjacent monomeric units have a meso configuration (isotactic). Similar configurational sequences are present for the



styrene-centered triads. The coisotacticity  $\sigma_m$  is calculated from the methoxy region in the proton NMR spectrum to be 0.44.<sup>34</sup> The other tacticities  $\sigma_{mm}$  and  $\sigma_m$  are taken from the carbon NMR spectra of the homopolymers: 0.23<sup>15</sup> and 0.29,<sup>16</sup> respectively. The terminologies (between brackets) of the peak signals for the statistical copolymers are as follow: the C1 carbon (X'', Y'', Z'') and the  $\alpha$ -methyl carbon (A, B, C, D).

#### 4.4.1 Proton NMR

The proton NMR spectra of statistical SMMA copolymers are well resolved for the methoxy protons<sup>34</sup>; the complex peak grouping in the methoxy region is sensitive to MMA-centered pentad sequence distributions and cotacticity on triad level as shown in Chapter 3. The  $\alpha$ -methyl proton region could not be assigned to sequence distributions and tacticities because of the unresolved peaks (Figure 3.3b).

In what follows we examine the carbon NMR spectra of the statistical copolymers, using the assignments of the alternating SMMA copolymers and both homopolymers polystyrene and polymethyl methacrylate. The aim of this work is to overcome some of the limitations described above for proton NMR, namely to develop a method whereby triad sequence distributions can be experimentally determined for SMMA copolymers utilizing carbon NMR.

#### 4.4.2 Carbon NMR

Figure 4.5 (c-e) show typical 100 MHz carbon NMR spectra of statistical SMMA copolymers of different copolymer composition, of the aromatic C1 region ( $\delta = 148-143$  ppm) and the  $\alpha$ -methyl region ( $\delta = 25-15$  ppm). It appears from this Figure 4.5(a-e) that the carbon resonances of statistical SMMA show additional splittings due to comonomer sequence distributions and configurational effects.<sup>45</sup>

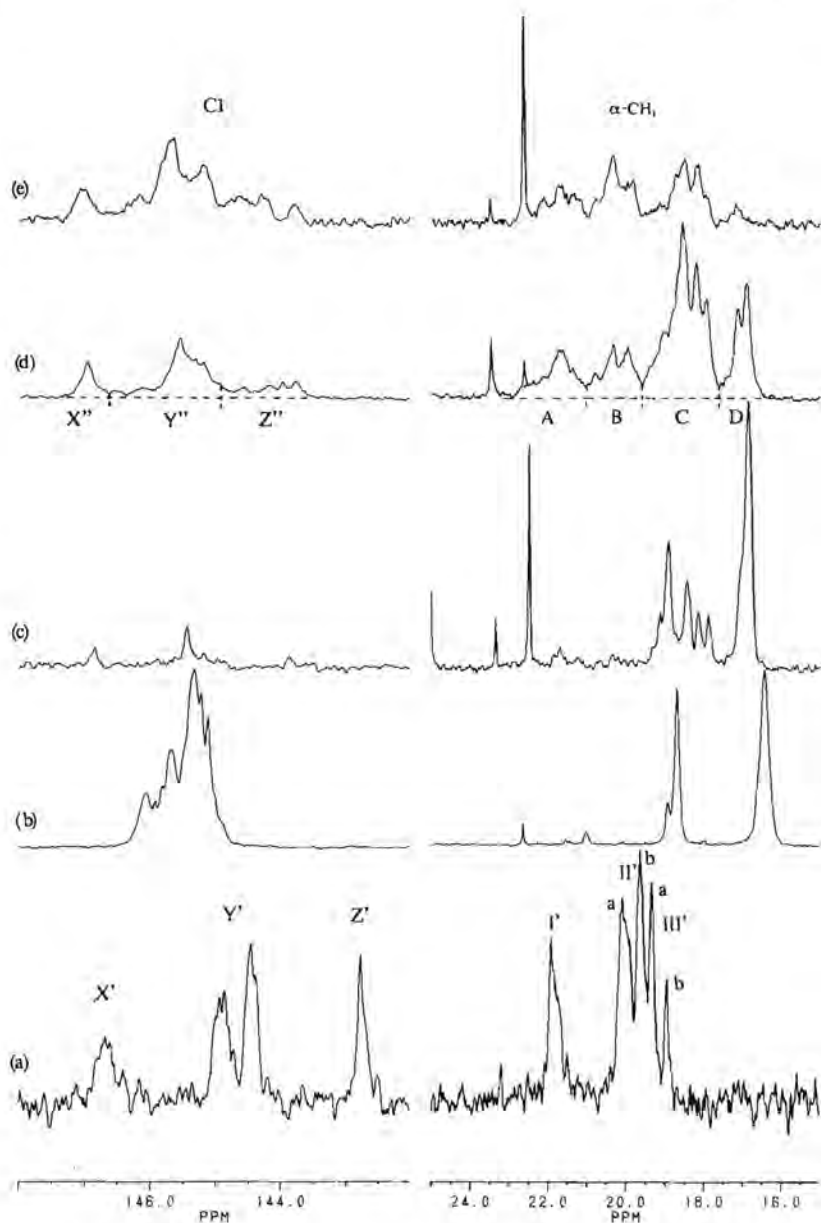


**Figure 4.5:** Expanded 100 MHz carbon-13 NMR spectra showing only the aromatic C1 region ( $\delta = 149\text{-}142$  ppm) and the  $\alpha$ -methyl carbon ( $\delta = 25\text{-}15$  ppm) of (a) alternating SMMA copolymer, (b) a mixture of Polystyrene and Polymethyl methacrylate polymer, (c) statistical SMMA copolymer with a molar feed composition styrene  $f_S = 0.073$ , (d) statistical SMMA copolymer with  $f_S = 0.262$ , (e) statistical SMMA copolymer with  $f_S = 0.557$ .

## a) C1 carbon

The C1 carbon resonances in statistical SMMA copolymers can be divided into three peaks, X'', Y'' and Z''. The assignments of the aromatic C1 resonance of Katritzky<sup>4</sup> and of Kato<sup>5</sup> are given in Table 4.3. From this Table it is clear that the two assignments are in contradiction. As described in the section of Chapter 4.3 dealing with alternating SMMA copolymers, Hirai<sup>7</sup> mentioned that the assignment of Kato should be used for the statistical SMMA

Table 4.3 Carbon C1 assignments of statistical SMMA copolymers

	X'' (147.5-146.8 ppm)	C1 Y'' (146.8-145.15 ppm)	Z'' (145.15-143.5 ppm)
Katritzky <sup>4</sup>	$\sigma_m^2$ MSM	$\sigma_m^2$ SSS $2\sigma_m(1-\sigma_m)$ SSS $\sigma_m\sigma_m$ SSM $(1-\sigma_m)\sigma_m$ SSM $2\sigma_m(1-\sigma_m)$ MSM	$(1-\sigma_m)^2$ SSS $\sigma_m(1-\sigma_m)$ SSM $(1-\sigma_m)(1-\sigma_m)$ SSM $(1-\sigma_m)^2$ MSM
Kato <sup>5</sup>	$\sigma_m^2$ SSS $(1-\sigma_m)^2$ MSM	$(1-\sigma_m)^2$ SSS $2\sigma_m(1-\sigma_m)$ SSS $(1-\sigma_m)(1-\sigma_m)$ SSM $(1-\sigma_m)\sigma_m$ SSM $2\sigma_m(1-\sigma_m)$ MSM	$\sigma_m(1-\sigma_m)$ SSM $\sigma_m\sigma_m$ SSM $\sigma_m^2$ MSM
This work	$(1-\sigma_m)^2$ MSM	$\sigma_m^2$ SSS $2\sigma_m(1-\sigma_m)$ SSS $(1-\sigma_m)^2$ SSS $(1-\sigma_m)(1-\sigma_m)$ SSM $\sigma_m(1-\sigma_m)$ SSM $2\sigma_m(1-\sigma_m)$ MSM	$(1-\sigma_m)\sigma_m$ SSM $\sigma_m\sigma_m$ SSM $\sigma_m^2$ MSM

copolymers as far as the C1 resonance is concerned, because the isotactic MSM triad resonates at higher field. In the process of evaluation of this assignment, we will reconsider all ten different S centered sequences.

In Figure 4.5b a carbon NMR spectrum of polystyrene is shown (aromatic C1 region only). The shielding differences in the three different SSS triads are very small, the meso SS dyad is shifted downfield by 0.2 ppm. Because of the small differences in chemical shifts, the iso- hetero-, and syndiotactic SSS triads are assigned to peak Y". Note that this is not in concurrence with Kato.<sup>5</sup>

In Figure 4.5a a carbon NMR spectrum of the alternating SMMA copolymer is given, showing only the aromatic C1 region. It is discussed in paragraph 4.3.2.a that the resonance, being indicated as X' in Figure 4.5a corresponds to syndiotactic MSM triad resonates at low field: this is peak X" in the statistical SMMA copolymer (see Figure 4.5d). The isotactic MSM triad resonates at high field (peak Z"), so the heterotactic MSM triad is assigned to peak Y". This all conforms to the work of Kato.<sup>5</sup>

The assignments of MSS and SSM triads are based on the chemical shift differences in SSS and MSM triads. For example,  $\sigma_m(1-\sigma_m)$  SSM resonates at lower field than  $(1-\sigma_m)\sigma_m$  SSM, because a meso SS dyad is shifted to lower field (+0.2 ppm) and a meso SM dyad to higher field (-1.5 ppm). This conforms to the text of Kato,<sup>5</sup> but the published assignments of Kato concerning the SSM triads do not follow this reasoning. In our opinion the  $(1-\sigma_m)(1-\sigma_m)$  SSM (Y"),  $\sigma_m(1-\sigma_m)$  SSM (Y"),  $(1-\sigma_m)\sigma_m$  SSM (Z") and  $\sigma_m\sigma_m$  SSM (Z") triads have to be assigned, in order to signals, from lower to higher magnetic field. The new assignments are given in Table 4.3.

#### b) $\alpha$ -methyl carbon.

In Figure 4.5(c-e) the  $\alpha$ -CH<sub>3</sub> main chain resonances are shown ( $\delta$ = 25-15 ppm), and are designated as A, B, C, and D. The assignments of these resonances, given by Katritzky<sup>4</sup> and Kato<sup>5</sup> are summarized in Table 4.4. There are a few differences between the assignments of Katritzky<sup>4</sup> and Kato.<sup>5</sup> The order of assignment of the configurational MMM triads are the same and in agreement with literature,<sup>15</sup> and also the order of assignment for the

configurational SMS triads are in agreement with the experiments in this chapter (see earlier paragraph 4.3.2.b). In our view, however, there is a misunderstanding in assigning the MMM and SMS triads to the correct peaks A, B, C, and D, as discussed in the next paragraph.

We agree with the assignments by Kato<sup>5</sup> of the  $\sigma_{mm}^2$  MMM,  $2\sigma_{mm}(1-\sigma_{mm})$  MMM and  $(1-\sigma_{mm})^2$  MMM triads to peak A, C and D, respectively (Figure 4.5d). The SMS triads are also well assigned by Kato,<sup>5</sup> with one exception; it is not immediately evident that peak IIIb could be assigned to peak C instead of to peak B (cf. Figure 4.5a and 4.5c-e).

Table 44: Carbon  $\alpha$ -methyl assignments of statistical SMMA copolymers

	$\alpha$ -CH <sub>3</sub>			
	A (23.0-21.2 ppm)	B (21.2-19.8 ppm)	C (19.8-17.8 ppm)	D (17.8-16.5 ppm)
Katritzky <sup>4</sup>	$\sigma_{mm}(1-\sigma_{mm})$ MMS $\sigma_{mm}\sigma_{mm}$ MMS	$\sigma_{mm}^2$ MMM $\sigma_{mm}^2$ SMS $2\sigma_{mm}(1-\sigma_{mm})$ SMS $(1-\sigma_{mm})^2$ SMS	$2\sigma_{mm}(1-\sigma_{mm})$ MMM $(1-\sigma_{mm})\sigma_{mm}$ MMS $(1-\sigma_{mm})(1-\sigma_{mm})$ MMS	$(1-\sigma_{mm})^2$ MMM
Kato <sup>5</sup>	$\sigma_{mm}^2$ MMM $\sigma_{mm}(1-\sigma_{mm})$ MMS $\sigma_{mm}^2$ SMS	$2\sigma_{mm}(1-\sigma_{mm})$ SMS $(1-\sigma_{mm})^2$ SMS	$2\sigma_{mm}(1-\sigma_{mm})$ MMM $(1-\sigma_{mm})\sigma_{mm}$ MMS $(1-\sigma_{mm})(1-\sigma_{mm})$ MMS $\sigma_{mm}\sigma_{mm}$ MMS	$(1-\sigma_{mm})^2$ MMM
This work	$\sigma_{mm}^2$ MMM $\sigma_{mm}\sigma_{mm}$ MMS $\sigma_{mm}^2$ SMS	$\sigma_{mm}(1-\sigma_{mm})$ MMS $2\sigma_{mm}(1-\sigma_{mm})$ SMS	$2\sigma_{mm}(1-\sigma_{mm})$ MMM $(1-\sigma_{mm})\sigma_{mm}$ SMM $(1-\sigma_{mm})(1-\sigma_{mm})$ SMM $(1-\sigma_{mm})^2$ SMS	$(1-\sigma_{mm})^2$ MMM

The MMS or SMM triads also have to be reconsidered, in the same manner as the SSM triads and the same reasoning can be used (see paragraph 4.4.2.a). The meso MM dyad resonates at even lower field (+2 ppm) than the meso SM dyad. This explanation is again also given by Kato *et al.*,<sup>5</sup> but there is no reason given for assigning, say  $\sigma_{mm}\sigma_{em}$  MMS to peak C. This may be one of the reasons why the authors failed to obtain a fit when the experimental peak areas were compared with theoretical predictions.

The following order of MMS configurational triads matches carbon NMR signals with increasing shielding:  $\sigma_{mm}\sigma_{em}$  MMS (A),  $\sigma_{mm}(1-\sigma_{em})$  MMS (B),  $(1-\sigma_{mm})\sigma_{em}$  MMS (C), and  $(1-\sigma_{mm})(1-\sigma_{em})$  MMS (C). The complete assignment is given in Table 4.4.

#### 4.5 Conclusions

It appears that in the proton and carbon NMR spectra of SMMA copolymers (both alternating and statistical) contradicting assignments in the literature have caused confusion. Although some of the original studies containing these assignments are rather dated, references to these sources are still made in modern studies. This severely hampers the progress in copolymerization studies of SMMA systems.

In this chapter some important rectifications are proposed in the assignments of the  $\alpha$ -methyl protons in the NMR spectra of alternating SMMA copolymers. With this result the  $\alpha$ -methyl carbon NMR resonances can be assigned correctly by means of selective decoupling NMR experiments. With this knowledge and with the assignments for the aromatic C1 and  $\alpha$ -methyl carbon NMR signals of polystyrene, polymethyl methacrylate and the alternating SMMA copolymers, it was possible to propose assignments for the statistical copolymers in the aromatic C1 and  $\alpha$ -methyl carbon NMR regions. These new peak assignments were made without comparing experimental and predicted peak areas from any theoretical copolymerization model, because the aim of Chapter 5<sup>2</sup> is to use the sequence distribution of SMMA copolymers for testing several models for copolymerization. Therefore, sequence distributions

should be obtainable from the NMR spectra for lack of alternatives. It is the aim of this Chapter to achieve this goal, see also paragraph 4.1 Introduction.

As shown in Chapter 5, the MMA-centered triads and the styrene-centered triads can be directly calculated from the  $\alpha$ -methyl and C1 peak areas in the carbon NMR spectra, respectively. This in contrast to the proton NMR spectra of the SMMA copolymers, where the peak splitting of the methoxy protons is so complicated that the peak areas cannot be translated directly into sequences. It is only possible to theoretically predict M-centered pentads, in which case the peak areas can be calculated and compared with experimental values.

## References

1. Koenig J.L., "Chemical Microstructure of polymer chains"; Wiley: New York, 1980.
2. This thesis, Chapter 6.
3. Aerdts A.M., Haan de J.W., German A.L., Velden van der G.P.M., *Macromolecules*, 24, 1473, 1991.
4. Katritzky A.R., Smith A., Weiss D.E., *J.C.S. Perkin II*, 1547, 1974.
5. Kato Y., Ando I., Nishioka A., *Nippon Kagaku Kaishi*, 501, 1975.
6. Tacx J.C.J.E., Velden van der G.P.M., German A.L., *J. Polym. Sci., Polym. Chem. Ed.*, 26, 1439, 1988.
7. Hirai H., Koinuma H., Tanabe T., Takeuchi K., *J. Polym. Sci. Polym. Chem. Ed.*, 17, 1339, 1979.
8. Hirai H., *J. Polym. Sci., Macromol. Rev.*, 11, 47, 1976.
9. Niknam M.K., University of Akron, Akron, OH, 1985, *Diss. Abstr. Int. B.* 46 (4), pp 331, 1196, 1985. Available from University Microfilms, Int. Order No DA 85 13339.
10. Koinuma H., Tanabe T., Hirai H., *Makromol. Chem.*, 181, 383, 1980.
11. Heffner S.A., Bovey F.A., Verge L.A., Mirau P.A., Tonelli A.E., *Macromolecules*, 19, 1628, 1986.
12. Tonelli A.E., "NMR Spectroscopy and Polymer Microstructure"; Marchand A.P., Ed; VCH Publishers, Inc.: New York, pp 126-127, 1988.
13. Koinuma H., Tanabe T., Hirai H., *Macromol. Chem.*, 183, 211, 1982.
14. Kale L.T., O'Driscoll K.F., Dinan E.J., Uebel J.J., *J. Polym. Sci., Part A*, 24, 3145, 1986.
15. Inoue Y., Nishioka A., Chujo R., *Makromol. Chemie*, 156, 207, 1972.
16. Inoue Y., Nishioka A., Chujo R., *Polym. J.*, 4, 535, 1971.



## Chapter 5

### Free Radical Copolymerization: An NMR Investigation of Current Kinetic Models

**ABSTRACT:** The ability of terminal model kinetics to predict copolymer microstructure was tested for the styrene-methyl methacrylate system copolymerized at 313 K at various fractions of monomers. Carbon-13 NMR studies (in Chapter 4) showed that previous peak assignments of the spectra of statistical styrene-methyl methacrylate copolymers were incorrect. The peak areas obtained for all copolymers were described in terms of triad sequences, and were also adequately predicted by the terminal model utilizing reactivity ratios calculated from non-linear least squares fit to the copolymer composition data determined by  $^1\text{H}$  NMR. The non-terminal model behaviour of the kinetics of the rate of polymerization described elsewhere can be successfully modelled by the 'restricted' penultimate model of Fukuda *et al.* It is shown that all current data can also be explained by various 'bootstrap' or monomer-polymer complex models. Further model discrimination awaits new independent experimental results.

#### 5.1 Introduction

The kinetic model that is most widely used to model free radical copolymerizations is the terminal model, also known as the Mayo-Lewis model.<sup>1</sup> For most copolymer systems the copolymer composition was well fitted by the terminal model equation.<sup>2</sup> Recently, however, there have been numerous reports of the inability of the terminal model to fit other types of

copolymerization data.<sup>3,7</sup> These discrepancies have been explained in at least two ways, which are described below.

First, the rate or mean propagation rate coefficient of copolymerization has been found not to obey the terminal model.<sup>5,6</sup> This deviation has been explained by invoking the penultimate model for copolymerization, in which the penultimate group from the polymeric free radical end is considered to affect the reactivity of the radical. In order to accommodate the fact that composition is well fitted by the terminal model a restricted penultimate model has been developed<sup>5,8</sup> in which the terminal model is a limit for the case of polymer composition.

Copolymer composition and monomer sequence distribution data for some copolymers are sensitive to the solvent utilized during polymerization.<sup>7,9</sup> A model which has been invoked to explain the effect of solvents upon both sequence distributions and copolymer composition in copolymerization is the so-called 'bootstrap' model.<sup>7</sup> This model was derived from the observation that copolymers of the same composition have the same microstructure irrespective of the solvent used during copolymerization. The assumption is that the conditional probabilities governing the propagation reactions are independent of the solvent. This model has been successful in explaining solvent effects in copolymerization.

One of the current difficulties in the field of free radical copolymerization is discrimination between models (there are at least 10 models for copolymerization<sup>1,3,7,10</sup>). On the basis of composition and rate data O' Driscoll and Davis<sup>11</sup> stated that nuclear magnetic resonance (NMR) experiments are incapable of model discrimination. However, Moad *et al.*<sup>12</sup> showed that the latter statement assumes that an adequate fit to polymer composition data of the terminal model justified the use of the terminal model. In fact Moad *et al.*<sup>12</sup> showed that an adequate fit to composition data by the terminal model does not discount penultimate unit effects on polymer composition. Further, these authors<sup>12</sup> pointed out the necessity of further experiments before model discrimination in copolymerization could proceed. This is the aim of this chapter.

Many workers have assumed that the inadequacy of the terminal model in

some cases automatically suggests penultimate unit effects, despite the fact that numerous other models of copolymerization have sufficient adjustable parameters to fit all current data. In fact, to our knowledge there is only one claimed experimental (electron spin resonance, ESR) observation of a penultimate unit effect,<sup>13</sup> and that is of the rather exotic homo-polymerization (or dimerization ?) of tert-butyl  $\alpha$ -tert-butylsulfenyl acrylate with various azo initiators in chlorobenzene at 297 K. The substituent groups on the initiator fragment were claimed to effect the ESR signal of the propagating radical. It is unclear why this would be the case following a few propagation steps after which substituents on the initiator would be unlikely to effect the propagating radical (obviously an oligomeric radical with degree of polymerization,  $d_p > 2$  cannot feel penultimate unit effects from the initiator fragment, simply because the penultimate unit is not the initiator fragment). Without further experimental details it is unlikely that this experimental data can be used as evidence for penultimate unit effects in bulk copolymerization.

In this chapter we endeavor to test a limited number of models for copolymerization by measuring the <sup>13</sup>C NMR triad sequence distributions for the 'model' bulk copolymerization system, styrene (S) and methyl methacrylate (MMA) at 313 K. These data may allow the discrimination between both terminal and penultimate unit effects and any other effects on copolymer composition data. Previous attempts to fit triad sequence distributions of this system by the terminal model are invalid since they utilize fine structures in <sup>1</sup>H NMR spectra, which are sensitive to (at least) pentad sequences.<sup>14</sup> Further, in Chapter 4<sup>15</sup> we show that all previous triad sequence assignments of <sup>13</sup>C NMR spectra are invalid, and propose new assignments for these spectra. One further advantage of <sup>13</sup>C NMR is that both styrene-centered and MMA-centered triad sequence distributions can be measured.<sup>15</sup> The <sup>13</sup>C NMR sequence distributions are measured for polymers polymerized at conditions utilized by Fukuda *et al.*<sup>5</sup> to determine the mean propagation rate coefficients for this system. We also determine the <sup>1</sup>H NMR polymer composition data, and with the mean propagation rate coefficient and triad sequence distribution data this provides the most complete set of copolymerization data on this system to date.

## 5.2 Theory

### Terminal model

The terminal model for copolymerization assumes that there are two types of polymeric radicals distinguished by their end units,  $S^0$  and  $M^0$ , where S and M represent the two monomer units in the system (in this study these represent styrene and MMA respectively). The rate of copolymerization is given by the rate of decrease of the total monomer concentration,  $C_m$ .

$$-\frac{dC_m}{dt} = -\frac{d[S]}{dt} - \frac{d[M]}{dt} = k_p ([S] + [M])([S^0] + [M^0]) \quad (5.1)$$

where  $[S^0]$  and  $[M^0]$  are the concentrations of the polymeric free radicals,  $[S]$  and  $[M]$  the concentrations of the monomers, and  $k_p$  is the mean propagation rate coefficient given by:<sup>5</sup>

$$k_p = \frac{r_s f_s^2 + 2f_s f_m + r_m f_m^2}{\frac{r_s f_s}{k_{ss}} + \frac{r_m f_m}{k_{mm}}} \quad (5.2)$$

in which  $f_s$  and  $f_m$  are the mole fractions of each monomer in the reaction, and  $r_s$  and  $r_m$  are the reactivity ratios given by:

$$r_s = \frac{k_{ss}}{k_{sm}} \quad r_m = \frac{k_{mm}}{k_{ms}} \quad (5.3)$$

$k_{ij}$  is the propagation rate coefficient for radical  $I^0$  with monomer J ( $i, j = s$  or  $m$ ; I, J = S or M). The instantaneous copolymer composition is given by the well-known copolymer equation:<sup>1</sup>

$$\frac{F_s}{F_m} = \frac{f_s(r_s f_s + f_m)}{f_m(r_m f_m + f_s)} \quad (5.4)$$

where  $F_s$  and  $F_m$  are the mole fractions of monomers S and M in the copolymer.

In this chapter we measure the  $^{13}\text{C}$  NMR spectra, of which some of the resonances can be assigned in terms of triad sequence distributions. These are given in terms of conditional probabilities, which themselves can be couched in terms of monomer ratios and reactivity ratios. We define the quantity  $x$  as the ratio of the monomer concentrations:

$$x = \frac{[\text{S}]}{[\text{M}]} \quad (5.5)$$

The fractions of each type of the styrene-centered triads are given by:<sup>16</sup>

$$F_{ssm} = \frac{r_s^2 x^2}{1 + 2r_s x + r_s^2 x^2} \quad (5.6)$$

$$F_{mssm} = \frac{1}{1 + 2r_s x + r_s^2 x^2} \quad (5.7)$$

$$F_{msm} = F_{smm} = \frac{r_s x}{1 + 2r_s x + r_s^2 x^2} \quad (5.8)$$

Similarly, the fractions of each type of MMA-centered triads are given by:<sup>16</sup>

$$F_{mmm} = \frac{r_m^2/x^2}{1 + 2r_m/x + r_m^2/x^2} \quad (5.9)$$

$$F_{smm} = \frac{1}{1 + 2r_m/x + r_m^2/x^2} \quad (5.10)$$

$$F_{mms} = F_{smm} = \frac{r_m/x}{1 + 2r_m/x + r_m^2/x^2} \quad (5.11)$$

*Penultimate model*

The penultimate model considers that there are four distinct types of polymeric free radicals, and that each is distinguished by the terminal and by the penultimate monomer units from the radical site. In the penultimate model the mean propagation rate coefficient is given by:<sup>5</sup>

$$k_p = \frac{\bar{r}_s f_s^2 + 2f_s f_m + \bar{r}_m f_m^2}{\bar{r}_s f_s / \bar{k}_{ss} + \bar{r}_m f_m / \bar{k}_{mm}} \quad (5.12)$$

where the mean reactivity ratios and propagation rate coefficients are given by:

$$\bar{r}_s = \frac{r_s' [f_s r_s + f_m]}{f_s r_s' + f_m} \quad (5.13)$$

$$\bar{r}_m = \frac{r_m' [f_m r_m + f_s]}{f_m r_m' + f_s} \quad (5.14)$$

$$\bar{k}_{ss} = \frac{k_{ssm} [f_s r_s + f_m]}{f_s r_s + f_m / s_s} \quad (5.15)$$

$$\bar{k}_{mm} = \frac{k_{mmm} [f_m r_m + f_s]}{f_m r_m + f_s / s_m} \quad (5.16)$$

The reactivity ratios, in turn, are:

$$r_i = \frac{k_{jii}}{k_{ijj}} \quad i, j = s \text{ or } m \quad i \neq j \quad (5.17)$$

$$r_i' = \frac{k_{jji}}{k_{jij}} \quad i, j = s \text{ or } m \quad i \neq j \quad (5.18)$$

$$s_i = \frac{k_{jji}}{k_{jii}} \quad i, j = s \text{ or } m \quad i \neq j \quad (5.19)$$

where the propagation rate coefficients for addition of monomer  $J$  to radical  $II^0$  is given by  $k_{ij}$  ( $i, j = s$  or  $m$ ;  $I, J = S$  or  $M$ ).

The instantaneous copolymer composition is given by the penultimate copolymer equation:<sup>5</sup>

$$\frac{F_s}{F_m} = \frac{f_s(\bar{r}_s f_s + f_m)}{f_m(\bar{r}_m f_m + f_s)} \quad (5.20)$$

The fractions for the styrene-centered triads are:<sup>16</sup>

$$F_{sss} = \frac{r_s r_s' x^2}{1 + 2r_s' x + r_s r_s' x^2} \quad (5.21)$$

$$F_{msm} = \frac{1}{1 + 2r_s' x + r_s r_s' x^2} \quad (5.22)$$

$$F_{smm} = F_{mms} = \frac{r_s' x}{1 + 2r_s' x + r_s r_s' x^2} \quad (5.23)$$

Similarly, for the MMA-centered triads:<sup>16</sup>

$$F_{mmm} = \frac{r_m r_m' / x^2}{1 + 2r_m' / x + r_m r_m' / x^2} \quad (5.24)$$

$$F_{smm} = \frac{1}{1 + 2r_m' / x + r_m r_m' / x^2} \quad (5.25)$$

$$F_{mms} = F_{mms} = \frac{r_m' / x}{1 + 2r_m' / x + r_m r_m' / x^2} \quad (5.26)$$

### *The bootstrap model*

Recently, the bootstrap model for copolymerization has been developed<sup>7</sup> for which the primary assumption is that the monomer ratio at the polymerization site is different from that in the bulk. Further, the monomer ratio is considered to have no effect upon the conditional probabilities or reactivity ratios. Therefore, polymers of the same overall composition in different solvents always have the same microstructure.

In principle the bootstrap model considers the actual or true monomer concentrations at the polymerization site,  $[S]$  and  $[M]$ , and allows the ratio of these quantities to be related to the ratio of the bulk monomer concentrations by an equilibrium constant,  $K$ . It has been suggested<sup>7</sup> that the true ratio of the monomers at the polymerization site,  $x_1$ , is given by:

$$x_1 = \frac{[S]}{[M]} = K \frac{[S]}{[M]} \quad (5.27)$$

Note that this equation assumes that the bootstrap effect is independent of factors such as monomer ratio and polymer composition, *i.e.* a single coefficient,  $K$ , describes the bootstrap effect. In principle, this equation can be applied to any other model for copolymerization. That is all quantities in, say, the terminal model that relate to the monomer concentrations, *i.e.*  $f_s$ ,  $f_m$ , and  $x_1$ , must be replaced by their true value as defined by the equilibrium constant,  $K$ .



### 5.3 Results and discussion

#### Testing of models

In this work we have used a non-linear least squares fitting technique known as the functional relationship model<sup>17</sup> which allows the fitting of multi-parameter models to data. One important feature of this technique is that it encompasses, as an input parameter, an estimate of the random error in both the experimentally observed dependent and independent variables. The errors indicated for all fitted parameters are standard deviations which can be related to both the variance and confidence limits through the variance-covariance matrix.<sup>17</sup> If the fit of the model to data is valid the size of the standard deviation indicates the significance of the fit. Alternatively, if there is more than one fitted parameter (which is not the case for the fit of the terminal model to <sup>13</sup>C NMR peak areas) joint confidence regions can be constructed, although in this work this has not been done, because of the number and complexity of models discussed.

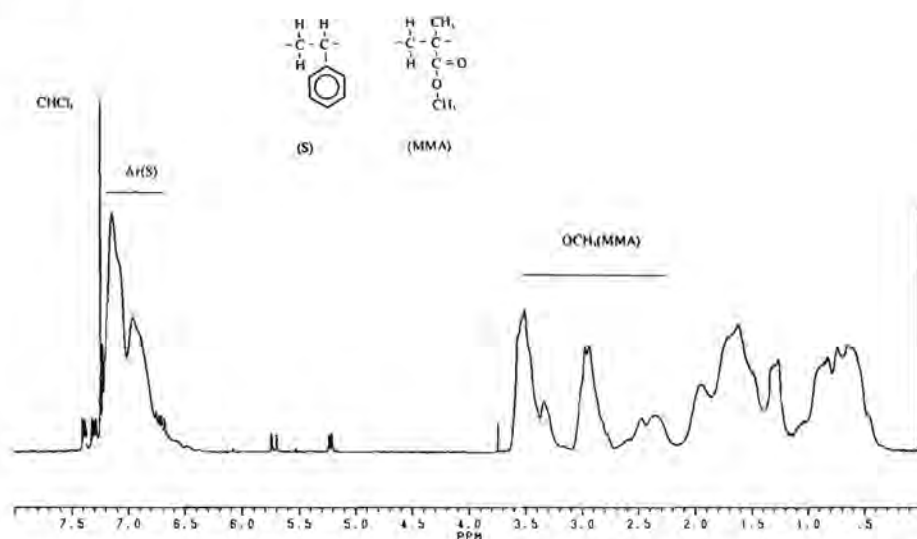


Figure 5.1: 400 MHz <sup>1</sup>H NMR spectrum of a low conversion bulk SMMA copolymer (fraction of styrene in feed,  $f_s = 0.377$ ) in CDCl<sub>3</sub> at 298 K. Styrene is represented by S. The symbol Ar(S) represents the resonance of the aromatic protons on the styrene unit, and OCH<sub>3</sub>(MMA) represents the resonance of the methoxy protons on the MMA unit.

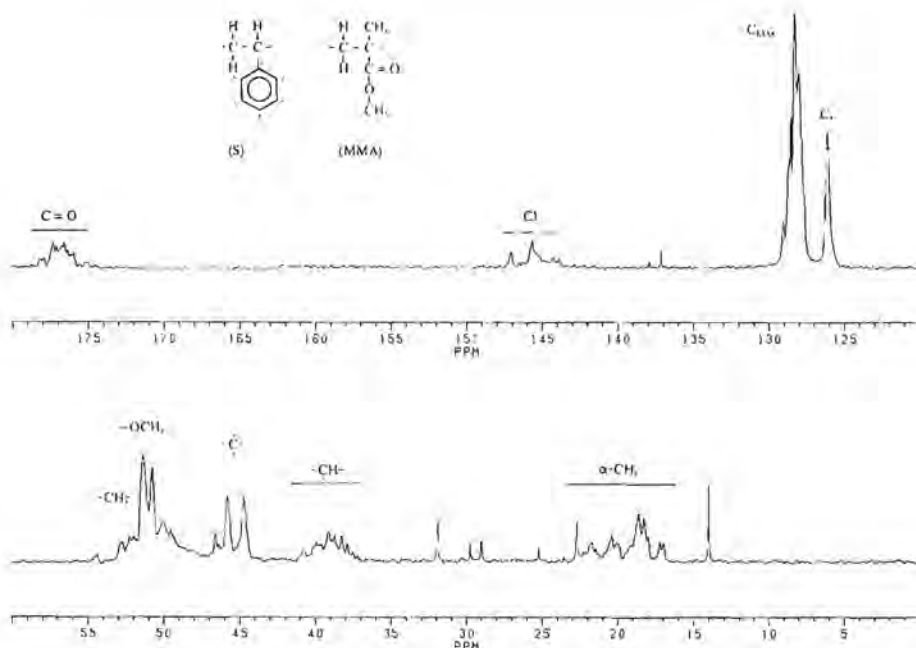


Figure 5.2: 100 MHz  $^{13}\text{C}$  NMR spectrum of a low conversion bulk SMMA copolymer (fraction of styrene in feed,  $f_s = 0.377$ ) in  $\text{CDCl}_3$  at 298 K. Styrene is represented by S. The C=O represents the resonance of the carbonyl carbon of the MMA unit,  $C_x$  (where  $x=1-6$ ) represents the aromatic carbon resonances of the styrene unit,  $\text{CH}_2$  represents the main chain carbon resonances,  $\text{OCH}_3$  represents the methoxy carbon resonances of the MMA unit, C represents the main chain carbon resonance of the MMA unit, CH represents the main chain carbon resonance of the styrene unit, and  $\alpha\text{-CH}_3$  represents the  $\alpha$ -methyl resonance of the MMA unit.

### Copolymer composition

The motivation for utilizing copolymerization conditions exactly the same as that used by Fukuda *et al.*<sup>5</sup> was to obtain copolymer triad sequence distribution data and hence to obtain a full set of copolymerization data, namely the mean propagation rate coefficients, the copolymer composition and the triad sequence distributions, all at various monomer ratios.

The copolymer composition data and sequence distributions data are obtained by  $^1\text{H}$  and  $^{13}\text{C}$  NMR respectively. A typical  $^1\text{H}$  NMR spectrum of a bulk SMMA copolymer is displayed in Figure 5.1, and in Figure 5.2 a typical  $^{13}\text{C}$  NMR spectrum is displayed.

The average copolymer composition of the SMMA copolymers can be readily obtained by using

$$F_s = 1.6 \frac{A(\delta=7.5-6.5)}{A(\delta=7.5-6.5) + A(\delta=3.7-0.2)} \quad (5.28)$$

where  $A(\delta=7.5-6.5 \text{ ppm})$  is the peak area of the aromatic protons of styrene and  $A(\delta=3.7-0.2 \text{ ppm})$  is the peak area of the aliphatic protons of styrene and MMA (Figure 5.1). Hence, before further analyses of the triad sequence data was performed we confirmed that the copolymer composition of the bulk polymers measured by  $^1\text{H NMR}$  were similar to those measured by Fukuda et al. In Table 5.1 these data are presented and in Figure 5.3 the copolymer compositions from the two sets of experiments are presented.

*Table 5.1: Comparison of copolymer compositions from bulk polymerizations performed in this work and by Fukuda et al.<sup>5</sup> Also the final conversions of copolymerizations performed in this work, and the mean propagation rate coefficient measured by Fukuda et al.*

$f_s$ this work	$f_s$ ref. 5	$F_s$ this work	$F_s$ ref. 5	% final conversion	$k_p/\text{dm}^3\text{mol}^{-1}\text{s}^{-1}$ ref.5
- <sup>a</sup>	0	-	-	-	377 <sup>b</sup>
0.073	0.073	0.135	0.118	1.77	247
0.109	0.109	0.198	0.184	0.76	193
0.199	0.199	0.307	0.284	1.20	149
0.262	0.262	0.355	0.340	0.44	139
0.377	0.377	0.419	0.402	1.14	135
- <sup>a</sup>	0.454	-	-	-	101
0.458	0.458	0.489	0.489	0.5	127
0.557	0.557	0.539	0.544	1.35	109
0.705	0.705	0.648	0.643	0.19	110
- <sup>a</sup>	1	-	-	-	120 <sup>b</sup>

<sup>a</sup> - not polymerized in this work

<sup>b</sup> - average of values in ref.5

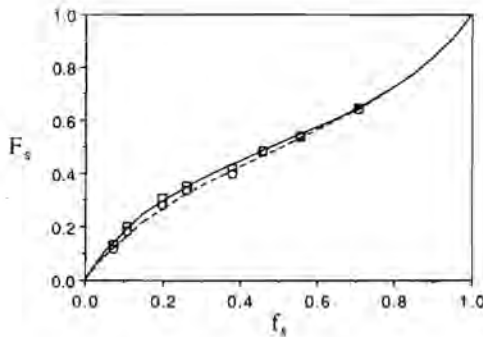


Figure 5.3: Fraction of styrene in copolymer versus fraction of styrene in feed. Experimental results; squares are this work, circles from ref.<sup>5</sup> The solid line represents the fit of the terminal model to the data of this work with  $r_s = 0.48$ ,  $r_m = 0.42$ . The dashed line represents the fit of the terminal model to the data of ref.<sup>5</sup> with  $r_s = 0.53$  and  $r_m = 0.49$ .

The terminal model (eq. 5.4) was fitted to the polymer composition data of both Fukuda *et al.*<sup>5</sup> and this work. For the polymer compositions measured by Fukuda *et al.* we found the following reactivity ratios  $r_s = 0.53 \pm 0.02$  and  $r_m = 0.49 \pm 0.02$ , where the subscripts *s* and *m* refer to styrene and MMA respectively. These values are similar to those fitted by Fukuda *et al.*,  $r_s = 0.523$  and  $r_m = 0.460$  for the same data. The composition data from this work were fitted by the same technique as above, and gave  $r_s = 0.48 \pm 0.03$  and  $r_m = 0.42 \pm 0.09$ . These values agree well with values proposed by O'Driscoll *et al.*<sup>18</sup> for the copolymerization of styrene and methyl methacrylate, namely  $r_s = 0.472$  and  $r_m = 0.454$ . Therefore the composition data of this study suggest that the copolymers studied in this work are those normally produced by these polymerizations.

#### Triad sequence distributions

For statistical copolymers there are 20 possible configurations of triads, 10 each for the styrene-centered and the MMA-centered triads. The fraction of each triad is given by  $F_{iii}$ , where *i*=*s* or *m*. The 20 possible configurations in terms of triad fractions are given in Tables 4.3 and 4.4 (here, MMM is the same

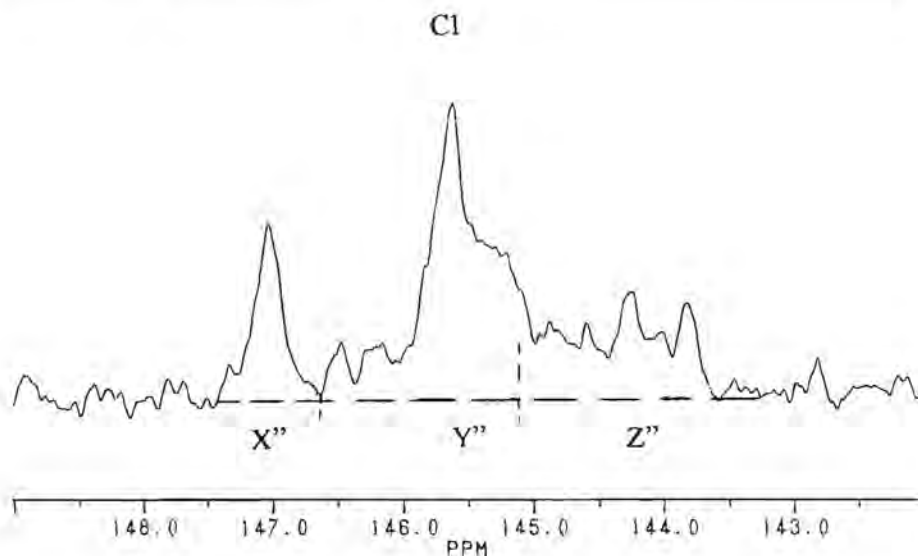


Figure 54: Expanded 100 MHz  $^{13}\text{C}$  NMR spectrum of SMMA copolymer (fraction of styrene in feed,  $f_s = 0.377$ ) in  $\text{CDCl}_3$  at 298 K, showing only the aromatic C1 region ( $\delta = 150 - 142$  ppm) and three designated signal areas X'', Y'' and Z''.

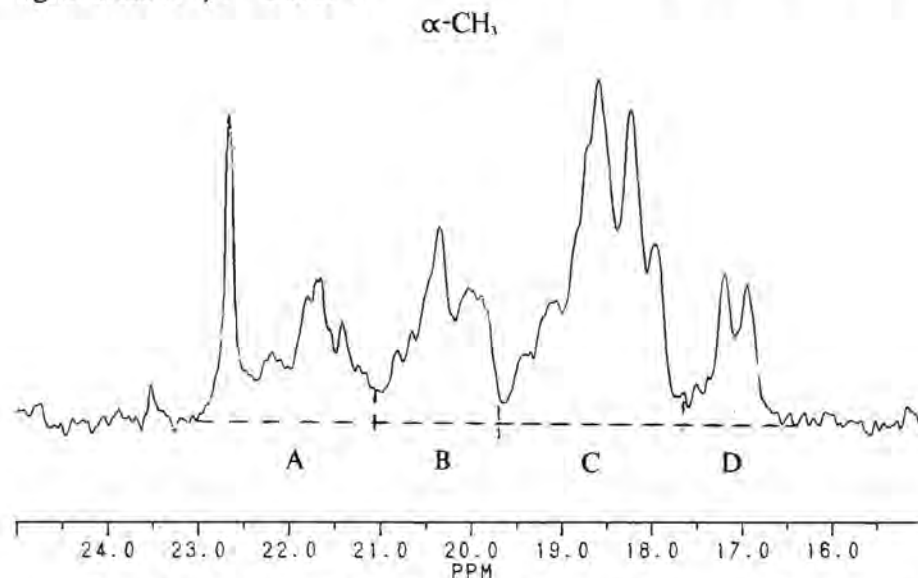


Figure 5.5: Expanded 100 MHz  $^{13}\text{C}$  NMR spectrum of SMMA copolymer (fraction of styrene in feed,  $f_s = 0.377$ ) in  $\text{CDCl}_3$  at 298 K, showing only the  $\alpha$ -methyl carbon region ( $\delta = 25 - 15$  ppm) and four designated signal areas A, B, C and D.

as  $F_{\text{mmm}}$ ). The probability that two adjacent monomer units have a meso configuration (isotactic) is given by a tacticity parameter  $\sigma$ . The coisotacticity parameter,  $\sigma_{\text{mm}}$ , is calculated<sup>15</sup> from the methoxy region in the  $^1\text{H}$  NMR spectra and is 0.44. The other tacticities,  $\sigma_{\text{ss}}$  and  $\sigma_{\text{ms}}$ , are taken from  $^{13}\text{C}$  spectra of the homopolymers, and are 0.29 and 0.23 respectively.<sup>15</sup>

The two regions of interest in the  $^{13}\text{C}$  NMR spectra of the SMMA copolymers are the aromatic C1 region of the styrene unit (chemical shift,  $\delta = 148$  -143 ppm) and the  $\alpha$ -methyl region of the MMA unit ( $\delta = 25$  -15 ppm). These two regions show induced splitting due to the various tacticities and sequences of the styrene-centered triads and MMA-centered triads respectively. In Figure 5.4 and 5.5 the  $^{13}\text{C}$  NMR spectra of these regions are displayed, showing the distinct signal areas. The assignments of these signal areas have been elucidated in Chapter 4,<sup>15</sup> and for each of the sets of triad fractions are given in Tables 4.3 and 4.4. For the styrene centered triads there are three distinct signal areas, labelled X'' ( $\delta = 147.5$  -146.8 ppm), Y'' ( $\delta = 146.8$  -145.15 ppm) and Z'' ( $\delta = 145.15$  -143.5 ppm). For the MMA-centered triads there are four distinct signal areas labelled A ( $\delta = 23$  -21.2 ppm), B ( $\delta = 21.2$  -19.8 ppm), C ( $\delta = 19.8$  -17.8 ppm) and D ( $\delta = 17.8$  -16.5 ppm). The relative areas of the signals for all copolymer compositions are given in Table 5.2. Note that, in what follows for the MMA-centered triad signal areas B and C are considered as one, since

Table 5.2: Summary of  $^{13}\text{C}$  NMR results showing fraction signal areas for copolymers produced at various fractions of styrene in the feed,  $f_s$ .<sup>15</sup>

$f_s$	MMA-centered triads				styrene-centered triads		
	A	B	C	D	X''	Y''	Z''
0.073	0.069	0.045	0.458	0.428	0.191	0.557	0.252
0.109	0.079	0.066	0.494	0.361	0.243	0.524	0.232
0.199	0.106	0.121	0.530	0.243	0.203	0.528	0.269
0.262	0.148	0.153	0.528	0.171	0.187	0.561	0.252
0.377	0.113	0.241	0.526	0.120	0.155	0.542	0.303
0.458	0.154	0.255	0.516	0.075	0.148	0.558	0.293
0.557	0.135	0.366	0.437	0.062	0.116	0.633	0.241
0.705	0.166	0.478	0.330	0.025	0.080	0.624	0.296

the configuration,  $(1-\sigma_{mn})^2 F_{smn}$ , is divided over these signal areas. Therefore, both the styrene-centered and the MMA-centered triads are split into 3 separate signals with corresponding areas. In the case of MMA-centered triads these are A, B+C, and D.

First, the peak areas were predicted by the reactivity ratios found by a fit of the terminal model to the copolymer composition data in the previous part of this section ( $r_s=0.48\pm 0.03$  and  $r_m=0.42\pm 0.09$ ). It is important to note that the styrene-centered triads are only determined by  $r_m$ . In Figure 5.6.a-b it can be seen that the reactivity ratios calculated from polymer composition data predict the signal areas of the  $^{13}\text{C}$  NMR spectra with spectacular success at all fractions of monomer. It is important to note that the assignments of the signal areas were elucidated by a technique entirely independent of any kinetic model for copolymerization, and rely entirely upon NMR experimental data. Further, these assignments are different from those previously deduced elsewhere.<sup>15</sup>

For completeness we utilized the  $^{13}\text{C}$  NMR data to predict reactivity ratios. From each set of data, *i.e.* styrene-centered and MMA-centered results, we find an independent reactivity ratio,  $r_s$  and  $r_m$  respectively. Utilizing the non-linear least squares technique discussed above we find,  $r_s=0.51\pm 0.05$  and  $r_m=0.52\pm 0.02$ . These values compare very well to those found from composition data: they are equal within experimental error. The fit of these parameters to the peak areas can be seen in Figure 5.7.a-b. A fit of the penultimate model to the  $^{13}\text{C}$  NMR peak area data showed no statistical improvement in the fit.

Hence, the  $^{13}\text{C}$  NMR data suggest that there are no penultimate unit effects on the triad fractions of the copolymers of styrene and MMA. This does not entirely disprove penultimate unit effects on polymer microstructure since it could be argued that penultimate unit effects may turn up in, say, pentad sequences. However, the fit of the terminal model presented above is much better evidence for the absence of penultimate unit effects on copolymer microstructure than simple polymer composition data.

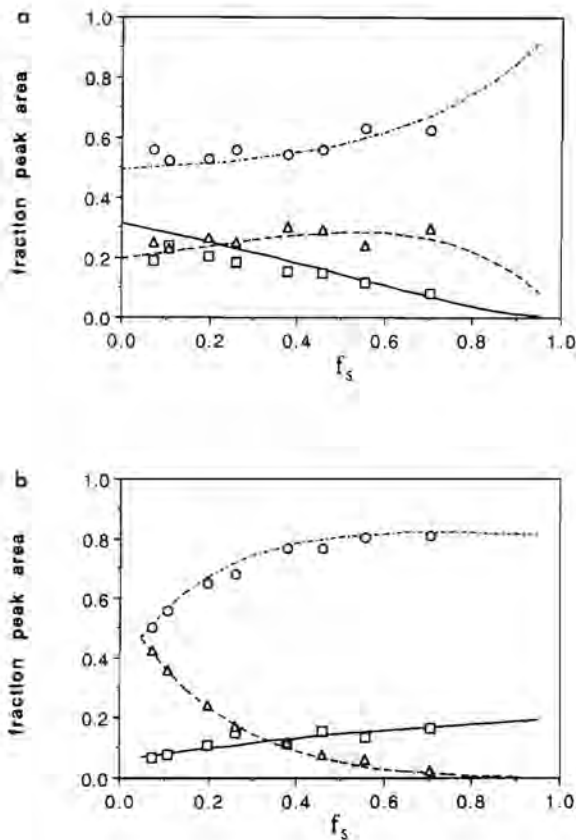


Figure 5.6: Fraction peak areas measured by  $^{13}\text{C}$  NMR of SMMA copolymers polymerized at various fractions of styrene in the feed. Lines are predictions of the terminal model utilizing reactivity ratios deduced from the copolymer composition data. (a) styrene-centered peak areas, squares-peak area X'', circles-peak area Y'', triangles-peak area Z''. Lines calculated with  $r_s = 0.48$ . (b) MMA-centered peak areas, squares-peak area A, circles-peak area B+C, triangles peak area D. Lines calculated with  $r_m = 0.42$ .



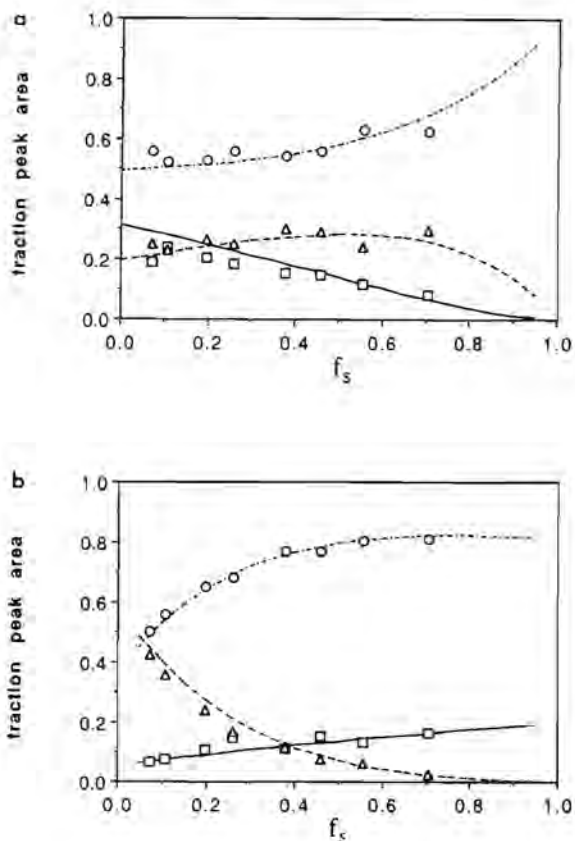


Figure 5.7: Fraction peak areas measured by  $^{13}\text{C}$  NMR of SMMA copolymers polymerized at various fractions of styrene in the feed. Lines are fits of the terminal model to the experimental points. (a) styrene-centered peak areas, squares-peak area X'', circles-peak area Y'', triangles-peak area Z''. Lines calculated with fitted reactivity ratio,  $r_s = 0.51$ . (b) MMA-centered peak areas, squares-peak area A, circles-peak areas B+C, triangles-peak area D. Lines calculated with fitted reactivity ratio,  $r_m = 0.52$ .

### Propagation rate coefficients in copolymerization

The evidence that we present in this chapter suggests that the terminal model is valid for both the polymer composition and the triad sequence distributions. The unusual feature of the copolymerization of styrene and methyl methacrylate is the now well documented non-terminal model behavior<sup>5,6,11</sup> of the mean propagation rate coefficient (see Figure 5.8). This behavior was explained by Fukuda *et al.*<sup>5,8</sup> by suggesting a restricted penultimate model. In this model the reactivity ratios,  $r_i$  and  $r_i'$  are set equal to each other, i.e.

$$r_i = r_i' \quad i=s \text{ or } m \quad (5.29)$$

From this equality it follows that the penultimate model reduces to the terminal model in the copolymer equation. Hence, although the mean propagation rate coefficient is influenced by penultimate unit effects, the composition and the triad sequence distributions are not.

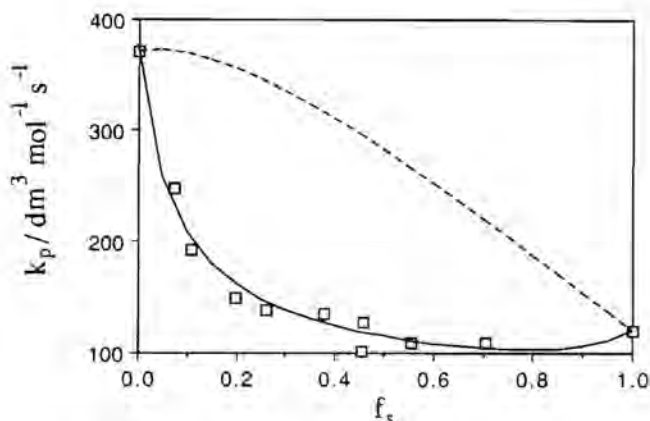


Figure 5.8: Plot of  $k_p$  versus  $f_s$  for SMMA copolymerization at 313 K. Experimental results (squares) from ref.5. Solid line predictions of restricted penultimate model with  $s_s = 0.30$  and  $s_m = 0.53$ . Dotted line prediction of terminal model with  $r_s = 0.52$  and  $r_m = 0.46$ .

The assumption that  $r_1=r_1'$  was initially made because of the good fit of the composition data to the terminal model. However, Moad *et al.*<sup>12</sup> showed that this did not necessarily mean that penultimate unit effects are not operating with regard to composition. Therefore, Fukuda *et al.*<sup>8</sup> justified the use of eq. 5.29 by considering a stabilization energy argument. There are problems with this justification, namely that to find eq. 5.29 Fukuda *et al.* made the following assumptions:<sup>8</sup>

(1) The energy change for the addition of a monomer to a radical may be expressed as the algebraic sum of a normal energy change which would be observed in the absence of conjugation (or other effects) plus corrections due to the latter.<sup>19</sup>

$$-\Delta H_{ijl} = -(\Delta H_p)_0 + U_j - (U_{ij} + U_l) \quad (5.30)$$

where  $-\Delta H_{ijl}$  is the energy change for the addition of monomer L to polymeric radical  $I_j^0$  (where  $i,j,l = s$  or  $m$ ;  $I, J, L=S$  or  $M$ ),  $(\Delta H_p)_0$  is the energy which would be observed in the absence of substituents, and  $U_{ij}$ ,  $U_j$  and  $U_l$  are the stabilization energies of the product radical, the initial radical and the monomer respectively.

(2) The use of the Polanyi rule for propagating free radicals is substantiated. Hence the activation energy of propagation radical  $I_j^0$  with monomer L,  $E_{ijl}$ , can be written as:<sup>19</sup>

$$E_{ijl} = (E_{ijl})_0 - \alpha(-\Delta H_{ijl}) \quad (5.31)$$

where  $(E_{ijl})_0$  and  $\alpha$  are constants.

(3) Finally, all constants and frequency factors were neglected and the penultimate propagation rate coefficients can be written as:<sup>8</sup>

$$k_{ijl} = \exp[\alpha(U_j - U_{ij} - U_l)] \quad (5.32)$$

The use of eq. 5.32 gives eq. 5.29. Ignoring the considerable assumptions<sup>19</sup> made in both the derivations and use of eq. 5.30-31 for polymeric radicals, we

would like to concentrate on the assumptions made in the derivation of eq. 5.32. The use of eq. 5.32 does not seem reasonable for the SMMA system when it is realized that pre-exponential factors may be significantly different for various polymeric radicals. For example, the pre-exponential factors,  $A$ , for the homopolymerizations of the following systems have been experimentally determined:<sup>6</sup> styrene ( $A=1.99 \times 10^7$ ), ethyl methacrylate ( $A=1.5 \times 10^6$ ), butyl methacrylate ( $A=3.44 \times 10^6$ ), MMA ( $A=4.92 \times 10^5$ ), and lauryl methacrylate ( $A=2.93 \times 10^5$ ). Note that the pre-exponential factors for the homopolymerization of styrene and MMA differ by approximately two orders of magnitude. In the copolymerization case there is no obvious *a priori* reason to assume that the pre-exponential factors for two radicals with differing penultimate units should be the same. In fact this is a major assumption made by Fukuda *et al.* (without comment) and ensures the result of eq. 5.29.

Despite the above theoretical doubts the restricted penultimate model<sup>5,8</sup> does explain all the data and hence deserves further study, especially from a theoretical point of view. The question remains whether the fit of the restricted penultimate model is only a function of the number of adjustable parameters in the model. Without doubt unambiguous experimental evidence of a penultimate unit effect must be observed before the restricted penultimate unit should be adopted. In the SMMA copolymerization system ESR may distinguish a penultimate unit effect, since the MMA propagating free radical has a well characterized signal.

#### *Monomer concentrations in copolymerization*

The mean propagation rate coefficients in copolymerization are measured by at least two techniques, rotating sector<sup>5</sup> and laser flash photolysis.<sup>6</sup> In both these techniques a major assumption is that the monomer concentration at the polymerization site is equal to that in the bulk phase. The bootstrap model<sup>7</sup> proposes a local monomer ratio at the polymerization site that is different from the bulk monomer ratio. For the SMMA polymerizing system it has been suggested that a bootstrap effect does in fact exist.<sup>9</sup> However, this work utilized data that calculated triad fractions from <sup>1</sup>H NMR spectra - an approach that is incorrect.<sup>14</sup> We also note that, if the ratio of monomers is affected by a

bootstrap effect then so may the total concentration of monomers. If this is the case then the measurements of the mean propagation rate coefficients are subject to artifact.

In what follows we consider two manners by which local monomer concentrations and/or ratios at the polymerization site could arise. First, we look at bulk thermodynamics to determine the relationship, if any, between the monomer concentration at the polymerization site and the bulk monomer phase. Secondly, we consider that the proposed local monomer concentration at the polymerization site is a result of molecular scale interactions between the monomers and polymer.

#### *Bulk monomer-polymer thermodynamics*

In polymer kinetic studies a bulk solution containing low percentages of polymer and two monomers where there is no entanglement of the polymer chains has normally been considered as a homogeneous system, but may in fact also be considered as an heterogeneous system containing globules of polymer surrounded by monomer. The dimensions of the globules will presumably be defined by the root-mean-square end-to-end distance of the polymer molecule in the particular monomer (solvent) mixture. The concentration of monomer in the globules may be lower than that in the bulk (monomer) phase. This is a situation analogous to latex particles swollen with monomer.

Maxwell *et al.*<sup>20</sup> measured the concentration of two monomers in latex particle systems. They found for a variety of monomers, with a number of polymer latices, that in each case the ratio of the monomer concentrations was equal in the free monomer phase and the polymer (latex particle) phase. Maxwell *et al.*<sup>20</sup> considered the thermodynamics of latex particle swelling by two monomers in terms of Flory-Huggins theory. By making reasonable assumptions theory predicted that the ratio of two monomers in the bulk phase will be equal to that in the polymer-monomer phase. This result has been proven for a variety of monomers and polymers in the latex particle situation, including the SMMA system<sup>21</sup>. This fact would argue against a bootstrap effect that was caused by bulk thermodynamic effects. However, as will be argued

later in this section this does not discount the possibility of local monomer ratios.

The concentrations of the two monomers in the latex particle system will always be less in the polymer phase than in the pure monomer phase. However, simple calculations utilizing Flory-Huggins theory show that it is unlikely, for monomers like styrene and MMA and copolymers thereof, that the concentration of monomer in the polymer globule phase will be significantly less than that in the pure monomer phase.<sup>19</sup> Even in latex particle systems where the degree of swelling of polymer by monomer is limited, not only by normal constraints, but also by the latex particle surface tension, the monomer concentration typically attains 75% of its maximum value.<sup>20,21</sup> Therefore it is very unlikely that the bulk monomer concentration in the polymer globule phase will cause a significant artifact in the measurement of mean propagation rate coefficients.

### *Monomer-polymer complexes*

As alluded to above the second manner by which the local monomer concentration at the polymerization site may differ from that in the bulk phase is by a 'template' effect or 'solvent-polymer complex' effect.<sup>10</sup> These concepts suggest that there are specific molecular interactions between the two monomers (solvents in the case of styrene and MMA) and polymer that cause the local monomer concentration and/or ratio to be different at the polymerization site than in the free monomer phase. This type of effect has been observed in many copolymerization systems.<sup>10</sup> It has also been noted that the apparent reactivity ratios of the SMMA copolymerization system are dependent upon the solvent utilized during polymerization.<sup>10</sup> These results can be interpreted by, *inter alia*, models based upon monomer-polymer complex effects.

For reasons discussed in the previous section we do not consider it likely that the total local monomer concentration could vary greatly from the bulk value. Hence, in what follows we assume that the deviation of the measured propagation rate coefficient from the predictions of the terminal model are caused by local monomer ratios that differ from the bulk monomer values.

First we develop the models that follow from these propositions. We then fit these models to the data and see whether the values of the fitted parameters are reasonable. In total, two different models are fitted to the data: one of these is a limit of the other.

In the following work an extension to the bootstrap model (eq. 5.27) is developed to account for true monomer ratios, since these may vary with monomer ratio or polymer composition (which itself depends on the monomer ratio). The motivation behind this approach is that if, say, a monomer-polymer complex exists, then it is possible that the relationship between the bulk and true monomer ratios will be non-linear in the monomer ratio. There is no *a priori* reason to think that the bootstrap effect is constant for various monomer ratios. We describe this complex bootstrap effect by an extension to eq. 5.27:

$$x_1 = \frac{[A]}{[B]} = K \frac{[A]^z}{[B]} \quad (5.33)$$

where  $K$  and  $z$  are dummy variables. This versatile empirical form of the monomer ratio will hopefully be capable of fitting any real functional form. Note that, if we set  $z=1$  eq. 5.33 reduces to eq. 5.27. In this case there is a single bootstrap parameter,  $K$ .

Now both the mean propagation rate coefficients and polymer compositions measured by Fukuda *et al.*<sup>5</sup> are simultaneously fitted by the terminal model (eq. 5.2 and 5.4) with the further adjustable parameters that describe the monomer partitioning in the 'complex' bootstrap model (eq. 5.33). We designate the case where  $z=1$  as the simple bootstrap terminal model (SBTM), and where  $z \neq 1$  as the complex bootstrap terminal model (CBTM): this latter model has one extra adjustable parameter,  $z$ . We do not fit these models to the triad sequence distribution data measured in this work since we have already determined that this data is well fitted by the terminal model. Hence, any set of parameters in the terminal model that reproduce the polymer composition also reproduce the triad sequence distribution data.

It should be noted that the penultimate model has six adjustable

parameters and that the restricted penultimate model described by Fukuda *et al.*<sup>5</sup> has four adjustable parameters. The two models utilized in this section have three (SBTM) and four (CBTM) adjustable parameters, respectively. Given the agreement to data of the limited penultimate model it is expected that both these models will provide adequate fits to experiment. It should be noted that a half-penultimate model<sup>22</sup> in which only one of the radicals is allowed to have a penultimate unit effect also fits both the polymer composition and rate data. This model has only three adjustable parameters. However, we cannot see any theoretical justification for the use of this model.

Utilizing the same non-linear least squares fitting package as described in an earlier section<sup>17</sup> the fit to the polymer composition and mean  $k_p$  data of Fukuda *et al.*<sup>5</sup> by both the simple and complex bootstrap terminal models gives the following parameters. (1) SBTM,  $r_1=2.41\pm 0.12$ ,  $r_m=0.11\pm 0.03$  and  $K=0.22\pm 0.05$ . (2) CBTM,  $r_1=2.32\pm 0.13$ ,  $r_m=0.05\pm 0.04$ ,  $K=0.15\pm 0.07$  and  $z=1.17\pm 0.16$ . In both cases a more than adequate fit to the data is described (Figures 5.9 and 5.10). Note that the use of four parameters in the CBTM when three parameters provide an adequate fit in the SBTM indicates a possible lack of uniqueness in some parameters. In fact the functional relationship model<sup>17</sup> indicates that in the SBTM parameters  $r_m$  and  $K$  are highly correlated (*i.e.* have

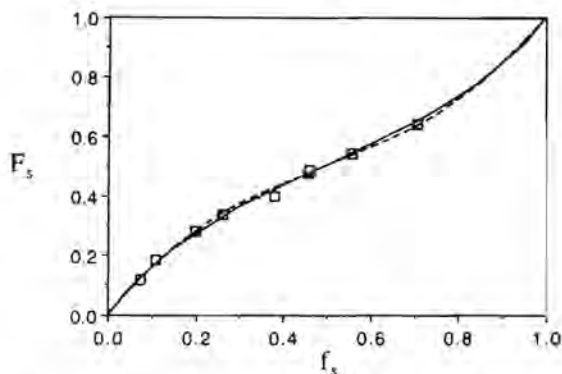


Figure 5.9: Fraction of styrene in copolymer versus fraction of styrene in feed. Experimental results (squares) from ref.5. The solid line represents the fit of the simple bootstrap terminal model (SBTM) with  $r_1=2.41$ ,  $r_m=0.11$  and  $K=0.22$ . The dashed line represents the fit of the complex bootstrap terminal model (CBTM) with  $r_1=2.32$ ,  $r_m=0.05$ ,  $K=0.15$  and  $z=1.17$ .



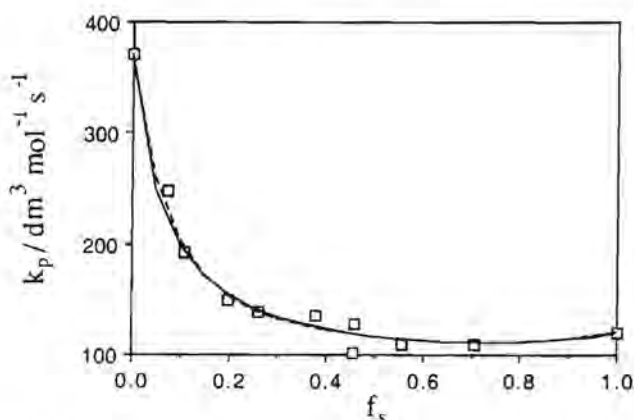


Figure 5.10: Plot of  $k_p$  versus  $f_s$  for SMMA copolymerization at 313 K. Experimental results (squares) from ref.5. The solid line represents the fit of the simple bootstrap terminal model (SBTM) with  $r_s=2.41$ ,  $r_m=0.11$  and  $K=0.22$ . The dashed line represents the fit of the complex bootstrap terminal model (CBTM) with  $r_s=2.32$ ,  $r_m=0.05$ ,  $K=0.15$  and  $z=1.17$ .

a large joint confidence region), and in the CBTM the parameters  $K$  and  $z$  are correlated to  $r_m$ . Statistically, the CBTM shows no improvement in the fit to the data over the SBTM.

The values of the reactivity ratios suggest that the 'apparent' reactivity ratios are very different from the real reactivity ratios predicted by this model. Deviations of this magnitude obviously need independent experimental correlation. More disturbing is the deviation of the bulk and true monomer concentrations. If we concentrate upon the results of the SBTM we see that the ratio of the concentrations of styrene and MMA is 0.22 times that in the bulk (or feed). That is, complex formation between the copolymer and MMA is favoured over that between copolymer and styrene. If a monomer-copolymer complex does exist then it is possible that this complex depends upon the copolymer structure. That is, say, a specific interaction between MMA in the copolymer and the MMA monomer could be favoured at high MMA content in the copolymer. If this is the case then the value of  $z$  in the CBTM should be far from unity. In the CBTM the fitted value of  $z$  is slightly larger than unity suggesting that there may be only a slight polymer composition effect on the

bootstrap effect.

There is some experimental basis for considering that monomer-polymer complex effects may occur in copolymerizations of styrene and MMA, namely the (sometimes large) solvent effect upon the reactivity ratios.<sup>10</sup> However, apart from this fact and the ability of the above models to fit data there is little evidence for the veracity of these bootstrap models. The same is also true of the penultimate and restricted penultimate models, which have no theoretical nor experimental grounding. One possible direct experimental test for the presence of monomer-polymer complexes would be a fluorescence study in which fluorescence probes built into the polymer are quenched by two monomers at different rates. Varying the monomer ratio in time resolved fluorescence studies may provide some direct evidence of a local monomer ratio around the polymer chain.

#### 5.4 Conclusions

Triad sequence distributions for the model copolymerization system, styrene and MMA have never been measured before since <sup>1</sup>H NMR spectra must be interpreted in terms of pentads<sup>14</sup> and all previous <sup>13</sup>C NMR spectra have been interpreted with erroneous signal assignments.<sup>15</sup> The triad sequence distribution of copolymers of styrene and MMA polymerized with differing monomer ratios in bulk were well fitted by the terminal model. This does not entirely disprove penultimate unit effects on polymer microstructure but is much better evidence for the absence of them than simple polymer composition data.

All the current copolymerization data on the SMMA system, including the triad sequence distribution data measured in this work, can be explained by the restricted penultimate model.<sup>5</sup> However, this model has no sound theoretical basis and is also difficult to test by direct experiment. The model may work simply because it contains sufficient adjustable parameters. Despite these doubts the model does explain all the data and hence deserves further study, especially from a theoretical point of view. Further experimental evidence of a

penultimate unit effect must be observed before the restricted penultimate unit is adopted. In the SMMA copolymerization system ESR may distinguish a penultimate unit effect.

New models which incorporate the bootstrap model<sup>7</sup> or monomer-solvent complex model<sup>10</sup> into the terminal model for polymerization can also explain all the existing data on the SMMA polymerizing system. These models presume that the local monomer ratio at the polymerization site is changed from that in the bulk monomer phase. There is some evidence for a solvent-polymer complex effect for this system, namely the variation in measured reactivity ratios with solvent.<sup>10</sup> If a complex between copolymer and monomers does in fact exist then this should be detectable by experiment. For example, quenching by monomers of fluorescence probe incorporated into copolymer could provide evidence for the presence or absence of monomer-polymer complexes.

In conclusion, the triad sequence distributions measured in this chapter for the SMMA system allow us to state with more authority that there is no penultimate unit effect on polymer chain structure. The presence of a non-terminal unit effect on the rate of polymerization (the mean propagation rate coefficient) can be explained by invoking a number of models. Many of these models have been previously described, and in this chapter new interpretations of previously existing models are developed: the monomer-polymer complex and bootstrap models are adapted to account for kinetic effects. Alternatively, new models can also be formulated that explain all extant copolymerization data, *e.g.* if the rates of propagation were dependent upon polymer tacticity then a model similar in algebraic form to the penultimate model could be developed, but with different interpretation of the various reactivity ratios. The content of this chapter suggests that a successful (and physically reasonable) copolymerization model must have at least three adjustable parameters. However, there is no doubt that model discrimination can only proceed if further independent experimental evidence designed to test particular models are performed.

## References

1. Mayo FR., Lewis EM., *J. Am. Chem. Soc.*, 66, 1954, 1944.
2. Bandrup J., Immergut E.H., *Polymer Handbook*, 3rd ed.; Wiley: New York, 1989.
3. Fukuda T., Ma Y-D., Inagaki H., *Polym. J.*, 14, 705, 1982.
4. Hill D.J.T., O'Donnell, J.H., O'Sullivan F.W., *Macromolecules*, 17, 3913, 1982.
5. Fukuda T., Ma Y-D., Inagaki H., *Macromolecules*, 18, 17, 1985.
6. Davis T.P., O'Driscoll K.F., Piton M.C., Winnik M.A., *Macromolecules*, 22, 2785, 1989.
7. Harwood H.J., *Makromol. Chem.*, *Macromol. Symp.*, 10/11, 331, 1987.
8. Fukuda T., Ma Y-D., Inagaki H., *Makromol. Chem. Rapid Commun.*, 8, 495, 1987.
9. Davis T.P., *Polymer Commun.*, 31, 442, 1990.
10. Barton J., Borsig E., 'Complexes in Free Radical Chemistry'; Elsevier: Amsterdam, 1988.
11. O'Driscoll K.F., Davis T.P., *J. Polym. Sci.*, 27, 417, 1989.
12. Moad G., Solomon D.H., Spurling T.H., Stone R.A., *Macromolecules*, 22, 1145, 1989.
13. Tanaka H., Sasai K., Sato T., Ota T., *Macromolecules*, 21, 3536, 1988.
14. Aerdts A.M., Haan de J.W., German A.L., Velden van der G.P.M., *Macromolecules*, 24, 1473, 1991.
15. Aerdts A.M., Haan de J.W., German A.L., *Macromolecules*, accepted; this thesis; Chapter 4.
16. Koenig J.L., *Chemical Microstructure of Polymer Chains*; Wiley: New York, 1980.
17. Hillegers L.T.M.E., *The Estimation of Parameters in Functional Relationship Models*; Ph.D. dissertation: Eindhoven University of Technology, The Netherlands, 1986.
18. O'Driscoll K.F., Reilly P.M., *Macromol. Symp.*, 10/11, 355, 1987.
19. Flory P.J., *Principles of Polymer Chemistry*, Cornell University Press: Ithica, NY, 1953.
20. Maxwell I.A., Kurja J., Doremaele van G.H.J., German A.L., *Makromol. Chem.*, 193, 2049, 1992.
21. This thesis; Chapter 6.
22. Maxwell I.A., Napper D.H., Gilbert R.G., to be published; Louis P. La Polymerisation Radicalaire Libre du Styrene en Milieux Heterogenes; Ph.D. dissertation: University of Liege, Belgium, 1990.

## Chapter 6

### Partial and Saturation Swelling in Latex Particles of Polybutadiene, Styrene Methyl Methacrylate Copolymers and Composite Particles

**ABSTRACT:** Partial and saturation swelling experiments in latex particles of SMMA copolymers, polybutadiene and composite particles containing polybutadiene with styrene and methyl methacrylate grafted were performed with the centrifugation method. Very good agreement is achieved between the experimental results of partial swelling and a simplified theoretical model. The behaviour of monomer partitioning when no monomer droplets are present is independent of polymer type, polymer cross-linking and latex particle diameter. The saturation monomer partitioning experiments also showed good agreement with a simplified thermodynamic theory. The polymer type does not influence the ratio of two monomers (styrene and methyl methacrylate) in the particle and droplet phases. Also, there is no preferential solvation of styrene in polybutadiene. This is an important result for the graft polymerization of styrene and methyl methacrylate. Differences observed in copolymer composition between graft and free copolymers thus cannot be ascribed to monomer partitioning.

#### 6.1 Introduction

Swelling behaviour of seed-latex particles by monomers is of great importance. For example, Methyl methacrylate/Butadiene/Styrene (MBS) and Acrylonitrile/Butadiene/Styrene (ABS) are prepared in two emulsion polymerization steps; in the first step a polybutadiene (PB) seed is prepared (the

rubbery core) and in the second step a monomer mixture (e.g. styrene/methyl methacrylate) is added and copolymerized (the glassy shell). Some of the latter monomers will graft onto the PB particles. The rest of the monomer will polymerize without chemically bonding onto the polybutadiene core, the so called 'free copolymer' (SMMA-f, see Table 6.1 for abbreviations used). The presence of a polybutadiene seed latex in principle may influence the partitioning behaviour of monomers due to different interactions between monomers and polymers. Different monomer concentrations will then influence the composition of the SMMA copolymer grafted onto PB and the free SMMA copolymer. Differences in copolymer composition between grafted SMMA and free SMMA copolymers can affect polymer phase separation<sup>1</sup>. Moreover, the properties of graft polymers depend on the degree of grafting<sup>2</sup>, particle morphology, the amount and length of the grafts, molecular weight and in the case of copolymers, the copolymer composition and compositional distribution.

The influences of process variables on the graft polymerization have been reported by several groups<sup>2,3,4</sup>. However, in order to understand the relations between process conditions, polymer characteristics and mechanical properties more fundamental research is necessary. The way monomers partition between several phases has been described by several investigators<sup>5,9</sup>. The saturation swelling of latex particles has been described by Morton *et al.*<sup>5</sup> and Maxwell *et al.*<sup>6</sup>, and the partial swelling where all monomer is solubilized in the aqueous phase and in the latex particles, by Vanzo *et al.*<sup>7</sup>, Gardon<sup>8</sup> and Maxwell *et al.*<sup>9</sup>. Some partitioning experiments of styrene (S) and acrylonitrile (AN) with polybutadiene latices and films have been reported by Mathey *et al.*<sup>10</sup> Mathey *et al.*<sup>10</sup> estimated the values for the interaction parameter and the surface tension, and showed that theoretically the particle size and cross-linking density of the polybutadiene latex influences the monomer concentration in PB particles. Actually, the interaction parameter and surface tension are hard to determine experimentally and may also be dependent on the volume fraction of polymer<sup>9</sup>. Experimentally<sup>10</sup>, only the styrene concentration in PB latex particles at saturation was measured. The concentrations of the two monomers as functions of different monomer

compositions would be of interest because this gives information about the monomer partitioning in copolymerization (it is known that the presence of S in SAN and graft polymer influences the AN concentration in the latex particles<sup>11</sup>). To understand the swelling behaviour of monomers in polybutadiene, it is better to first understand the swelling behaviour of partially water soluble monomers which are good solvents for their own polymer.

In this chapter experimental results of partial and saturation swelling of the monomers styrene (S) and methyl methacrylate (MMA) in styrene-methyl methacrylate copolymer (SMMA-i), PB and in SMMA-f and PB-SMMA-g (from the MBS graft polymerization) are discussed and compared to predicted results from the semi-empirical equations developed recently by Maxwell *et al*<sup>69</sup>. The following parameters were varied in the monomer partitioning experiments: latex particle diameter (of PB), cross-linking density (of PB), polymer type, copolymer composition and degree of grafting (of MBS).

## 6.2 Experimental section

The polybutadiene latices were prepared by emulsifier free emulsion polymerization<sup>12</sup> (Table 6.2), leading to monodisperse seed latexes. Butadiene (DSM, Hydrocarbons, Geleen, The Netherlands) was purified by distillation. The polymerizations were performed in a 5 L stainless steel reactor fitted with two twelve-bladed turbine impellers. A conversion of 95% was reached after 20 hours. The larger PB particle diameter sizes were made in a 2.5 L stainless steel reactor fitted with a helical ribbon rotator; the first 4 hours at 353 K, then 92 hours at 333 K (85 % conversion). The average particle sizes and particle size distributions were determined by Transmission Electron Microscopy (TEM). The details of the PB latices are given in Table 6.3. Different cross-linking densities are achieved by varying the mercaptan concentrations and by polymerizing to higher final conversions<sup>13</sup>. High degrees of cross-linking can also be achieved by heating a PB latex for 8 hours at 363 K. The gel content was measured as an indication of the degree of cross-linking of the PB. This was

determined by the solvent extraction method of the soluble fraction of the polybutadiene. The insoluble residue is by definition the gel fraction. Before using the PB for the monomer partitioning experiments, the latex was dialysed in a membrane tube in order to remove excess surfactant and monomer (Medicell International Ltd, London, England). The water was changed five times every four hours, during two days<sup>14,15</sup>. After this the solid contents were determined by gravimetry.

*Table 6.1: Abbreviations used for different types of polymers*

PB	polybutadiene
SMMA-i	styrene-methyl methacrylate copolymer formed independently, <i>i.e.</i> in the absence of PB seed
PB-SMMA-g	a composite polymer of PB with grafts of S and MMA copolymer
SMMA-f	free SMMA copolymer formed during MBS graft polymerization
MBS	product of grafting process, <i>viz.</i> PB-SMMA-g + SMMA-f

The SMMA copolymers (SMMA-i) were made in a 1 L stainless steel reactor fitted with a twelve bladed turbine impeller, under nitrogen according to a standard recipe given in Table 6.2. Also in this table the recipe for the graft polymerization MBS is given, made in the same reactor. These latices were dialysed in the same manner as the PB latices. The monomers used in the monomer partitioning experiments were applied as received without any further purification. The presence of a free radical inhibitor prevents polymerization during the monomer partitioning experiments.

The determination of the monomer partitioning was performed with the centrifugation method<sup>69</sup>. In the partial swelling experiments the latex was mixed with known amounts of MMA and in the saturation experiments with MMA and S. After 2 hours shaking, equilibrium was reached. It is necessary to know the solid content of the latex, the copolymer composition and for the MBS polymer also the degree of grafting. Polymer densities were calculated by



the appropriate averaging of the densities of the homopolymers. For the experiments with the MBS polymers the amount of PB-SMMA-g polymer and SMMA-f were calculated from the degree of grafting (measured by NMR)<sup>6</sup> and the total weight. The swollen polymer particles phase and aqueous phase (and monomer phase) were separated using an ultracentrifuge (55000 rpm Centrikon T-2060, 6-15 hours) at room temperature. Monomer concentrations in polymer and aqueous phases were determined by gas chromatography (GC). The PB and PB-SMMA-g phases were swollen in toluene with acetone as an internal standard. The SMMA-i and SMMA-f copolymers were dissolved in acetone with toluene as an internal standard. The concentration of MMA in the aqueous phase was determined after adding a standard 2-propanol solution in water to a sample of the aqueous phase. In the monomer phase samples only the monomer ratio was determined.

*Table 6.2: Seed latex recipes of some polybutadiene, SMMA-i copolymers and graft polymers MBS, in parts by weight.*

ingredients	PBI	PBII	SMMA-i 25/75	SMMA-i 52.5/47.5	MBSI	MBSII
water	2800	691	600	600	600	762
S	-	-	30.9	64.18	23.18	22.015
MMA	-	-	89.1	55.82	66.82	62.658
But(PB)	1200	691	-	-	30 <sup>a</sup>	29.75 <sup>a</sup>
SDS	-	-	2	2	1.297	-
(S)KPS	15.14	3.74	0.2	0.2	1.427	-
(S)KCB	7.74	1.91	-	-	0.638	-
(t)nDM	-	12	6.91	1.2	1.2	0.90.85
CHP	-	-	-	-	-	0.213
SFS	-	-	-	-	-	0.213
FeSO <sub>4</sub> /EDTA	-	-	-	-	-	0.005

where But is the butadiene monomer, SDS is sodium dodecyl sulfonate (Merck), (S)KPS is sodium or potassium persulfate, (S)KCB is sodium or potassium carbonate, (t)nDM is tertiary or normal dodecyl mercaptan, CHP is cumene hydroperoxide, SFS is sodium formaldehyde sulfoxylate, FeSO<sub>4</sub>/EDTA is iron(II)sulfate chelated with ethylenediaminetetraacetic acid.

### 6.3 Results and discussion; Partial swelling of latex particles by one monomer

The partial swelling by monomers and solvents of latex particles composed of a cross-linked polymer can be described by the Vanzo equation in combination with the Flory-Rehner theory<sup>9</sup>:

$$\ln(1 - v_p) + v_p(1 - 1/M_n) + \chi v_p^2 + (2 V_m \gamma v_p^{1/3} / R_0 R T) + (V_m d_p / M_c)(v_p^{1/3} - v_p/2) = \ln ([M]_p/[M]_{p,sw}) \quad (6.1)$$

- where
- $v_p$  = the volume fraction of polymer in the latex particles
  - $M_n$  = the number average degree of polymerization
  - $R$  = the gas constant
  - $T$  = the temperature
  - $\chi$  = the Flory-Huggins interaction parameter
  - $V_m$  = the partial molar volume of the monomer
  - $\gamma$  = the particle-water interfacial tension
  - $R_0$  = the unswollen radius of the latex particle
  - $d_p$  = the density of the polymer
  - $M_c$  = the molecular weight between crosslinks
  - $M_{aq}$  = the monomer concentration in the aqueous phase
  - $M_{aq,sw}$  = the monomer concentration in the aqueous phase at saturation

The monomer partitioning behaviour between the aqueous phase and the latex particles can be predicted by this equation. It is necessary to know the values for the interfacial tension ( $\gamma$ ) and for the interaction parameter ( $\chi$ ). Unfortunately, these values are hard to determine and dependent on the volume fraction of the polymer. For describing the partitioning, however, it is not longer necessary to know these parameters. Maxwell *et al.*<sup>9</sup> derived a semi-empirical equation where the value of the sum of the residual free energy and the particle-water surface free energy terms in the Vanzo equation are estimated from the saturation swelling volume fraction of polymer<sup>9</sup>.

$$\ln(1 - v_p) + v_p(1 - 1/M_n) + \text{corr.} = \ln(M_{aq}/M_{aq,sw}) \quad (6.2)$$

in which the correction term is calculated from the Morton equation and saturation swelling data<sup>9</sup>:

$$\text{corr.} = - [ \ln(1 - v_{p,sw}) + v_{p,sw}(1 - 1/M_n) ] \quad (6.3)$$

where  $v_{p,sw}$  is the volume fraction of polymer at saturation in the latex particles and  $M_n$  is the number average degree of polymerization. Equation 6.2 showed very good agreement with experimental results for several SMA copolymers and other polymers<sup>9</sup>. The experimental monomer concentrations of MMA in latex particles of SMMA-i, PB, SMMA-f and PB-SMMA-g during partial swelling are discussed below and compared with the predictions of equation 6.2.

#### Type of polymer

In Figure 6.1 the partitioning results are displayed for MMA in two SMMA-i copolymers. The latices differ only in copolymer composition (see Table 6.2). As has already been shown for the SMA system<sup>9</sup>, the copolymer composition has little effect on the partitioning of MA in seed latices. Although

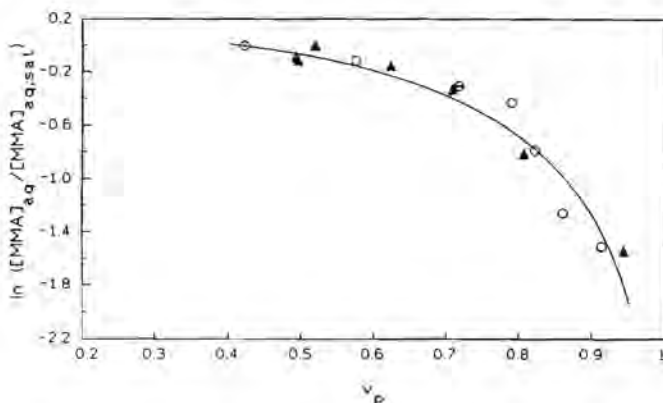


Figure 6.1: Comparison of theoretical predictions (according to equation 2) with experimental results of MMA partitioning for copolymer seed latices SMMA-i (25/75) (open circles) and SMMA-i (50/50) (closed triangles).

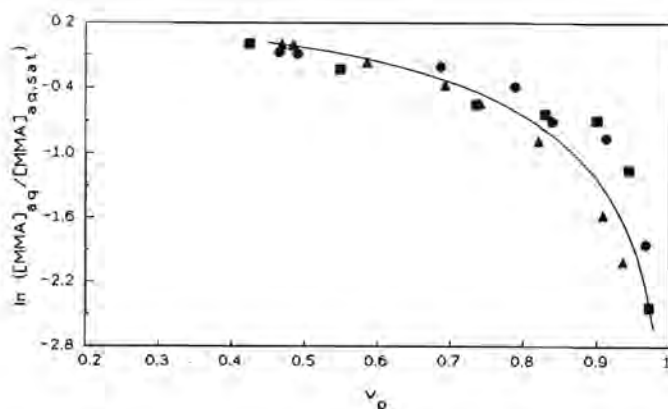


Figure 6.2: Comparison of theoretical predictions (according to equation 2) with experimental results of MMA partitioning for a seed latex PB1a (closed circles), PB1b (closed squares) and PB1I (closed triangles).

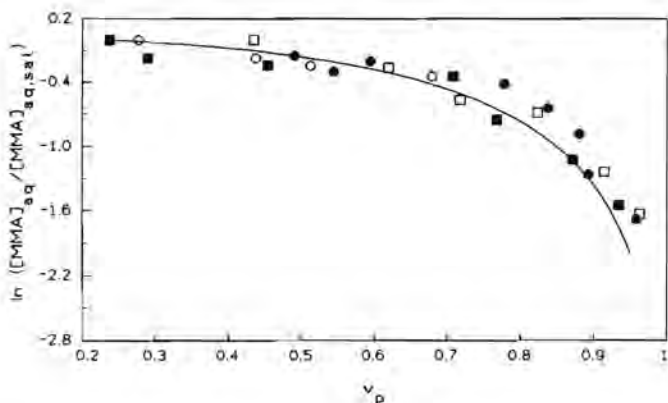


Figure 6.3: Comparison of theoretical predictions (according to equation 2) with experimental results of MMA partitioning for PB-SMMA-g (closed circles) and SMMA-f (closed squares) of MBSI, and PB-SMMA-g (open circles) and SMMA-f (open squares) of MBSII.

the interaction parameter will change with changing copolymer composition, the value of this interaction parameter has a small influence on the monomer partitioning. This also holds for the swelling MMA in polybutadiene latex (PBIa, Figure 6.2) and for PB-SMMA-g (Figure 6.3). From this it can be concluded that for varying polymer latices, including those of PB, the free energy associated with the configurational entropy of mixing of monomer and polymer is the dominant term in equation 6.2. Hence the change in partial swelling of different seed latices with one monomer is small.

#### Particle size and degree of cross-linking

The polybutadiene latices are prepared by batch emulsion polymerization processes. Depending on the conversion, the temperature and the mercaptan concentration, the degree of cross-linking will vary<sup>13</sup>. In order to show effect of the particle size and degree of cross-linking on the partial swelling of latex particles with MMA, experiments were performed with different PB latices (Table 6.3). The gel content is used as an indication of the degree of cross-

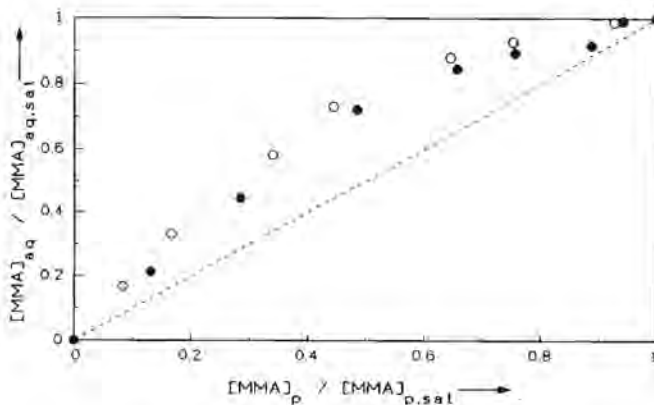


Figure 6A: Experimentally determined MMA concentrations in the aqueous phase as function of the MMA concentration in the particle phase (concentrations normalized to saturation) in SMMA-i (25/75) (closed circles) and in PBIa (open circles)

linking. PBI has an average particle diameter of 209.7 nm, PBIa and PBIb have a gel content of 72% and 95%, respectively. PBII has an average particle diameter of 305 nm and a gel content of 70%. Experimental results of the swelling of different PBs with MMA are shown in Figure 6.2. Neither the particle size nor the degree of cross-linking significantly affect the monomer partitioning, which is in agreement with the results of Maxwell *et al.*<sup>9</sup>, who showed that the free energy due to the configurational entropy of mixing of monomer and polymer is the dominant factor.

Table 6.3: Number average, weight average unswollen particle diameter, polydispersity and gel content of some PB seed latices.

	D <sub>n</sub> (nm)	D <sub>w</sub> (nm)	P <sub>n</sub>	gel content (%)
PBIa	209.7	212.7	1.014	72
PBIb	209.7	212.7	1.014	95
PBII	305	401	1.313	70

Table 6.4: Characteristics of two MBS latices measured by NMR<sup>16</sup>.

	degree of grafting	F <sub>s</sub> in SMMA-g	F <sub>s</sub> in SMMA-f
MBSI	0.42	0.18	0.26
MBSII	0.85	0.19	0.28

Higher degrees of cross-linking occur when a polybutadiene seed is used for a graft polymerization, resulting from six hours of polymerization at 323 K and from grafting. Partial swelling experiments were performed with two types of MBS (Table 6.4), only differing in the degree of grafting (defined as the ratio of graft-SMMA over PB in PB-SMMA-g polymer). Again, no difference is found in partitioning between the PB-SMMA-g and the SMMA-f formed during graft polymerization (Figure 6.3). From Figure 6.1-6.3, it appears that during partial swelling (stage III in emulsion polymerisation) the

relation between the monomer concentration in the aqueous phase and the monomer concentration in the particle phase ( $1-v_p$ ) is convex. Thus the monomer concentration in the aqueous phase is closer to saturation than in the particle phase. This relation does not change if the monomer concentration in the aqueous phase is plotted on a non-logarithmic scale (Figure 6.4). This means that in interval III of emulsion polymerization with highly water soluble monomers, a significant amount is resides in the aqueous phase, which reduces the monomer concentration and the rate of polymerization in the latex particles<sup>17</sup>.

**6.4 Results and discussion; saturation swelling of latex particles by two monomers**

At equilibrium the partial molar free energy of each monomer will be equal in each of the three phases, *i.e.* the particle, the monomer droplet and the aqueous phase. This leads to the following equation for monomer  $i$ :

$$\ln v_{pi} + (1-m_i)v_{di} + v_p + \chi_i v_{pi}^2 + \chi_w v_p^2 + v_{pi}v_p(\chi_i + \chi_p - \chi_w m_w) + (2V_{mi}\gamma v_p^{1/3})/RR_0T = \ln v_{di} + (1-m_i)v_{di} + \chi_i v_{di}^2 = \ln([M]_i/[M]_{i, sat}) \quad (6.4)$$

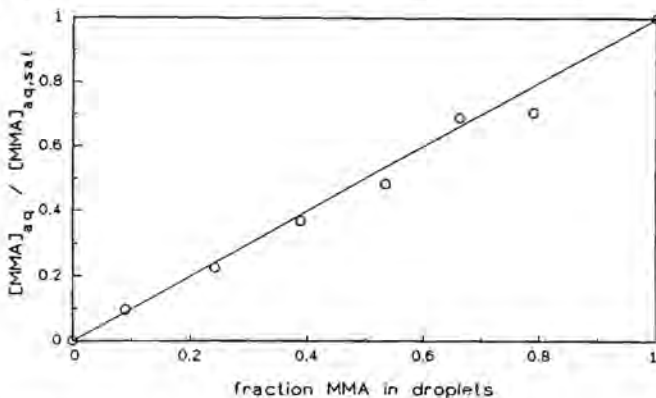


Figure 6.5: Experimentally determined MMA concentrations in the aqueous phase as function of the fraction MMA in the droplet phase with S as comonomer in the presence of a polybutadiene latex.

where  $v_{pi}$  and  $v_{pj}$  are the volume fractions of monomer  $i$  and  $j$  in the latex particles, respectively,  $\chi_{ij}$  the interaction parameter between monomers  $i$  and  $j$ ,  $\chi_{ip}$  and  $\chi_{jp}$  are, the interaction parameters between either of the monomers  $i$  and  $j$  and the polymer. The term  $m_i$  is the ratio of the molar volumes of monomers  $i$  and  $j$ ,  $\gamma$  is the particle-water interfacial tension and  $R_0$  the unswollen radius of the latex particle,  $v_{di}$  represents the volume fraction of monomer  $i$  in the droplets, and  $v_{dj}$  the volume fraction of monomer  $j$  in the droplets,  $[M]_i$  and  $[M]_{i,sat}$  are the monomer concentrations in the aqueous phase and in the aqueous phase at saturation, respectively.

A similar equation applies to monomer  $j$ .

An important assumption made in equation 6.4 is that a polymer seed does not change the relation between aqueous and monomer phase<sup>69</sup>; water soluble monomers show a proportional relationship between the aqueous phase and the monomer phase, obeying Henry's Law<sup>6</sup>. From Figure 6.5 it can now be derived that the same assumption of Henry's law can be made in the presence of polybutadiene seed latex particles: the concentrations of monomer in the aqueous phase and droplets are still proportional.

Equation 6.4 and a similar equation for monomer  $j$  can be used to predict the monomer partitioning for latex systems containing two monomers. However, the values for the interaction parameters and the interfacial tension are hard to determine and are dependent on the volume fraction of polymer in the latex particle as well as on the monomer ratio. So the monomer partitioning is very hard to predict.

Simplifications to the theory of swelling of latex particles with two monomers recently made by Maxwell *et al.*<sup>6</sup>, are: the volume fractions of monomers are equal or similar, the interaction parameter of mixing of two monomers is rather small, and the interaction parameters for each monomer with the same polymer are equal ( $\chi_{ip} = \chi_{jp}$ ). These assumptions then lead to the following result<sup>6</sup>:

$$f_{pi} = f_{di} \quad (6.5a)$$

$$f_{pj} = f_{dj} \quad (6.5b)$$



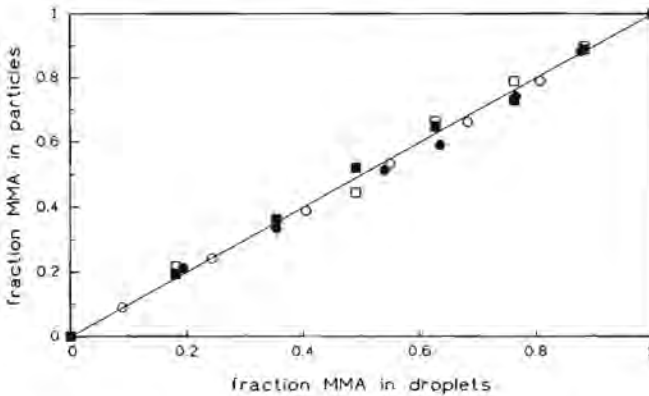


Figure 6.6: Experimentally determined fractions MMA in latex particles as a function of the fraction MMA in the droplet phase. MMA and S in : PB1a (open circles), SMMA-i 25/75 (closed circles), SMMA-f from MBSI (open squares), and PB-SMMA-g of MBSI (closed squares). The solid line gives the theoretical prediction according to equation 6.5.

where the monomer volume fraction of monomers  $i$  and  $j$  in the droplets is given by  $f_{d(i)}$  and in the particle phases by  $f_{p(i)}$  (the volume of the polymer in the latex particles is not included in these fractions). With the additional assumption of  $m_i = m_j$ , the monomer molar fractions in droplet and particle phases are also equal.

The actual concentrations of two monomers in the particle phase can also be estimated<sup>6</sup>. These calculations only require the values of the individual saturation concentrations of the two monomers in the latex particles. The total concentration should be proportional to the ratio of monomers in the droplets. For a particular seed latex the concentration of monomer  $i$  within the particles ( $C_i$ ) as a function of the fraction of monomer  $i$  in the droplets, is given by<sup>6</sup>:

$$C_i = f_{di}[(C_{im} - C_{jn})f_{di} + C_{jn}] \quad (6.6a)$$

Similarly for monomer  $j$ :

$$C_j = f_{d_j}[(C_{jm} - C_{im})f_{d_i} + C_{im}] \quad (6.6b)$$

where  $C_{im}$  and  $C_{jm}$  are the maximum saturation concentrations of monomers  $i$  and  $j$  in the latex particles. For the monomers styrene-methyl acrylate, styrene butyl acrylate and methyl acrylate-butyl acrylate in their homopolymers and copolymers good agreement was observed between experimental results and this simplified theory<sup>6</sup>. From these results it was concluded<sup>6</sup> that the entropy of mixing of the two monomers is the dominant thermodynamic contribution to the free energy, and the presence of the polymer has no significant effect upon the ratio of the two monomers in the polymer and in monomer droplet phases, respectively.

Figure 6.6 shows the experimental results of the partitioning of styrene and MMA between particle and monomer droplet phase in two SMMA- $i$  copolymers of different compositions. For both polymers it can be seen that the fraction of the monomer in the droplet and particle phases are equal, as predicted by equation 6.5. Utilizing a different polymer, PB, the same characteristics are observed. This means that the assumptions made in the derivation of equation 6.5 are also valid for PB: the type of polymer has no effect on the mixing of two monomers. This is an important result because polybutadiene is often used as a seed in graft copolymerization, for instance in the preparation of MBS or ABS. Also for modelling purposes and for the understanding of the resulting MBS copolymer microstructure, the monomer partitioning of the two monomers is of great importance. For this reason saturation monomer swelling experiments were also performed with MBS polymers.

Centrifugation of MBS polymers at saturation swelling give four layers in the centrifugation tube. From the bottom to the top the successive layers contain: the SMMA- $f$  copolymer, the aqueous phase, the composite polymer PB-SMMA- $g$  and the monomer phase. Note that the particle phase in this case is composed of individual PB-SMMA- $g$  polymer and SMMA- $f$  copolymer

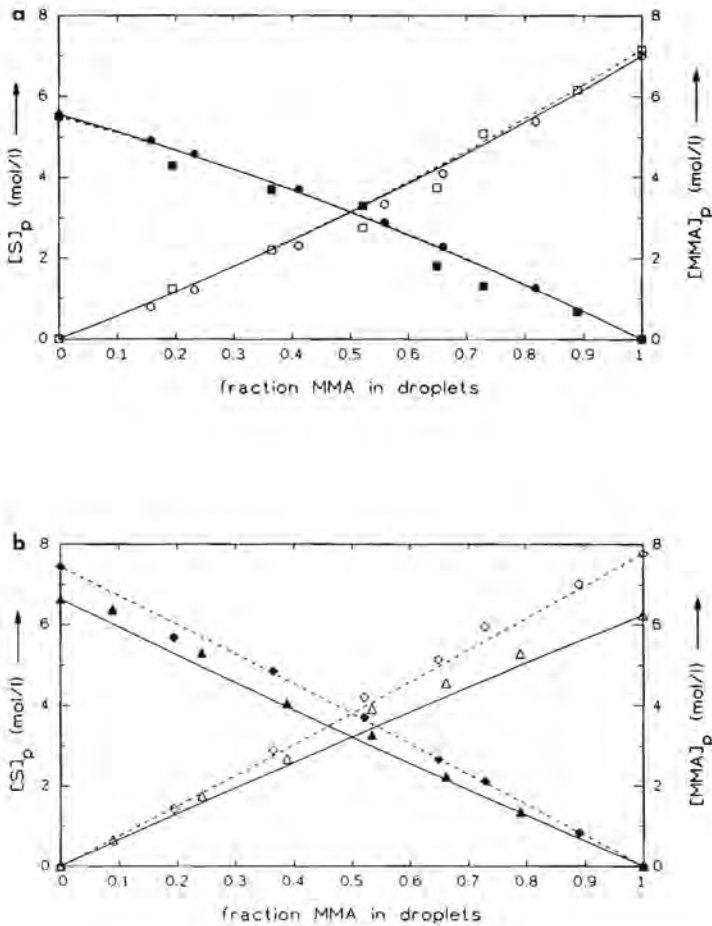


Figure 6.7: Experimentally determined monomer concentrations in the latex particle phase as a function of the fraction MMA in the droplet phase (symbols) compared with theoretical predictions of equation 6.6 (lines); (a) MMA concentrations (open symbols), S concentrations (full symbols) in SMMA(25/75) copolymer (full lines and circles) and in SMMA-f of MBSI (dotted lines and squares). (b) MMA concentrations (open symbols), S concentrations (full symbols) in PB1a (solid lines and triangles) and in PB-SMMA-g of MBSI (dotted lines and diamonds).

phases. The monomer concentrations and the monomer ratios in all four layers were determined. Again, no differences were observed in the fraction of monomer in the droplet and particle phases between SMMA-f, PB-SMMA-g, SMMA-i and PB as can be seen in Figure 6.6. From this Figure 6.6 we can conclude that the molar fraction of the monomers is the same in PB, SMMA-i and SMMA-f copolymer, as well as in PB-SMMA-g polymer. This again shows that the ratio of the two monomers is independent of the polymer type. The observed differences in copolymer composition between PB-SMMA-g and SMMA-f (Table 6.4) thus cannot be ascribed to monomer partitioning effects.

In Figure 6.7a the concentrations of the monomers S and MMA in the SMMA-i and SMMA-f copolymer particle phases are plotted against the fraction of MMA in the droplet phase. In Figure 6.7b the concentrations of the monomers S and MMA in the PB and PB-SMMA-g particle phases are plotted against the fraction of MMA in the droplet phase. The absolute value of the degree of swelling depends upon polymer and monomer type (an effect of different interaction parameters and interfacial tensions). The monomer concentrations in SMMA copolymers and in the free copolymer formed during the grafting process are the same (see Fig 6.7a). Obviously (Fig 6.7b) the MMA concentration in the PB-SMMA-g polymer is higher than in PB, and that the S concentration is also increased, but not to the same extent. However, it should be emphasized that the higher concentrations in the particle phases do not change the ratio between the two monomers, but only could have an effect on the polymerization rates in the latex particles. The lines in Figure 6.7a,b are the predictions of equation 6.6; only the concentrations of the two monomers, when exclusively swelling a particular latex, are required. In these calculations a very good agreement is achieved between the experimental results and the theoretically predicted monomer concentrations according to equation 6.6, at any ratio of monomers in the droplets.

## 6.5 Conclusions

MMA monomer concentrations in the latex particle, monomer droplet and aqueous phases were measured with the centrifugation method. Experiments showed that the partitioning of MMA is independent of the type of polymer/SMMA copolymers of different composition and PB. Moreover, the partitioning of MMA in polybutadiene is independent of particle size, polymer degree of cross-linking and the presence of SMMA-g. These experiments also show that the partitioning of monomer between the aqueous and latex particles phases, when there is no separate monomer phase present can be predicted using the semi-empirical equation of Maxwell *et al.*<sup>5</sup>, which requires only the values of the saturation concentration of the monomer in the particle and aqueous phases. This result can be understood<sup>9</sup> when realizing that the contribution of the configurational entropy of mixing of monomer and polymer dominates the free energy of monomer partitioning, and that both the interfacial free energy and residual free energy terms do not significantly influence the degree of swelling.

Experiments were also carried out at saturation swelling of different polymers by two monomers. The results of these experiments show that the mixing of the two monomers, S and MMA, is independent of the polymer type and that again the ratio of monomers in droplet and particle phases is equal. The saturation partitioning of monomers between latex particles and droplet phases can be predicted by the simplified equations of Maxwell<sup>6</sup>. This equation only requires the individual saturation concentrations of the two separate monomers in the latex particles. These results were based on the finding that the entropy of mixing of two monomers is the dominant contribution to the thermodynamic equilibrium reached<sup>6</sup>. Hence, the monomer ratio becomes independent of the type of polymer phase considered. Only the absolute value of the degree of swelling depends upon monomer and type of polymer. This is an important result in regard of the graft polymerization of S and MMA onto polybutadiene. In all systems considered, *viz.* SMMA-i, polybutadiene, PB-SMMA-g, SMMA-f, and monomer droplets, the ratio of the two monomers is equal.

## References

1. Molau, G.E., *J. Polym. Sci.*, A3, 1965, 4235.
2. Baum B., Holley W.H., Stiskin H., White R.A., Willis P.B., Wilde A.F., (DeBell and Richardson, Inc, Enfield, Conn.), *Adv. Chem. Ser.*, 1976, (Thoughness and Brittleness Plast. Symp., 263, 1974)
3. Locatelli J.L., Riess G., *Angew. Makromol. Chem.*, 28, 161, 1973.
4. Locatelli J.L., Riess G., *Angew. Makromol. Chem.*, 35, 47, 1974.
5. Morton M., Kaizerman S., Atlier M.W., *J. Colloid Sci.*, 9, 300, 1954.
6. Maxwell I.A., Kurja J, Doremaele van G.H.J., German A.L., *Makromol. Chem.*, 193, 2065, 1992
7. Vanzo E., Marchessault R.H., Stannett V., *J. Colloid Sci.*, 20, 62, 1965.
8. Gardon J.L., *J. Polym. Sci.*, PartA-1, 6, 2859, 1968.
9. Maxwell I.A., Kurja J, Doremaele van G.H.J., German A.L., Morrison B.R., *Makromol. Chem.*, 193, 2049, 1992.
10. Mathey P., Guillot J., *Polymer*, 32, 5, 934, 1992.
11. Locatelli J.L., Riess G., *J. Polym. Sci.*, *Polym. Let. Ed.*, 11, 257, 1973.
12. Verdurmen E.M.F.I., German A.L., to be published.
13. Weerts P, Ph.D-thesis, Technische Universiteit Eindhoven, 1990.
14. Vanderhoff J.W., Hul van der H.J., Tausk R.J.M., Overbeek J.T.H.G., 'The Preparation of Monodisperse Latexes with Well-characterized Surfaces Clean Surfaces', in 'Clean Surfaces: Their Application and Characterization for Interfacial Studies', G. Goldfinger Ed., Marcel Dekker, Inc. New York (1990)
15. Ahmed S.M., El Aasser M.S., Pauli G.H., Poehlein G.W., Vanderhoff J.W., *J. Colloid and Interfac. Sci.*, 2, 73, 1980.
16. Aerdts, A.M., Kreij de J.E.D., Kurja J, German A.L., "Emulsifier Free Grafting of Styrene and Methyl methacrylate onto Polybutadiene and Determination of the Copolymer Microstructure" to be published.
17. Maxwell I.A., Verdurmen E.M.F.I., German A.L., *Makromol. Chem.*, 193, 2677, 1992.

## Chapter 7

### Emulsifier free Grafting of Styrene and Methyl Methacrylate onto Polybutadiene and Determination of the Copolymer Microstructure

**ABSTRACT:** Styrene / methyl methacrylate monomer mixtures (75/25) were copolymerized at 323 K in the presence of a polybutadiene seed latex using either a water soluble (potassium persulfate) or an oil soluble (cumene hydroperoxide) initiator. The PB seed latex was made via an emulsifier free emulsion polymerization process. The graft copolymerizations were performed over a range of emulsifier concentrations. The emulsifier free polymerization with cumene hydroperoxide shows a very high degree of grafting while neither secondary nucleation nor coagulation was observed. Furthermore, the graft polymers have been extensively studied in terms of intra- and intermolecular microstructure. For this purpose breaking of the polymer backbone by means of ozonolysis was necessary. The grafted styrene methyl methacrylate copolymer is less rich in styrene than the free copolymer. The chemical composition distributions of the graft copolymer were broader than those of the free copolymer.

#### 7.1 Introduction

Various important physical and mechanical properties of the methyl methacrylate/butadiene/styrene (MBS) polymers are affected by many variables, such as the degree of grafting, the particle morphology, the heterogeneity in the inter- and intramolecular microstructure. Differences in microstructure can cause phase separation<sup>1</sup> and reduction of the transparency. The chemical microstructure of the copolymers depends on the reactivity ratios

of the monomers, the monomer partitioning behaviour between the various phases in the emulsion system, and the type of process used (batch or (semi-)continuous). Batch processes are known to give bimodal or very broad chemical composition distributions, when there is a strong composition drift<sup>2</sup>.

In seeded emulsion polymerization the monomers are distributed between the polymer phase (polybutadiene or graft polymer), the aqueous phase, and if present the monomer droplets. During emulsion polymerization the local monomer ratio can be quite different from the overall monomer ratio. Any possible differences in monomer concentrations between the reaction domains of graft and free polymer (even when no second crop of particles is formed, since domain formation within the particle may occur), will lead to a different intramolecular microstructure of the free copolymer as compared with that of the graft copolymer. The relevant monomer partitioning data were measured and discussed in Chapter 6<sup>3</sup>. It was found for the composite particles of MBS<sup>3</sup> as well as for other styrene-acrylate systems<sup>4</sup>, that the configurational entropy of mixing of two monomers is the dominant thermodynamic factor and that the presence of polymer has no significant effect upon the ratio of the two monomers when comparing the polymer and monomer droplet phases. It was quite remarkable that notwithstanding these results of the monomer partitioning experiments, significant differences were found between the microstructure of the graft and free copolymer.

A study was performed to prepare copolymers of styrene and methyl methacrylate grafted onto polybutadiene. There are some limiting conditions in order to perform this study in a reliable way. Firstly, it is important to avoid coagulation and the formation of new particles. Secondly, a certain minimum degree of grafting is required to allow accurate analysis of the grafts. In a series of preliminary experiments the proper conditions to meet these requirements were determined by varying some process parameters, in particular the type of initiator and the emulsifier concentration. The purpose of this study was to investigate the intramolecular microstructure (sequence distribution)<sup>5,6</sup> and intermolecular microstructure (average copolymer composition, chemical composition distribution<sup>7</sup>, molecular weight distribution) of the SMMA copolymer grafted onto PB and of the free SMMA copolymer.



## 7.2 Experimental

### 7.2.1 Procedures and analytical techniques used in emulsion homopolymerization of butadiene

#### *Materials and preparation of the polybutadiene<sup>8</sup>*

The butadiene (DSM, Hydrocarbons, Geleen, The Netherlands) was purified by condensing the vapour from a 27 L storage vessel into a cooled steel recipient. In Table 6.2 (PBI)<sup>3</sup> the standard recipes of the emulsion polymerization of butadiene are given. The polybutadiene latices were made by means of an emulsifier free emulsion polymerization process<sup>9</sup>, which gives a monodisperse latex. The polymerizations were performed in a 5 L stainless steel reactor fitted with two twelve bladed turbine impellers. The temperature was 353 K and the impeller speed was 400 rpm.

#### *Particle size analysis*

The average particle sizes and particle size distributions were determined by means of transmission electron microscopy (TEM, Jeol 2000 FX). The polybutadiene samples were first diluted 400 times, after which the double bonds of the PB were stained with osmium tetroxide (OsO<sub>4</sub>). Subsequently, the latices were dried on a 400 Mesh grid. Typically 750-1000 particles were counted with a Zeiss TGA-10 particle analyzer. The polydispersity is defined as:

$$P_n = \frac{d_w}{d_n} \quad (7.1)$$

where  $d_w = (\sum n_i d_i^4) / (\sum n_i d_i^3)$  (the weight average diameter),  $d_n = (\sum n_i d_i) / (\sum n_i)$  (the number average diameter) and  $n_i$  represents the number of particles with diameter  $d_i$ .

The characteristics of the seed latices produced during this research are summarized in Table 6.3 (PBIa)<sup>3</sup>. From this table it is obvious that the particle diameters of these latices show a narrow distribution, i.e. the polydispersity is close to unity.

### *Gel content*

The determination of the gel content is based on a toluene extraction of the soluble fraction of the polybutadiene (PB)<sup>8</sup>. The insoluble part is the gel fraction by definition. The isolation of the emulsifier free polybutadiene was difficult due to the high degree of stabilization of the latex by the sulfate groups of the initiator. Precipitation only occurs when aluminium nitrate was added in combination with an excess of methanol. The coagulum was washed three times with water and methanol and then dried under nitrogen at 323 K during 5 hours. To 1 gram of an accurately weighed PB sample in a stoppered flask, 100 ml toluene was pipetted, after which the mixture was gently shaken for at least 48 hours at room temperature in the dark. The mixture is then filtered over a 100 mesh filter, and 50 ml of the filtrate was evaporated to dryness in a weighed aluminium dish. The gel content is calculated according to  $(w_{PB} - 2w_f) / w_{PB}$ , where  $w_{PB}$  is the weight of the PB sample and  $w_f$  is the weight of the dried filtrate.

### **7.2.2 Processes developed and analytical techniques used in emulsion graft copolymerization of styrene and methyl methacrylate onto polybutadiene seed particles**

#### *Materials and preparation of the graft polymers*

The batch graft polymerizations were performed in a 1 L stainless steel reactor under nitrogen at 323 K with a twelve-bladed turbine impeller and at a stirrer speed of 300 rpm.

Before using a PB latex in the graft copolymerizations, the latex was dialysed in a membrane (Medicell International LTD, London, England). The water was changed five times every four hours and this has been found sufficient to remove most inorganic ingredients<sup>10</sup>. After this, the solid content was determined.

The monomers styrene (S, Merck) and methyl methacrylate (MMA, Merck) were distilled under nitrogen at reduced pressure and subsequently stored at 277 K under nitrogen. The chain transfer agent n-dodecyl mercaptan

(nDM, Fluka, for synthesis), the emulsifier sodium dodecylsulfate (SDS, Fluka, purity ~99%) and the buffer sodium hydrogen carbonate ( $\text{NaHCO}_3$ , Merck, p.a.) were used as received without further purification. The water was distilled twice and stored under nitrogen. The initiators used will be discussed in more detail. The emulsion graft polymerization processes were performed with a water soluble initiator potassium persulfate ( $\text{K}_2\text{S}_2\text{O}_8$ , KPS, Fluka, p.a.) or with a more oil-soluble initiator cumene hydroperoxide (CHP) in combination with a redox system<sup>11</sup>. The redox initiator system, CHP ( $\text{C}_9\text{H}_{12}\text{O}_2$ , Fluka, 80% pure), sodium formaldehyde sulfoxylate (SFS) ( $\text{CH}_3\text{NaO}_3\text{S}\cdot 2\text{H}_2\text{O}$ , Fluka), Iron(II)sulfate ( $\text{FeSO}_4$ , Fluka) and Ethylenediamine tetraacetic acid (EDTA, Fluka) were also used without further purification. The CHP was used as received, a solution was made of SFS, and of  $\text{FeSO}_4$  and EDTA as well, all in oxygen free water at pH=4. The ratio of the components in the redox system added, CHP/EDTA- $\text{Fe}^{2+}$ /SFS, was 1/0.02/1 (w/w/w). The mechanism of the formation of the initiating species is shown in Figure 7.1<sup>12</sup>.

The reactor was filled with the ingredients in the following order; first, the PB seed latex was added to the reactor together with an emulsifier solution (when emulsifier was used). Next, the reaction medium was degassed and purged with nitrogen. After this the monomers were added together with the mercaptan (nDM). The initiator was added after the polybutadiene seed latex had been allowed to swell with the monomers for 1 hour at reaction temperature. Addition of EDTA- $\text{Fe}^{2+}$  and SFS solutions at the beginning of the swelling would lead to premature polymerization (and might yield a conversion of 10-30%). Evidence of this phenomenon was already found by Anderson *et al.*<sup>13</sup>, who stated that the iron/EDTA complex and SFS interact to give free radicals. The standard recipes of the MBS graft polymerizations are given in Table 6.2.<sup>3</sup> MBSI is the graft copolymerization with potassium persulfate (KPS) and an emulsifier concentration at the cmc (critical micelle concentration), i.e. 30.4 mg SDS/g PB + cmc water (= 2.26 mmol/L), and MBSII is the graft copolymerization with cumene hydroperoxide (CHP) and without emulsifier.

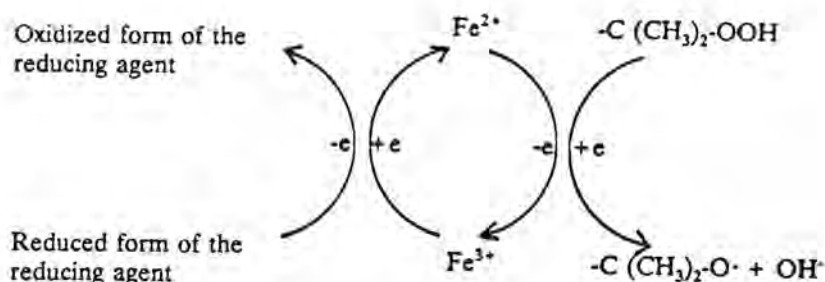


*Figure 71: Schematic illustration of the interactions between the various components of hydroperoxide-iron-reducing agent initiating system<sup>12</sup>.*

#### *Separation of graft and free copolymer by solvent extraction.*

In the graft polymerizations, not all of the monomer added to the polybutadiene seed latex will become grafted onto the PB backbone (PB-SMMA-g), but part of it will polymerize without being chemically bonded onto the PB. This is the so-called free copolymer (SMMA-f). In literature several methods are described to separate the free copolymer from the graft polymer. One of the methods is based on the formation of reversible gels<sup>14,16</sup>. Another method which has been used in the present investigation, will be described here: the solvent extraction method<sup>17</sup>. A good solvent is chosen for the free copolymer, whereafter in principle separation can be achieved by ultracentrifugation.

Solvation of MBS took place in acetone, however, at high fractions styrene in the copolymer methyl-ethyl-ketone (MEK) was used instead of acetone. The procedure is as follows: to 1 gram of accurately weighed MBS polymer 100 ml acetone is added, followed by shaking for 70 hours at room temperature. The soluble polymer was then separated from the insoluble polymer in an ultracentrifuge (Centrikon T- 2060), at 45000 rpm for 45 minutes. After centrifugation the clear solution was poured out in an excess of cold heptane, leading to precipitation of the polymer. The precipitated polymer, SMMA-f, as well as the non-soluble residue were collected and dried in a vacuum oven at  $10^{-2}$ Torr and 323 K for at least 48 hours.

*Determination of the degree of grafting and the graft efficiency.*

The degree of grafting (DG) and the graft efficiency (GE) were calculated from a material balance over the insoluble polymer and the MBS polymer which was added to the acetone solution, according to the following equations:

$$DG = \frac{\text{amount of SMMA-g}}{\text{amount of PB}} = \frac{w_{\text{res}} - w_{\text{PB}}}{w_{\text{PB}}} \quad (7.2)$$

$$GE = \frac{\text{amount of SMMA-g}}{\text{amount of SMMA polymerized}} = \frac{w_{\text{res}} - w_{\text{PB}}}{w_{\text{MBS}} - w_{\text{PB}}} \quad (7.3)$$

where  $w_{\text{res}}$  is the weight of the non-soluble PB-SMMA-g residue resulting from the solvent extraction (g),  $w_{\text{PB}}$  is the polybutadiene weight in the MBS sample (g), calculated from  $w_{\text{PB-a}} * (w_{\text{MBS}} / (w_{\text{mon}} + w_{\text{PB-a}}))$ , where  $w_{\text{PB-a}}$  is the weight of PB added to the reaction (g),  $w_{\text{mon}}$  is the weight of polymerized monomers (g), and  $w_{\text{MBS}}$  is the weight of the MBS sample used for the solvent extraction.

The data for DG and GE of low conversion samples show larger relative errors (Figure 7.2), because at lower conversions the determinations suffer from lower graft levels. Since the method relies upon the ability to extract free copolymer chains from the grafted rubbery polymer domains, the size of the

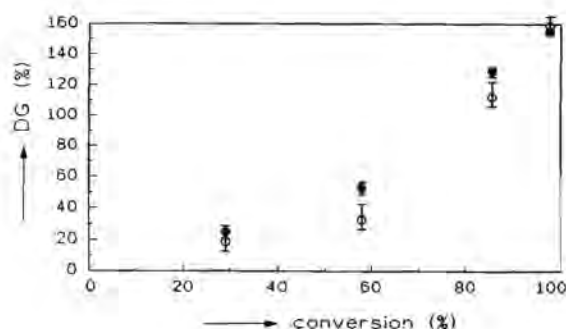


Figure 7.2: Degree of grafting obtained by solvent extraction (open symbols) and by NMR (closed symbols).

rubbery polymer granules influences the extraction. The samples at high conversions tended to be almost powdery in the dry state and could be easily dispersed in the acetone extraction solvent. Samples at low conversions, however, were tough and rubbery, preventing the formation of a good dispersion.

#### *Determination of DG, GE, and F<sub>S</sub> by means of NMR*

After the solvent extraction of MBS, the separated polymers (SMMA-f and PB-SMMA-g) can be analysed by <sup>1</sup>H NMR. The SMMA-f is dissolved in chloroform-d<sub>6</sub> and the PB-SMMA-g is swollen with chloroform-d<sub>6</sub>. The conditions for measuring <sup>1</sup>H NMR spectra are the same as described in par.4.2. The fraction styrene of SMMA-f (F<sub>S</sub>-f) can be determined easily from equation 5.28<sup>8</sup>. For the PB-SMMA-g, a new set of equations had to be derived to determine the DG, GE and F<sub>S</sub>-g (the fraction styrene in SMMA-g copolymer grafted onto PB). In Figure 7.3 a typical <sup>1</sup>H NMR spectrum of a grafted polymer (PB-SMMA-g) is shown. From the different signal areas we can calculate the amount of styrene per proton ("S"), the amount of butadiene per proton ("PB") and the amount of MMA per proton ("MMA") using the following equations:

$${}^{\circ}\text{S}^{\circ} = \frac{A_{\delta 7.5-6.5}}{5} \quad (7.4)$$

$${}^{\circ}\text{PB}^{\circ} = \frac{A_{\delta 5.4} - 1/2A_{\delta 4.9}}{2} + \frac{A_{\delta 4.9}}{2} \quad (7.5)$$

$${}^{\circ}\text{MMA}^{\circ} = \frac{A_{\delta 3.7-0.2} - 3/5A_{\delta 7.5-6.5} - 3/2A_{\delta 4.9} - 2[A_{\delta 5.4} - 1/2A_{\delta 4.9}]}{8} \quad (7.6)$$

Where  $A_{\delta 7.5-6.5}$  is the total signal area of the aromatic protons of styrene,  $A_{\delta 5.4}$  is the signal area of the olefinic protons of the cis and trans units and one methine proton of the olefinic protons of the vinyl sequence,  $A_{\delta 4.9}$  is the signal area of olefine CH<sub>2</sub> of the vinyl-1,2 sequence, and  $A_{\delta 3.7-0.2}$  is the signal area of all aliphatic protons of styrene, MMA and PB.

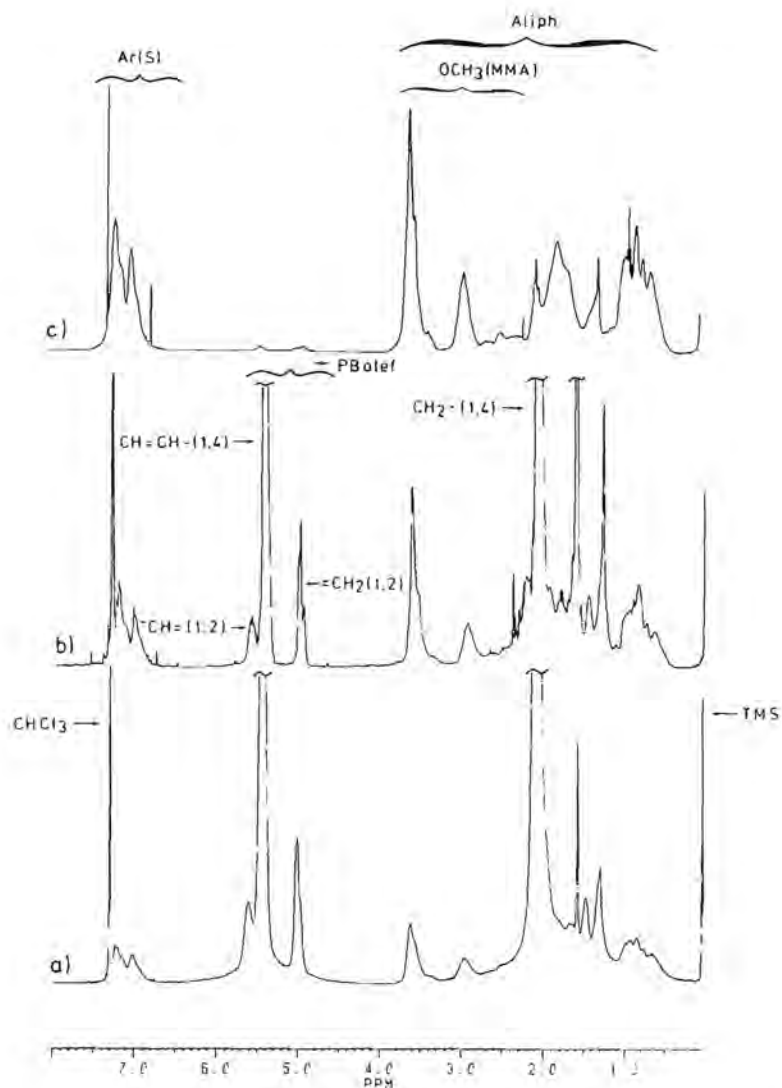


Figure 73: 400 MHz  $^1\text{H}$  NMR spectra in  $\text{CDCl}_3$  at 298 K of a) PB-SMMA-g polymer from MBSII at 78% conversion, b) PB-SMMA-g polymer from MBSII at 95% conversion and c) free SMMA copolymer from MBSII at 95% conversion. The symbol Ar(S) represents the resonance of the aromatic protons of the styrene unit, PBolef. represents the olefinic protons of the PB unit, Aliph. represents all the aliphatic protons of the styrene, MMA and PB units.

With these formulas we can easily calculate the mole fraction of styrene in the SMMA-g copolymer ( $F_{S-g}$ ) by using equations 7.4 and 7.6:

$$F_{S-g} = \frac{S}{S+MMA} \quad (7.7)$$

The (molar) degree of grafting (DG) can be calculated using the following definition:

$$DG = \frac{\text{amount of SMMA-g}}{\text{amount of PB}} = \frac{S+MMA}{PB} \quad (7.8)$$

If the equations 7.4-7.6 are multiplied by the molecular weight of styrene ( $M=104.15$  g/mol), butadiene ( $M=54.09$  g/mol) and MMA ( $M=100.12$  g/mol) respectively, the degree of grafting and grafting efficiency by weight are obtained.

$$GE = \frac{\text{amount of SMMA-g}}{\text{amount of SMMA polymerized}} = \frac{DG(wt) * w_{PB-a}}{w_{mon}} \quad (7.9)$$

where DG is measured by NMR,  $w_{PB-a}$  is the added amount of PB and  $w_{mon}$  is total monomer polymerized in the graft polymerization. The DG and GE by weight can be compared with the solvent extraction data. This is shown for one experiment (MBSII without nDM) in Figure 7.2. It appears that the agreement between the two independent methods is satisfactory. The NMR results are believed to provide the more reliable values.

#### *Breaking the polymer backbone by ozonolysis*

In order to determine the molecular weight and the chemical composition distribution of the copolymers grafted onto PB, these grafted chains have to be isolated. This can be done by breaking the polymer backbone through oxidation of the residual double bonds of the PB. A number of methods have been developed to achieve this purpose; Kranz *et al.*<sup>19</sup> made an overview and compared several methods based on the use of  $OsO_4$  and  $KMnO_4$ . Barnard<sup>20</sup>



showed that the use of ozone gives good results when applied to isolate grafted copolymers. Ozone reacts with the double bound of PB to form an ozonide. This ozonide then can be reduced or oxidized. In this study the polybutadiene backbone has been broken by the ozone method.

Ozone was generated by passing oxygen gas through an ozone generator (OREC) at room temperature. Each graft phase sample of 0.5-3.5 g was dispersed and homogenized in 250 ml of methylene chloride. Before the ozone was purged through the solution, 5 ml of butyl sulfide (Aldrich) was added and the solution mixture was cooled with dry ice and acetone to a temperature of approximately 196K. This temperature was maintained during the whole

Table 71: Comparison of the average molecular weight (measured by SEC) of a PB-SMMA-g sample after one and two exposures to ozone.

ozonolysis passes	analysis #	Ultra Violet			Refractive Index		
		Mn (kg/mol)	Mw (kg/mol)	Mw/Mn (-)	Mn (kg/mol)	Mw (kg/mol)	Mw/Mn (-)
single	1	33.8	180	5.32	36.6	159	4.33
	2	33.4	138	4.12	34.7	137	3.96
double	1	29.4	158	5.37	31.7	185	5.82
	2	28.0	109	3.9	29.9	87.6	2.93

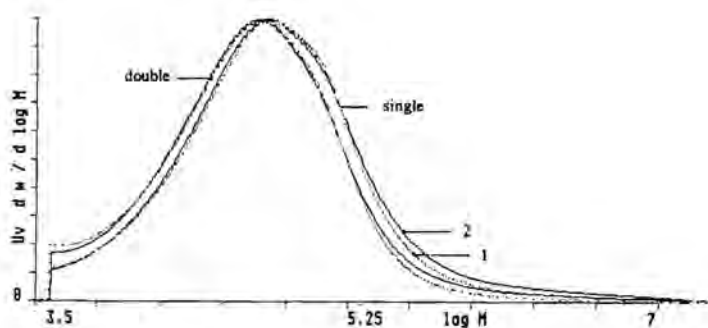


Figure 74: MMDs of one PB-SMMA-g, samples, a) and b): single ozonolysis (duplo), c) and d): double ozonolysis (duplo).

ozonolysis. A flow of approximately 2% of 2.5 l/min ozone was passed through the solution for 40 minutes. After about 30 minutes, the solution mixture turned blue, indicating that no more ozone could be absorbed by the sample and the butyl sulfide.

The ozonides were then reduced by adding a solution of 0.5 g of sodium borohydride ( $\text{NaBH}_4$ , Aldrich) dissolved in 100 ml methylene chloride and 100 ml methanol.<sup>21,22</sup> The mixture was stirred for at least one hour at room temperature. The borohydride reaction was quenched by adding 100 g of a 15% aqueous HCl solution. The solvent is substantially removed in a rotavaporator until the polymer precipitates. Then the remaining solution was decanted and the polymer was redissolved in methylene chloride, rotavaporated until dryness and loosened from the sides of the flask by adding 150 g methanol. The liquid and polymer were poured into a fritted filter and washed twice with additional methanol. Finally, the copolymers were dried in an air-circulating oven at 50 mbar and 323 K for at least 24 hours. The SMMA copolymer is somewhat attacked by ozone, as is shown in Table 7.1 and Figure 7.4 where the number and weight average molecular weights ( $M_n$  and  $M_w$ , respectively) of one sample after single and double exposure to ozone were measured twice. Figure 7.4 shows that after two exposures to ozone the molecular weight distributions (MMDs) of the SMMA-g copolymer are somewhat shifted to lower molecular weights, which is also reflected in the average values of  $M_n$  and  $M_w$  (Table 7.1).

#### *Determination of the chemical composition distribution*

High Performance Liquid Chromatography (HPLC) equipped with UV detection or with a "moving wire FID" has been found to be a useful method of determining the chemical composition distribution of styrene-acrylate copolymers<sup>7</sup>. UV detection causes problems at low fractions of styrene in the copolymer. By contrast, the "moving wire FID" (a carbon sensitive detector) can detect even acrylate homopolymers.

Solvent gradients were created with a system controller (Model 720) and two HPLC pumps (Model 510, Millipore-Waters Corp., Milford, MA, USA). A Waters Intelligent Sample Processor (Wisp, Model 710) was used to inject 10 to 200  $\mu\text{l}$  of the samples (0.2 wt% copolymer solution in THF). The

measurements of SMMA and SMA copolymers were performed on a silica column at ambient temperature.

In the case of SMMA copolymers an elution gradient according to equation 7.10 was applied as shown in Table 7.2.

$$\%A = \%A \text{ start} + (\%A \text{ end} - \%A \text{ start}) \left( \frac{t-t_0}{t_1-t_0} \right)^{(2)} \quad (7.10)$$

Where A is heptane,  $t$  is the time elapsed after injection,  $t_0$  is the time elapsed from the beginning of the segment,  $t_1$  is the time elapsed from the end of the segment. Under these conditions the separation was probably dominated by the so-called precipitation mechanism<sup>23</sup>, and the retention time then will be independent of molecular weight<sup>24</sup>. Low conversion solution SMMA copolymers were used to calibrate the HPLC measurements.

*Table 7.2: Elution gradient used in the HPLC measurements, determining the CCD of the SMMA copolymers.*

time (min)	flow (ml/min)	%A <sup>a</sup>	%B <sup>b</sup>
initial	1.0	80	20
7	1.0	35	65

<sup>a</sup>A = heptane

<sup>b</sup>B = 90 v% dichloromethane + 10 v% methanol

#### *Determination of the molecular weight.*

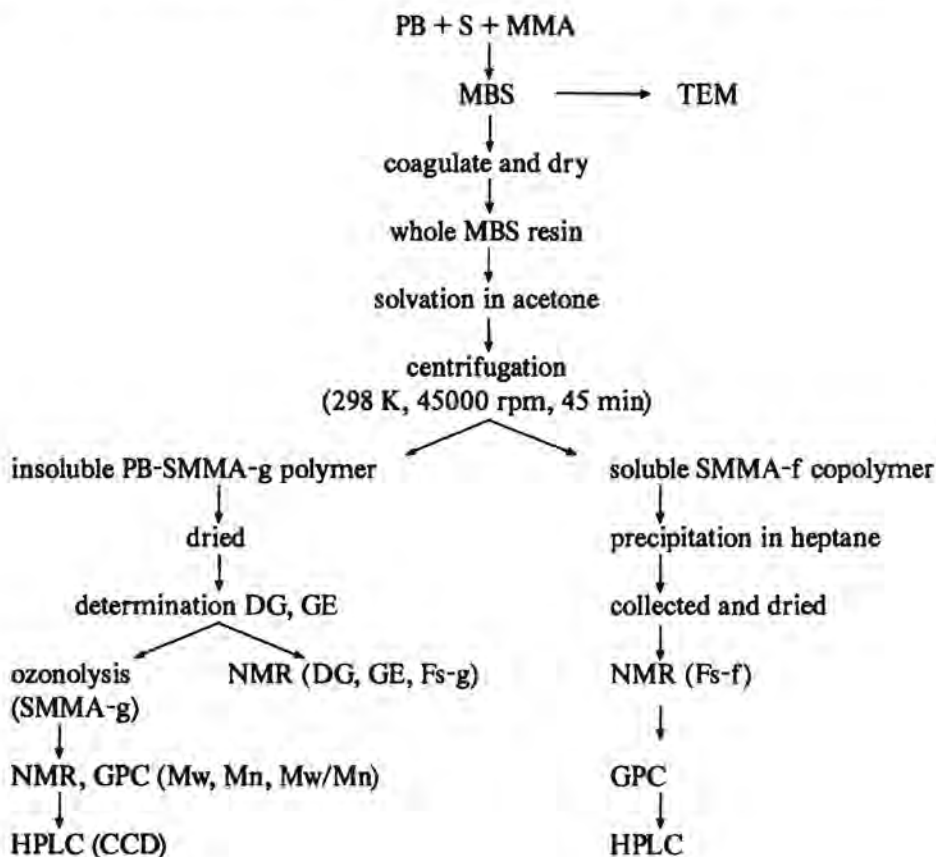
Size Exclusion Chromatography (SEC) of SMMA copolymers (also of the isolated SMMA-g after ozonolysis) was performed on a chromatographic system (Waters Associates) equipped with both a differential refractometer (Waters 410) (313 K) and an ultraviolet (UV) detector (Waters 440) (254 nm, 295 K). A series of two columns (Shodex KF-80 M) thermostated at 313 K was used. The SEC columns were calibrated using 12 polystyrene (PS) samples (Polymer Labs.), with narrow molecular weight distributions. The PS standards could be used here, since it was shown that the individual calibration curves for

PS and PMMA in THF are in extremely close proximity<sup>25</sup>. The THF flow rate was set at 1.0 ml/min. All emulsion copolymers were dissolved in THF and after 24 hours the samples were filtered over a 0.2  $\mu\text{m}$  filter, and 100  $\mu\text{l}$  of this sample (0.05 (%w/v)) was injected.

#### *Determination of the morphology*

The latices were diluted 400 times with distilled water to a concentration of 0.05 (%w/v). To this solution 1 ml of a 2 % aqueous  $\text{OsO}_4$  solution was added, and allowed to stain the PB in the grafted polymer for one hour. The stained latex was placed on a 400 mesh grid and dried. The morphology was examined by transmission electron microscopy (TEM, Jeol 2000 FX).

*The complete experimental procedure is summarized in the next scheme:*



## 7.3 Results and Discussion

### 7.3.1 Grafting of styrene and methyl methacrylate onto polybutadiene.

Commonly in emulsion polymerization a water soluble initiator like potassium persulfate (KPS) is used. In emulsion graft polymerizations, however, oil soluble initiators are more widely used because these tend to give higher grafting efficiencies. Nevertheless, it is found in literature that oil-soluble initiators of different water solubility do not show much variety in their grafting efficiencies<sup>11</sup>. In this research batch processes of grafting styrene and MMA onto polybutadiene were studied using both types of initiators, *i.e.* (KPS) or cumenehydroperoxide (CHP), over a range of emulsifier concentrations and conversions.

#### *Emulsifier concentration and type of initiator*

The seeded batch graft polymerizations were performed in the so-called stage III of emulsion polymerization. This means that there is no separate monomer phase present. The swelling behaviour of styrene and methyl methacrylate in polybutadiene is described in Chapter 6 of this thesis. At a comonomer feed composition of 25 % styrene, there will be no separate monomer phase at a monomer to polymer molar ratio of 77/23. The polybutadiene seed latex was prepared by means of the emulsifier free polymerization process, so the latex particles will be stabilized by sulfate groups (from the initiator) chemically bonded to the surface<sup>9</sup>.

In Table 6.2<sup>3</sup> the standard polymerization recipes are given for both types of initiators. Before the seeded reactions were performed, the apparent critical micelle concentration (cmc) in the presence of the PB seed latex was measured by means of conductometric titration. Note, however, that the possible decrease of the cmc caused by addition of monomer to the system was not taken into account<sup>26</sup>. From these titration experiments for recipe MBSI, an amount of 30.4 mg SDS/g PB is found taking into account that the cmc in water in the presence of KPS and NCB is 2.26 mmol/L. The same experiments were done for recipe MBSII in the presence of the initiator system CHP/FeSO<sub>4</sub>/SFS. With

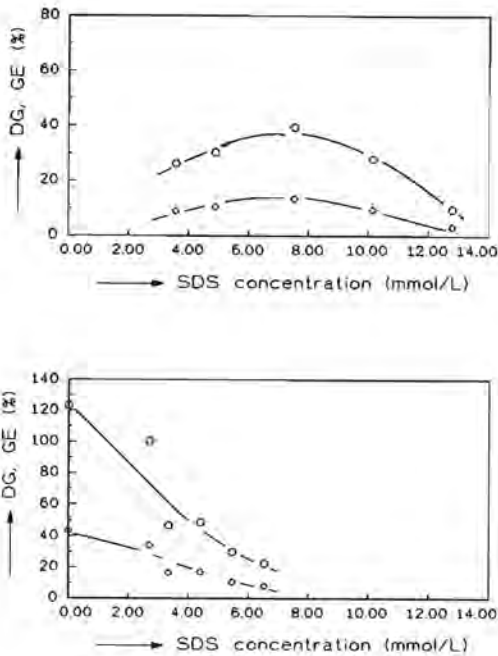


**Figure 7.5:** Degree of grafting (DG, open circles) and grafting efficiency (GE, open diamonds), as a function of the emulsifier concentration; (top) KPS as initiator (MBSI) and (bottom) CHP/FeSO<sub>4</sub>/SFS as initiator (MBSII).

a cmc of 3.78 mmol/L in the water phase an amount of 31.5 mg/g PB was determined.

In Figure 7.5 the DG and GE at 100% conversion (measured by NMR) are displayed as function of the emulsifier concentration for the polymerizations with KPS (MBSI) and CHP (MBSII), respectively.

At the left hand side of Figure 7.5(top) below the cmc(= 7.5 mmol/L) a decrease of DG and GE is shown. As a result of the decrease of emulsifier concentration coagulation occurs, probably due to a lack of electrostatic repulsion. If coagulation takes place at decreasing emulsifier concentrations, the total surface area will decrease and along with that the degree of grafting will also decrease. Furthermore, it should be noted that there are no data available for an emulsifier free polymerization with KPS as initiator. The grafting of styrene and MMA onto PB seeds, emulsifier free with KPS as

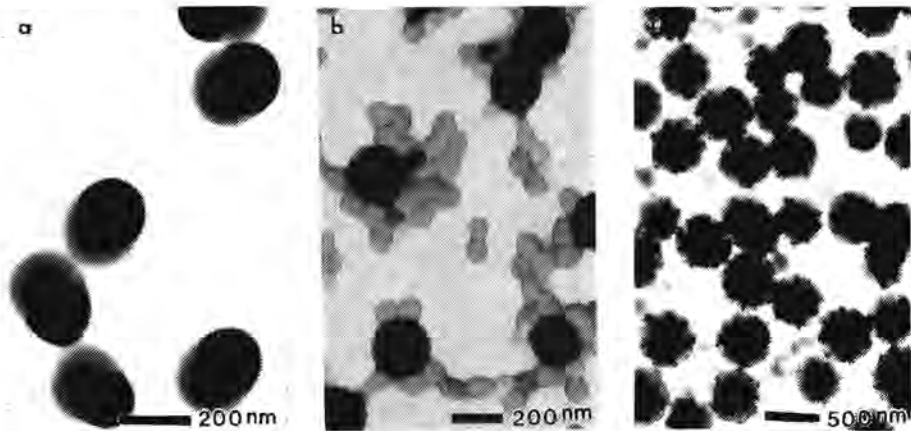


*Figure 7.6: Transmission electron micrographs of MBS graft polymer (100% conversion), prepared with different initiators and emulsifier concentrations: a) MBSI (KPS) at the cmc, b) MBSII (CHP) at the cmc, and c) MBSII (CHP) without emulsifier.*

initiator, gives latices with a very high viscosity, resulting in a relatively creamy stable dispersion of small aggregates rendering the grafting behaviour incomparable with that in the other experiments. In the right hand site of Figure 7.5(top) it can also be seen that above the cmc ( $= 7.5 \text{ mmol/L}$ ) the DG decreases, due to the occurrence of secondary nucleation. Above the cmc more free micelles exist in the water phase: these can be initiated to form a new crop of particles, so there will be less monomer left for grafting. Figure 7.6a shows the morphology of MBSI at cmc, where the maximum DG was reached.

In Figure 7.5(bottom) the DG and GE are shown as function of the emulsifier concentration for grafting taking place with the CHP/FeSO<sub>4</sub>/SFS redox system. In these polymerizations a different behaviour is observed: at the cmc the DG is very low due to the occurrence of secondary nucleation (Figure 7.6b). Therefore, no experiments were performed above the cmc. Below the cmc the degree of grafting is strongly increased and neither coagulation nor secondary nucleation of any importance takes place (Figure 7.6c). In the latter case the latex remains stable. This can be understood when realizing that the

PB latex particles are stabilized by chemically bonded sulfate groups. The sulfate groups can migrate to the surface during the seeded polymerization step provided that the diffusion of the chains with a sulfate end group is fast enough, which implies that these chains are not cross-linked. Taking into account the particle morphology (occlusions and a very thin shell) it can be assumed that during grafting batch reaction the chemically bonded sulfate groups do not become shielded, thus maintaining latex stability.

The strong increase of DG and GE when lowering the emulsifier concentration can be explained by the enhanced presence of initiator at the surface. Some components of the redox initiator system are in the aqueous phase and others in the oil phase, therefore it is to be expected that the initiator will be most active at the surface.

#### *Emulsifier free grafting with CHP as initiator*

The further discussion in this chapter concerns the emulsifier free batch graft polymerization with CHP/FeSO<sub>4</sub>/SFS as the redox initiator system. It has been shown in par.7.2.2 that the average copolymer composition can be determined simultaneously with the degree of grafting and the grafting efficiency, directly from the proton NMR spectrum of PB-SMMA-g. For the determination of the CCD, Mn and Mw of SMMA-g, breaking of the PB polymer backbone is necessary.

#### *Degree of grafting and grafting efficiency*

In Figure 7.7a the DG and GE are shown as function of the conversion. There are several striking points in this figure.

(1) According to literature, in the very beginning (< 10% conversion) of the polymerization the GE is assumed to be high (almost 100%) as a result of the highly probable penetration of free radicals into the polybutadiene seed particles<sup>27-30</sup>. (2) As the polymerization proceeds the GE will decrease and then remain constant<sup>27</sup> (between 10 and 85% conversion). (3) Then, at high conversions (> 85%), a sudden increase in the DG and GE takes place, which is not observed in other studies of grafting styrene onto PB<sup>27-30</sup>. The sudden increase in the grafting efficiency can be explained by the decrease in the



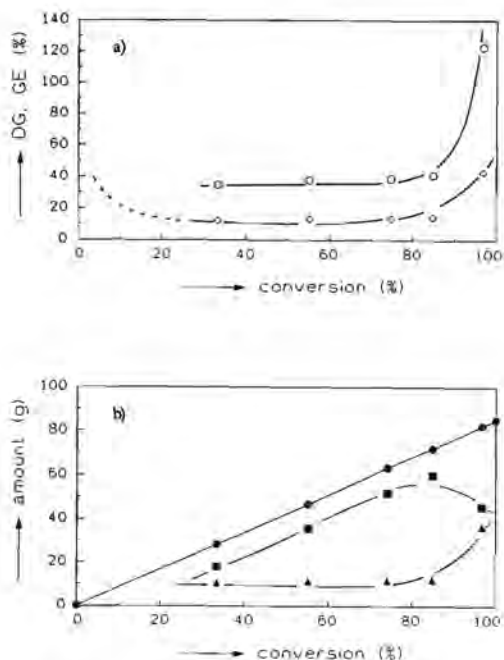


Figure 77: a) Degree of grafting (DG, open circles), grafting efficiency (GE, open diamonds), as a function of the conversion with  $\text{CHP}/\text{FeSO}_4/\text{SFS}$  as initiator and emulsifier free; b) Amount of SMMA-g (closed triangles) and SMMA-f (closed squares) with conversion. The closed circles are the total amount of S and MMA polymerized.

monomer concentration at higher conversion. There, at low monomer concentration, the probability of chain transfer to PB will increase, so more graft sites ( $N$ ) will be initiated (Table 7.3), leading to an increased GE. Transfer reactions are certainly dependent on the type of monomer, *i.e.* on the chemical structure and the mobility of the monomer, as shown in the literature<sup>27-30</sup> discussing the different patterns of behaviour of the DG as function of the conversion.

Figure 7.7b shows a decrease in the absolute amount of free copolymer with conversion instead of remaining constant as would be expected. Probably cross linking reactions take place between SMMA-f and either PB or PB-SMMA-g. Above 85% conversion styrene is almost depleted. The aqueous phase is acting as a buffer for MMA, so the monomer concentration in the particles is very low. At high weight fraction of polymer in the particles the

Table 73: Characteristics of MBSII as function of the conversion.

X <sup>a</sup> (%)	DG wt%	GE wt%	F <sub>S</sub> -g mol%	Mn-g kg/mol	Mw-g kg/mol	P(g) <sup>b</sup> -	N <sup>c</sup> 10 <sup>4</sup>	F <sub>S</sub> -f mol%	Mn-f kg/mol	Mw-f kg/mol	P(f) <sup>b</sup> -
33.3	34.9	12.2	21	49.8	101	2.03	3.79	32	60.8	181	2.98
55.1	37.9	13.2	24	63.8	115	1.81	3.21	28	69.8	162	2.32
74.7	39.0	13.6	32	61.4	107	1.75	3.44	27	-	-	-
84.9	41.1	14.3	24	-	-	-	-	27	-	-	-
96.8	123.2	43.1	21	50.6	116	2.3	13.1	24	64.9	148	2.28

<sup>a</sup> X = conversion

<sup>b</sup> P(g) and P(f) = the polydispersity = Mw/Mn of SMMA-g and SMMA-f, respectively.

<sup>c</sup> N = mol chains grafted / mol butadiene units

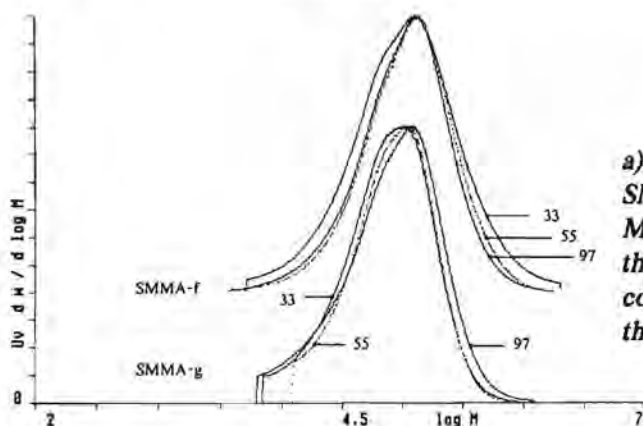


Figure 78: MMDs of a) SMMA-g and b) SMMA-f copolymer of MBSII as a function of the conversion (% conversion is indicated in the figure).

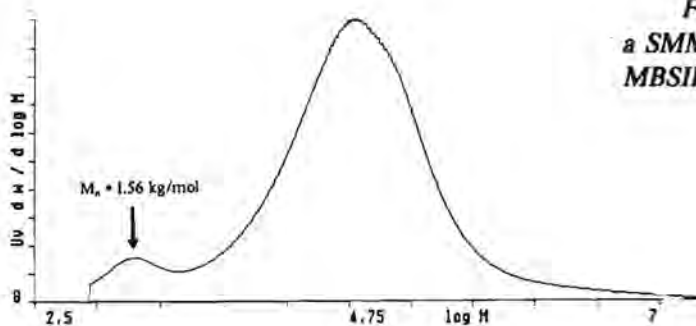


Figure 79: MMD of a SMMA-g copolymer of MBSII at 97% conversion.

intraparticle viscosity increases, which in turn increases the average number of radicals in the particle because termination is diffusion controlled. The SMMA-f chains then may be reinitiated by the increasing of transfer by PB radicals or by SMMA-g radicals, and thus become grafted chains.

#### *The average molecular weights $M_w$ , $M_n$ and molecular weight distributions*

The molecular weights are given in Table 7.3 and the MMDs in Figure 7.8 and 7.9. In Table 7.3 it is seen that SMMA-g copolymer has a lower molecular weight than SMMA-f in spite of the possible cross-linking reactions in the latter case. Differences in molecular weight may not only be caused by the destroyed PB chain parts after ozonolysis, but also by chain transfer processes. The number average chain length,  $M_n$ , will be equal to the rate of chain propagation divided by the total rate of termination plus chain transfer. The propagation rate of the polymer chains is assumed to be almost equal for SMMA-f and SMMA-g. So different mechanisms of transfer and termination leading to SMMA-g or to SMMA-f should explain the different molecular weights. These have been discussed in Chapter 2. From the molecular weight data as function of the conversion listed in Table 7.3, the MMDs in Figure 7.8, and the absolute amount of graft and free copolymer as function of the conversion (Figure 7.7b), it can be concluded that cross-termination between a free polymeric radical and either a PB-SMMA-g or a PB radical, can not be neglected. In Figure 7.8 it is shown that with increasing conversion an increase in the relative amount of chains with a higher molecular weight occurs, resulting in a somewhat bimodal molecular weight distribution.

It should be noted that in all MMDs of SMMA-g (Figure 7.9a) a second peak exists around  $M_n=1500$  g/mol, *i.e.* about 15 monomeric units. The appearance of these small chains is believed to arise from either the attack of ozone or from chain transfer or cross-termination of a growing polymeric chain coming from the aqueous phase to PB or with a PB radical.

#### *The average copolymer composition, CCD, and sequence distributions*

Another ambiguity is arising from Table 7.3. There is a small difference in copolymer composition (measured by NMR) between SMMA-g and SMMA-f

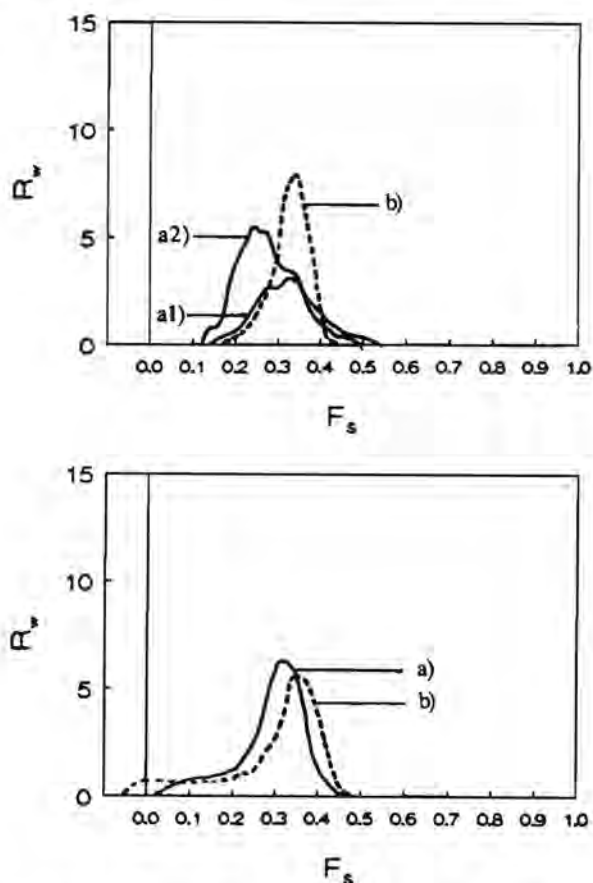


Figure 7.10 (top): CCDs of MBSII determined by means of HPLC of a) SMMA-g at two different conversion (a1) 33% and a2) 97% conversion) and b) SMMA-f at 97% conversion.

Figure 7.11 (bottom): CCDs determined by means of HPLC of a) SMMA with  $M/W = 0.2$  and b) SMMA with  $M/W = 0.05$ .

which cannot easily be explained. This difference in  $F_s$  between the SMMA-g and SMMA-f copolymer is confirmed by an independent HPLC experiment. In Figure 7.10 two CCDs of SMMA-g as function of the conversion and the CCD of SMMA-f (MBSII, at 97% conversion) are displayed. The average fraction of styrene at 97% conversion in SMMA-g is 19% and in SMMA-f 29%. This is comparable with the NMR results of 18% and 28%, respectively (Table 7.4). The distribution of the chemical composition of SMMA-g is broader and has more composition drift towards MMA-rich copolymers than

the CCD of SMMA-f, which is clearly shown in Figure 7.10. The CCD is broad but the copolymers formed over this wide range of composition would not phase-separate or demix. Nevertheless some haze may occur due to the wide range of refractive indices as a result of these broad CCDs. In principle, MBS copolymers can be transparent because the refractive indices of styrene ( $n^D=1.595$ ) and MMA ( $n^D=1.492$ ) may, depend on copolymer composition, match that of butadiene ( $n^D=1.5155$ ).

It should be noted that the broadening of the CCD may have been slightly increased by the selective adsorption of the hydroxy endgroups of the SMMA-g chains onto the silica column. These hydroxy groups are in the ozonolysis procedure when the ozonides are reduced. This is not assumed to be a significant effect at molecular weights higher than 20 kg/mol, which is supported by the fact that the  $F_s$  determined by NMR perfectly agrees with that measured by HPLC.

The CCDs of SMMA-g and SMMA-f can be compared with the CCD of a conventional SMMA copolymer prepared in batch emulsion. In Figure 7.11 the CCDs of two SMMA copolymers (25/75) are shown prepared at monomer to water ratios of 0.2 and 0.05, respectively, (see also SMMA-i Table 6.2<sup>3</sup>). The CCDs of SMMA-g and SMMA-f in Figure 7.10 clearly show differences with those in Figure 7.11. The differences in composition drift between SMMA-g and SMMA-f cannot be explained unambiguously. From Chapter 6 it becomes

*Table 7: Experimental values of the cumulative average chemical composition and triad sequences (measured by carbon NMR) of SMMA-g and SMMA-f high conversion batch graft polymerization prepared at  $(M/W)_0 = 0.11$  (g/g) and  $(S/MMA)_0 = 0.33$  (mol/mol) ratios (MBSII).*

	X	$F_s$	MMM	MMS	SMS	SSS	SSM	MSM
SMMA-g	33.3	21	0.45	0.40	0.15	0.05	0.34	0.61
	96.8	18	0.5	0.38	0.12	0.03	0.32	0.65
SMMA-f	33.3	32	0.35	0.48	0.17	0.08	0.36	0.56
	96.8	28	0.41	0.45	0.14	0.07	0.33	0.60

obvious that the main factor determining the partitioning of the two monomers is the configurational entropy of mixing. So monomer partitioning behaviour cannot provide an explanation for the above discrepancy. It is expected that chain transfer or cross-termination processes involving growing polymeric chains coming from the aqueous phase and PB play an important role.

The sequence distributions of the MMA-centered and styrene-centered triads of SMMA-g and SMMA-f measured by carbon-13 NMR (discussed in Chapter 4 and 5) fail to provide additional information. The sequence distributions of SMMA-g and SMMA-f at two different conversions are listed in Table 7.4. The differences between these copolymers are small, and the peak assignment of the C1 and the  $\alpha$ -CH<sub>3</sub> carbons are too complex to obtain significant results in this case. Therefore, in par.7.3.2 the sequence distributions of the grafted styrene methyl acrylate (SMA-g) and the SMA-f copolymers, which are easier to obtain, will be compared, where similar differences between F<sub>S</sub>-g and F<sub>S</sub>-f are observed.

### 7.3.2 Grafting of styrene and methyl acrylate onto polybutadiene

In an attempt to obtain more insight into the behaviour of grafted systems, the composition drift was also studied in the batch emulsion graft copolymerization of styrene and methyl acrylate onto polybutadiene seed particles. The composition drift occurring during the copolymerization of styrene and methyl acrylate in batch emulsion processes is very large. This is caused by a large difference between the reactivity ratios, namely  $r_{ma} = 0.19 \pm 0.05$  and  $r_s = 0.73 \pm 0.05$ , and by the large difference in water solubility between the monomers, i.e.  $[S]_{max} = 3 \text{ mmol/l}$  and  $[MA]_{max} = 600 \text{ mmol/l}$  at 323 K. Larger effects in composition drift will enhance the compositional and microstructural phenomena already observed in the graft copolymerization of styrene and MMA. The methyl acrylate-butadiene-styrene graft polymers (MABS) were polymerized according to the recipe of MBSII (Table 6.2)<sup>3</sup>, where MMA is replaced by MA and the monomer ratio is kept at 25 mol% styrene

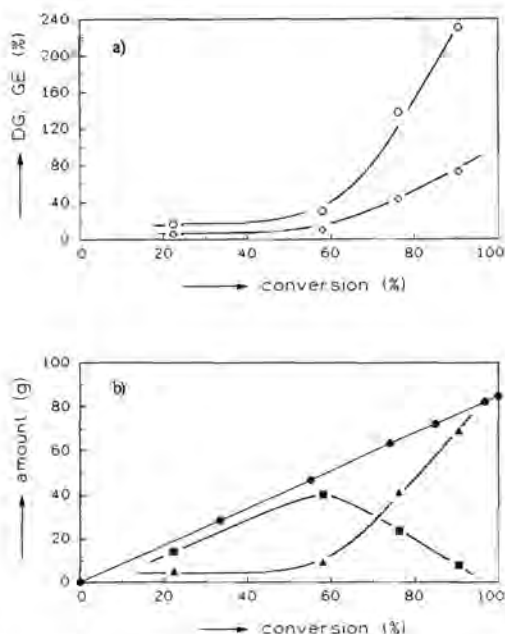


Figure 7.12: a) Degree of grafting (DG, open circles), grafting efficiency (GE, open diamonds), as a function of the conversion with  $\text{CHP}/\text{FeSO}_4/\text{SFS}$  as initiator and emulsifier free, b) variation of the amount of SMA-g (closed triangles) and SMA-f (closed squares) with conversion. The closed circles are the total amount of S and MA polymerized.

and 75 mol% MA.

In Figure 7.12a the DG and the GE are displayed. When compared with Figure 7.7a, in the present case the DG and GE do not remain constant over the entire conversion range till 85% conversion, but already increase from 60% conversion on. Figure 7.12b shows that simultaneously the absolute amount of SMA-f copolymer is decreasing dramatically. It has been shown before<sup>31</sup> that at a monomer/water ratio of 0.11, styrene is almost depleted at 60% conversion, leaving a substantial amount of MA in the water and polymer phases. This means that from this point on the monomer concentration in the latex particles is decreasing, and the freely formed SMA copolymers become chemically bonded by grafting. From Table 7.5 it is obvious that with increasing conversion the fraction styrene in SMA-g is decreasing more rapidly than the fraction styrene in SMA-f. Normally, in the batch emulsion copolymerizations of

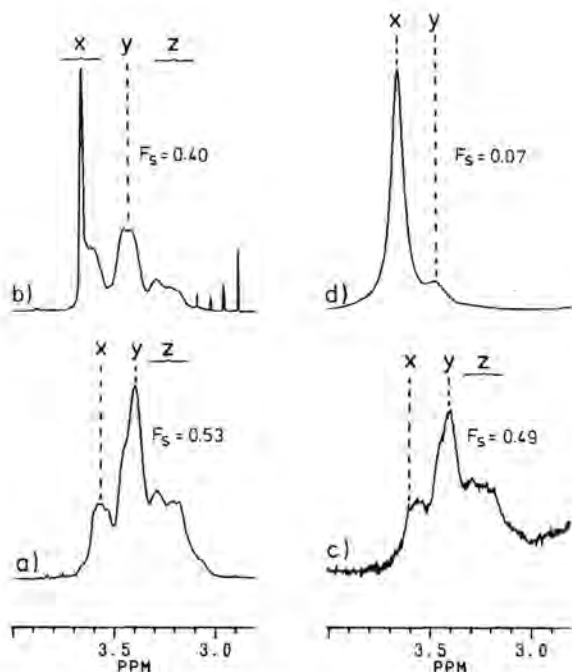


Figure 7.13: Expanded 400 MHz proton NMR spectra of the methoxy region of a) SMA-f 22.3 % conversion, b) SMA-f 94.9% conversion, c) SMA-g 22.3 % conversion and d) SMA-g 94.9% conversion.

styrene and MA, the average fraction of styrene will change from 50 to 25 mol% styrene at a molar feed ratio S/MA of 25/75.<sup>31</sup> See also the expanded NMR spectra in Figure 7.13 where only the methoxy region is shown of SMA-g and SMA-f at two different conversions. The assignment of the methoxy protons as function of compositional and configurational sequences is given in literature<sup>31</sup>. Peak X is mainly determined by the MMM sequence. Clearly, it is shown, that there is stronger composition drift towards MA rich copolymers in the SMA-g (strong increase of peak X) as compared with the SMA-f copolymer. It should be noted that the SMA-g copolymers obtained (after ozonolysis) at conversions higher than 58%, could no longer be dissolved in chloroform but gave a swollen gel. This behaviour indicates that the SMA copolymers become part of a cross-linked network. Therefore, HPLC could only be applied to the samples up to 58% conversion.

The CCDs shown in Figure 7.14 are in agreement with the composition



Table 7.5: Experimental values of the cumulative average chemical composition and triad sequences in (%) (MA-centered by proton NMR and S-centered by carbon NMR) of SMA high conversion batch graft polymerizations all prepared at  $(M/W)_0 = 0.11$  (g/g) and at  $(S/MA)_0 = 0.33$  (mol/mol) ratios. The coisotacticity parameter  $\sigma=0.9$ .

	X	F <sub>s</sub>	MMM	MMS	SMS	SSS	SSM	MSM
SMA-g	22.3	48.5	8.1	40.9	51.0	-	-	-
	57.9	40.1	30.5	48.8	20.7	-	-	-
	76.2	20.9	55.3	37.6	7.1	1.8	20.6	77.6
	94.9	7.0	84.4	15.6	0.0	0.0	12.9	87.1
SMA-f	22.3	53.4	12.3	46.0	41.7	-	-	-
	57.9	47.1	20.6	48.0	31.4	-	-	-
	76.2	43.0	19.5	49.6	30.9	3.8	22.1	74.1
	94.9	40.2	20.1	48.5	31.4	-	-	-

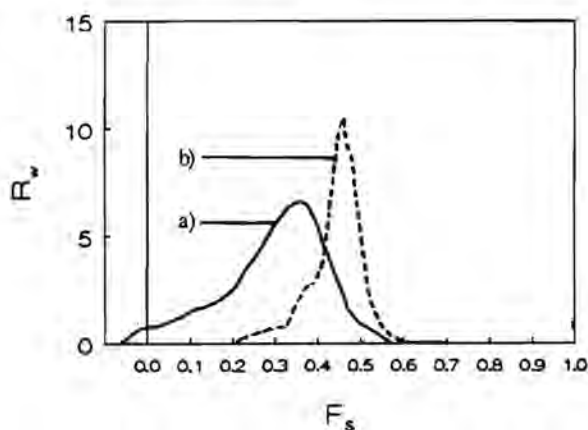


Figure 7.14: CCDs of MABS (with S/MA=25/75 %mol/mol) determined by means of HPLC of a) SMMA-g (58% conversion) and b) SMMA-f (95% conversion).

drift over the 58% conversion range of the average copolymer composition as listed in Table 7.5. It is obvious from Figure 7.14 that the CCD of SMA-f (95% conversion) and the CCD of SMA-g till 58% conversion are both unimodal, in contrast to the conventional batch emulsion process of SMA<sup>31</sup>. However, the CCD of SMA-g is very broad. It can be concluded that it is likely that at high

conversion bimodality will occur in SMA-g, especially because styrene is practically depleted at ca. 60 % conversion. This composition drift towards homopolymer MA directly shows up from the styrene-centered sequences and also the MA-centered sequences presented in Table 7.5.

Two main differences between MMA and MA exist. Firstly, the chemical structure is different which can lead to different transfer mechanisms. It is known that grafting can take place onto a polybutyl acrylate seed, the so-called ASA type of graft polymers<sup>32</sup>. The chemical structure of butyl acrylate is similar to that of methyl acrylate (except for the alkoxy group) leading to the assumption that grafting can take place due to the abstraction of a proton from the polymer backbone in both systems. Secondly, the respective homopolymers have different glass transition temperatures ( $T_g$ ). The polymerization of styrene and methyl acrylate at 323 K probably takes place above the  $T_g$  of all copolymer fractions formed, which can lead to higher grafting efficiencies<sup>33</sup>.

#### 7.4 Conclusions

Grafting of styrene and MMA onto polybutadiene seed particles, stabilized by sulfate end groups, gives stable composite particles. By using emulsifier free grafting processes high degrees of grafting were achieved, while neither coagulation nor formation of a new crop of particles occurred.

The intramolecular microstructure of SMMA-g copolymer shifts stronger to higher MMA contents than that of SMMA-f. The chemical composition distribution of SMMA-g is broad but not bimodal. Moreover, the lower fractions of styrene in the grafted copolymer are believed to be caused by the dominant grafting on the PB backbone of polymeric free radicals originating from the aqueous phase or by particle pre-cursor coagulation. This mechanism will of course depend on the monomer type and its water solubility in combination with the monomer to polymer ratio and reaction temperature, and gains importance as styrene becomes depleted.

The initiator type, on the other hand, has no influence on the copolymer microstructure, but affects the latex stability and through its intrinsic radical activity, the degree of grafting.

## References

1. Kollinsky F, Markert G, *Makromol. Chemie*, 121, 117, 1969.
2. Doremaele v. G.H.J., Herk v. A.M., German A.L., *Polymer*, 29, 2087, 1988.
3. This thesis; Chapter 6.
4. Maxwell I.A., Kurja J, Doremaele v. G.H.J., German A.L., *Makromol. Chem.*, 193, 2065, 1992.
5. Aerdts A.M., Haan de J.W., German A.L., Velden v.d. G.P.M., *Macromolecules*, 24, 1473, 1991.
6. Aerdts A.M., de Haan J.W., German A.L., *Macromolecules*, in press.
7. Doremaele v. G.H.J., Kurja J, Claessens H.A., German A.L., *J. Chromatogr.*, 31 (9/10), 493, 1991.
8. Weerts P.A., Ph.D. thesis, "Emulsion Polymerization of Butadiene, a Kinetic Study", Eindhoven University of Technology, 1990.
9. Verdurmen E.M., Albers J.G., Dohmen E.H., Zirkzee H., Maxwell I.A., German A.L., in preparation.
10. Vanderhoff J.W., Van der Hul H.J., Tausk R.J.M., Overbeek J.T.H.G., "The Preparation of Monodisperse Latices with Well Characterized Surfaces", in "Clean Surfaces Their Application and Characterization for Interfacial Studies", G. Goldfinger Ed., Marcel Dekker, Inc. New York (1990).
11. Daniels E.S., Dimonie V.L., El Aasser M.S., Vanderhoff, J.W., *J. Polym. Sci. Polym. Chem. Ed.*, 41, 2463, 1990.
12. Blackley D.C., "Emulsion Polymerization", Applied Science Publisher, LTD, London, 1975
13. Andersen H.M., Proctor (Jr) S.I., *J. Polym. Sci. Part A*, 3, 2343, 1965.
14. Llauro-Daricades M.F, Banderet A., Riess G., *Makromol. Chem.*, 174, 105, 1973.
15. Llauro-Daricades M.F, Banderet A., Riess G., *Makromol. Chem.*, 174, 117, 1973
16. Locatelli J.L., Riess G., *Eur. Polym. J.*, 10, 545, 1974.
17. Moore L.D., Moyer W.W., Frazer W.J., *Appl. Polym. Symp.*, 7, 67, 1968.
18. This thesis; Chapter 5.

19. Kranz D., Dinges K., Wendling P, *Angew. Makromol., Chem.*, 51, 25, 1976.
20. Barnard D., *J. Polym. Sci.*, 22, 213, 1956.
21. Kuczkowski R.L., *Chem. Soc. Rev.*, 21, 79, 1992.
22. Sousa J.A., Bluhm A.I., *J. Org. Chem.*, 25, 108, 1960.
23. Glöckner G., "Gradient HPLC of Copolymers and Chromatographic Cross Fractionation", Springer, Berlin, 1991.
24. Sparidans R.W., Claessens H.A., Doremaele v. G.H.J., Herk v. A.M., *J. Chromatogr.*, 508, 319, 1990.
25. Davis T.P., O'Driscoll K.F, Piton M.C., Winnik M.A., *J. Polym. Sci. Polym. Lett. Ed.*, 27, 181, 1989.
26. Janssen R.Q.F, Herk v. A.M., German A.L., XXIst Fatipecc Congress Book, 1992, Amsterdam, Vol 1, p. 74.
27. Brydon A., Burnett G.M. Cameron G.G., *J. Polym. Sci. Polym. Chem. Ed.*, 11, 3255, 1973.
28. Brydon A., Burnett G.M., Cameron G.G., *J. Polym. Sci. Polym. Chem. Ed.*, 12, 1011, 1974.
29. Sundberg D.C., Arndt J., Tang M-Y, *J. Dispers. Sci. Techn.*, 5, 433, 1984
30. Chern C.S., Poehlein G.W., *J. Polym. Sci. Polym. Chem Ed.*, 25, 617, 1987.
31. Doremaele v. G.H.J., Ph.D. thesis, "Model Prediction, Experimental Determination, and Control of Emulsion Copolymer Microstructure", Eindhoven University of Technology, 1990.
32. Schildknecht C.E., Sheist I., "Polymerization Processes", High Polymers, John Wiley, New York, 29, 228, 1977.
33. Dimonie V., El Aasser M.S., Klein A., Vanderhoff, J., *J. Polym. Sci. Polym. Chem. Ed.*, 22, 2197, 1984.

## Chapter 8

### Grafting of Styrene and Methyl Methacrylate onto Polybutadiene in Semi-Continuous Emulsion Processes and Determination of Copolymer Microstructure

**ABSTRACT:** Styrene and methyl methacrylate were copolymerized at 323 K in the presence of a polybutadiene seed latex in emulsifier free semi-continuous and for comparison batch processes using cumene hydroperoxide as initiator. Graft polymer characteristics were studied including the intra- and intermolecular microstructure. In contrast to expectation the free and graft copolymers resulting from the semi-continuous processes under starved conditions appeared to have even broader distributions than the copolymers formed in the batch processes.

#### 8.1 Introduction

Two-step emulsion polymers can be produced by various types of polymerization processes: *e.g.* batch, semi-continuous (semi-batch), or continuous processes. These different types of polymerization processes can have a large effect on polymerization kinetics, microstructure, and thus on polymer properties.

Although many studies are concerned with the qualitative<sup>1-3</sup> and some with the quantitative<sup>4-7</sup> interpretation of the grafting of two monomers onto a rubbery polymer, there is a lack of information on composition drift occurring during the grafting of two monomers on a rubbery polymer seed in emulsion. The combined interpretation of many graft polymer characteristics, as discussed in Chapter 7, is also a neglected aspect in this line of research.<sup>8</sup>

The semi-continuous emulsion copolymerization process is widely used in industry, due to a number of advantages as compared with the conventional emulsion batch processes. These advantages include a convenient control of emulsion polymerization rate in relation with heat removal, and control of particle morphology and chemical composition of the copolymer. In particular for the high performance polymer latices it can be important to produce copolymers which are homogeneous in chemical composition. High-impact graft polymers are mostly produced by the semi-continuous process, because higher degrees of grafting can be achieved and one might expect smaller distribution according to chemical composition and core-shell morphology<sup>9</sup>.

Several monomer addition strategies can be employed, of which the addition of a given monomer mixture at constant rate is most widely used. Two basically different situations can be distinguished with respect to the monomer addition rate. (1) Flooded conditions: the addition rate is higher than the polymerization rate. (2) Starved conditions: the monomers are added at a rate lower than the maximum attainable polymerization rate. In order to obtain homogeneous copolymers it is necessary to perform the semi-continuous processes under starved conditions, however, this requires long addition times. The latter problem can be overcome by using the optimal monomer addition strategy<sup>10</sup>.

The present investigation focuses primarily on differences in homogeneity between the two copolymers formed during graft copolymerization, *viz.* graft copolymer and free copolymer. Therefore, the semi-continuous graft copolymerizations were performed using the strategy of monomer addition under starved conditions. Styrene and methyl methacrylate were grafted onto a polybutadiene seed latex (prepared in emulsifier free emulsion polymerization), in batch and semicontinuous processes, while varying some crucial parameters.

## 8.2 Experimental procedures and techniques used in emulsion graft copolymerization

### *Semi-continuous graft copolymerizations of styrene and methyl methacrylate onto polybutadiene*

The dosage of the monomers in the seeded semi-continuous reactions was performed via an automatic burette (Metrohm, type 665 Multi Dosimat, refillable 10 ml burette). Every 15 minutes a sample was taken from the reactor for the GC and solid weight determination performed to measure the conversion. The reactor was filled with the polybutadiene seed, water and part of the initiating system, namely, SFS and  $\text{FeSO}_4$ . After this the reactor was purged with nitrogen in order to remove the oxygen. The reaction mixture was thermostated at 323 K. The monomer mixture containing n-dodecyl mercaptan (nDM) and cumenehydroperoxide (CHP) was added dropwise to the PB seed by means of an automatic burette over 6 hours. The emulsion was stirred with a six-bladed turbine impeller at 300 rpm. The conversion was determined by means of gas chromatography (GC) and dry solid content analysis. The total volume of all samples taken during the entire course of the reaction was always less than 4% of the total volume.

The same total amounts were used as mentioned in recipes of the batch experiment of MBSII in Table 6.2<sup>11</sup>. In Table 8.1 the different MBS polymers discussed in this chapter are given codes indicating the deviations from the standard recipe.

*Table 8.1: Codes for the different MBS polymers used here, indicating the deviations from the standard recipe MBSII in Table 6.2<sup>11</sup>. B=batch and SC=semi-continuous,  $f_s$  = feed fraction styrene.*

---

B1	: MBSII: 1 wt% nDM, $f_s = 0.25$ , T = 323 K
B2	: 0 wt% nDM
B3	: 2 wt% nDM
B4	: $f_s = 0.5$
SC1	: MBSII: 1 wt% nDM, $f_s = 0.25$ , T = 323 K
SC2	: $f_s = 0.5$
SC3	: T = 348 K

---

### 8.3 Results and discussion

Results are shown of batch and semicontinuous graft emulsion copolymerization processes to demonstrate the differences in microstructure, DG, GE, and Mn of the SMMA-g and SMMA-f copolymers (abbreviations see Table 6.1<sup>4</sup>) in both processes. As already shown in Chapter 7, the CCD of a SMMA-g copolymer in batch is very broad. One of the key questions leading to the investigation described in this chapter was whether it would be possible with semi-continuous polymerizations to obtain narrower distributions.

#### 8.3.1 Batch emulsion graft copolymerization

Additional batch experiments were performed, in which some process parameters including the mercaptan concentration (nDM) and the monomer feed ratio were varied.

##### *Effect of the mercaptan concentration*

Three experiments were performed with different mercaptan concentrations: 0, 1, 2 wt% per wt monomer. Figure 8.1a shows the effects of the four different mercaptan concentrations on the degree of grafting and Figure 8.1b shows the effects on the grafting efficiency, as a function of the conversion. From Figures 8.1a and b it can be seen that once mercaptan is added the amount of mercaptan does not further influence the course of DG and the GE. The latter remains constant over a wide conversion range and steeply increase at a conversion of ca. 90%. In contrast with the latter experiments, experiment B2 where no mercaptan is used shows that DG and the GE are increasing continuously with conversion. These results are in agreement with experiments published before by other groups<sup>6,7</sup>. The degree of grafting is reduced by using a chain transfer agent (CTA), because the radical activity of a grafted chain or polymer backbone is then most likely to transfer to the CTA. Few of the new chains formed by this CTA radical will graft again. Table 8.2 shows in the case of no mercaptan (MBS B2), the degree of grafting, grafting efficiency, copolymer composition and molecular weight



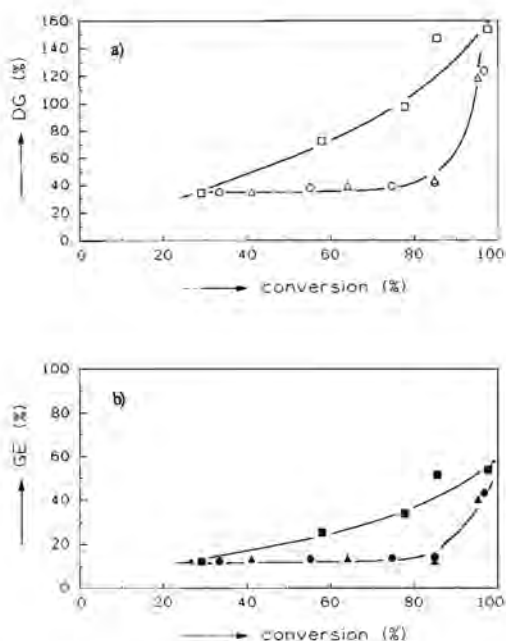


Figure 8.1: a) DG (open symbols) and b) GE (closed symbols) as function of conversion of MBS B1 (1 wt% nDM, circles), B2 (0 wt% nDM, squares), B3 (2 wt% nDM, triangles).

of grafted and of free copolymer, as well as the number of graft sites. The data of experiment B1 (1wt% nDM) were listed in Table 7.3. From a comparison of Table 8.2 and Table 7.3 it becomes clear that from the beginning of the reaction on more graft sites are initiated in the absence of mercaptan. However, the DG and GE are approximately the same in the beginning of the polymerization (< 50% conversion). At the end of the reaction the number of graft sites ( $N$ ) of MBS B1 (1wt% nDM) is still less than that of MBS B2 (0wt% nDM). In experiment B2, there is no transfer to CTA, so more transfer to PB and monomers will take place and as a result more cross-linking will occur at an earlier stage of the reaction than with mercaptan containing recipes.

There are some striking differences in molecular weight of SMMA-g and SMMA-f between the two experiments labelled B1 (1wt% nDM) and B2 (0wt% nDM) (Table 7.3 and 8.2, respectively). The molecular weight of the SMMA-g copolymer and more clearly that of the SMMA-f copolymer is affected by the

Table 8.2: Characteristics of MBS experiment B2 (without nDM) as function of the conversion.

$X^a$ (%)	DG wt%	GE wt%	$F_s$ -g mol%	Mn-g kg/mol	Mw-g kg/mol	$P(g)^b$ -	$N^c$ $10^{-4}$	$F_s$ -f mol%	Mn-f kg/mol	Mw-f kg/mol	$P(f)^b$ -
29.0	34.2	11.9	26	28.4	47.8	1.68	6.50	32	60.2	226	3.75
57.9	72.2	25.2	25	46.7	82.3	1.76	8.33	-	-	-	-
77.8	97.2	33.9	22	54.9	120	2.19	9.55	29	128	675	5.28
85.5	146.8	51.3	25	-	-	-	-	28	-	-	-
97.7	153.3	53.6	23	45.6	126	2.76	18.1	26	137	584	4.26

Table 8.3: Characteristics of MBS experiment B4 ( $f_s=0.5$ ) as function of the conversion.

$X^a$ (%)	DG wt%	GE wt%	$F_s$ -g mol%	Mn-g kg/mol	Mw-g kg/mol	$P(g)^b$ -	$N^c$ $10^{-4}$	$F_s$ -f mol%	Mn-f kg/mol	Mw-f kg/mol	$P(f)^b$ -
95.7	54.8	19.8	43	39.1	84.5	2.16	7.61	52	62.2	143.7	2.31

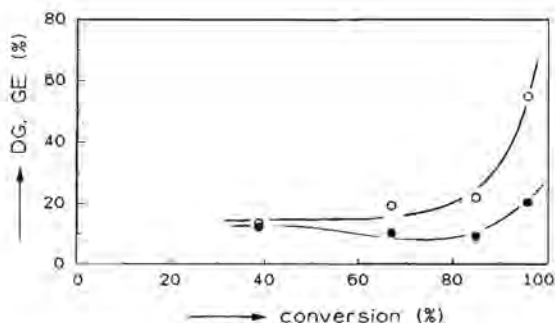


Figure 8.3: DG (open symbols) and the GE (closed symbols) as function of the conversion of MBS B4 ( $f_s=0.5$ )

Table 8.4: Characteristics of MBS SC1 (standard) as function of the conversion.

X <sup>a</sup> (%)	DG wt%	GE wt%	F <sub>S</sub> -g mol%	Mn-g kg/mol	Mw-g kg/mol	P(g) <sup>b</sup> -	N <sup>c</sup> 10 <sup>-4</sup>	F <sub>S</sub> -f mol%	Mn-f kg/mol	Mw-f kg/mol	P(f) <sup>b</sup> -
22.9	32.1	47.6	22	-	-	-	-	25	21.9	75.3	3.44
40.6	-	-	-	18.5	39.9	2.16	-	25	16.2	71.2	4.41
45.3	70.7	50.4	20.	19.5	48.5	2.49	20.7	24	30.0	83.8	2.80
49.9	123.6	79.0	22	-	-	-	-	23	25.3	92.1	3.64
60.0	-	-	-	20.0	50.0	2.47	-	-	20.7	113	5.43
80.2	180.1	67.1	22	19.9	57.5	2.88	48.9	21	-	-	-

Table 8.5: Characteristics of MBS SC2 ( $f_s=0.5$ ) as function of the conversion.

X <sup>a</sup> (%)	DG wt%	GE wt%	F <sub>S</sub> -g mol%	Mn-g kg/mol	Mw-g kg/mol	P(g) <sup>b</sup> -	N <sup>c</sup> 10 <sup>-4</sup>	F <sub>S</sub> -f mol%	Mn-f kg/mol	Mw-f kg/mol	P(f) <sup>b</sup> -
47	111.5	81.2	38	46.2	122	2.64	13.1	-	46.7	164	3.51
61	169.2	92.8	35	44.2	117	2.65	20.7	42	-	-	-
77	194.8	82.9	42	46.9	123	2.63	22.3	45	-	-	-
90	278.3	97.2	46	33.7	167	4.96	44.5	44	51.3	196	3.82

Table 8.6: Characteristics of MBS SC3 ( $T=348$  K) as function of the conversion.

X <sup>a</sup> (%)	DG wt%	GE wt%	F <sub>S</sub> -g mol%	Mn-g kg/mol	Mw-g kg/mol	P(g) <sup>b</sup> -	N <sup>c</sup> 10 <sup>-4</sup>	F <sub>S</sub> -f mol%	Mn-f kg/mol	Mw-f kg/mol	P(f) <sup>b</sup> -
45	-	-	-	20.6	53.3	2.60	-	21	-	-	-
58	122.3	70.3	21	20.0	54.8	2.74	33.0	-	12.2	32.4	2.65
77	142.7	70.0	19	19.0	54.0	2.85	40.6	23	-	-	-
96	207.8	68.8	20	19.1	55.2	2.89	59.1	34	19.8	63.4	3.20

<sup>a</sup>X = conversion

<sup>b</sup>P(g) and P(f) = the polydispersity (Mw/Mn) of SMMA-g and SMMA-f, respectively.

<sup>c</sup>N = mol chains grafted / mol butadiene unit

presence of mercaptan. It is expected that the SMMA-f and the SMMA-g copolymers are formed in different domains, which will have consequences for several important parameters such as the local glass transition temperature ( $T_g$ ), the mobility of the chains, and the number of radicals in the particle.

#### *Influences of monomer feed ratio*

On the grounds of the observations in the batch reactions, one would expect more composition drift in SMMA-g as the feed of the monomers contains more styrene. This makes it interesting to change the monomer feed ratio.

Experiment B1 is performed with a monomer molar feed ratio of 25% styrene and 75% of MMA. In bulk copolymerizations of S/MMA the azeotrope lies at a molar ratio of 52.5/47.5. Experiment B4 is performed under azeotropic conditions, therefore the composition drift should be far less. In Figure 8.2 the DG and GE of MBS B4 ( $f_s=0.525$ ) are given, and appear to be comparable with those found in MBS B1 ( $f_s=0.25$ ). Other characteristics of MBS B4 are given in Table 8.3. It cannot be concluded that there is azeotropic behaviour in these seeded emulsion polymerizations, because the SMMA-g and SMMA-f show different behaviour in copolymer composition. However, the conclusions drawn in Chapter 6, that the monomer feed ratios inside the particles are always equal to those in the monomer droplets lead to the conclusion that rather than different monomer ratios, locally different kinetic mechanisms, reactivities or conditions must be operative.

### **8.3.2 Semi-continuous emulsion graft copolymerizations under starved conditions**

#### *Stability of the semi-continuous process*

The semi-continuous processes were performed by adding a monomer/initiator mixture of constant composition, while maintaining starved conditions. The transmission electron micrograph of experiment SC1 (standard) in Figure 8.6c shows a uniform core-shell morphology. However,

there are some stabilization problems when the conversion reaches 68%. Addition of 0.5 mmol/l emulsifier SDS could avoid the formation of coagulum. The cause of this coagulum formation can be twofold: firstly, the surface area is growing so rapidly that too few sulfate groups are present to stabilize the particle. Secondly, the sulfate groups which stabilize the PB particles may become shielded because the migration of these groups to the surface of the latter particle is hindered by diffusion (far below  $T_g$ , say around 350 K). The  $T_g$  of a polymer is somewhat lowered by the presence of monomer. The experiment carried out at 348 K (SC2) supports the above second hypothesis, because under the same conditions as in experiment SC1 ( $T=323$  K), except for the higher temperature, no coagulum is formed. This means that with the same growth of surface area (Figure 8.6d) and the same amount of sulfate groups, this amount of sulfate groups is enough to stabilize the particle, so the second

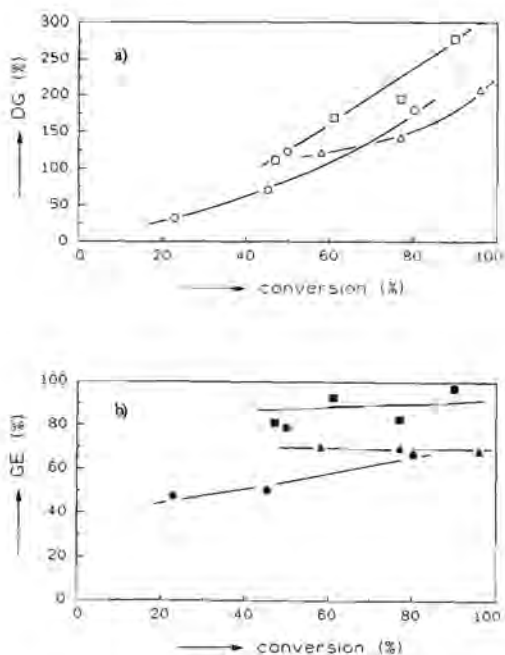


Figure 8.3: a) DG (open symbols) and b) GE (closed symbols) as function of the conversion of MBS SC1 (standard, circles), SC2 ( $T=348$  K, squares) and SC2 ( $f_s=0.5$ , triangles).

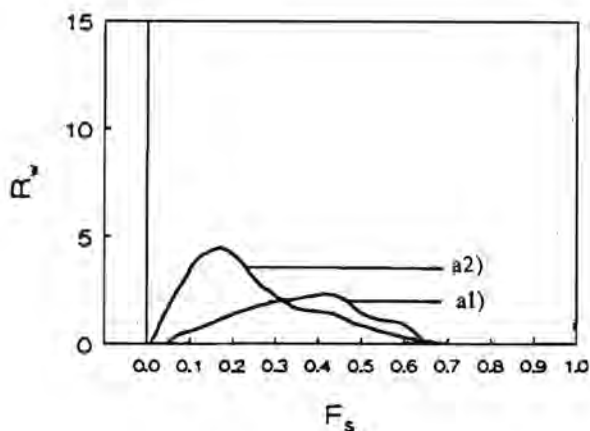


Figure 84: CCDs of SMMA-g copolymer of MBS SC1 (standard) a) 40.6% conversion and b) 80% conversion.

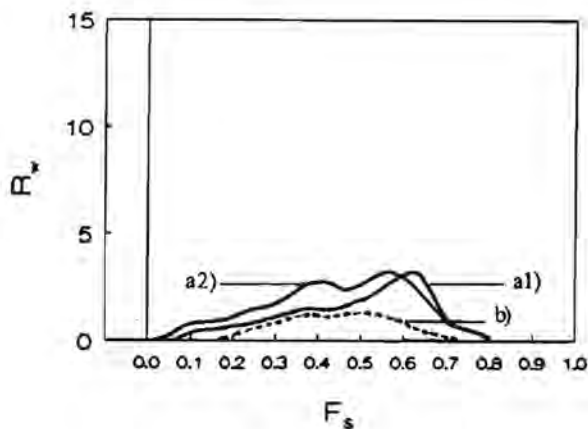


Figure 8.5: CCDs of MBS SC2 ( $f_s=0.5$ ) a1) SMMA-g at 47% conversion, a2) SMMA-g at 90% conversion and b) SMMA-f at 90% conversion.

explanation given above is the most likely one. At 348 K and at a weight fraction of 0.9 of polymer in the particle, the migration of the sulfate groups to the surface area is apparently fast enough. This shows at the same time that most of the sulfate group containing chains are not completely immobilized onto the polybutadiene network.

#### *Influence of temperature and feed composition*

In Figure 8.3 a and b the dependencies of DG and GE on conversion are shown for the semi-continuous experiments SC1, SC2 and SC3. A steady increase of the DG is observed over the entire conversion range. As compared with the batch processes the semi-continuous processes lead to much higher values of DG and GE. This must be caused by the low monomer concentration, maintained over the entire conversion range. The probability of chain transfer of monomeric and polymeric radicals to the PB backbone then will increase, so initiating more graft sites, which in turn leads to higher graft efficiencies. In Table 8.4 the number of graft sites (N) is listed for experiment SC1 (under standard conditions) as a function of the conversion. The final product has about four times more graft chains than the batch products (Table 7.3), however, due to the low monomer concentration in the particle, the average molecular weight is low. As a result, the core-shell structure shown in Figure 8.6c-e should have a morphology of long-term-stability. The average copolymer composition of SMMA-g and SMMA-f listed in Table 8.4 do not show significant differences. In Figure 8.4 two CCDs of SMMA-g (SC1, standard) at two different conversions are shown. The distributions are very broad, and a composition drift is observed towards more MMA rich copolymers in SMMA-g.

In Figure 8.5 the CCDs are shown of MBS SC2 ( $f_s=0.5$ ). The same effects in composition drift are observed as in MBS SC1 ( $f_s=0.25$ ). In Tables 8.5 and 8.6 the characteristics are listed of MBS SC2 ( $f_s=0.5$ ) and SC3 ( $T=348$  K), respectively. When comparing the three experiments in Figure 8.3b it can be seen that the graft efficiency of SC2 ( $f_s=0.5$ ) is the highest ( $\langle GE \rangle = 90\%$ ) but the number of graft sites is lower and the chains have higher average molecular weights.

The higher graft efficiencies at higher temperatures ( $\langle GE \rangle = 70\%$ ) can be explained by the very low actual monomer concentrations in the latex particles. Also the higher temperatures will give an increase in penetration of free radicals from the aqueous phase. This should promote a large number of graft sites at the expense of shorter chains.

The present results, indicating a constant or even an increasing GE (when a shell is already formed), do not completely fit in with the conclusions reported by Merkel et al.<sup>12</sup> for MMA grafting on PB in emulsion. These authors inferred that as soon as a certain shell thickness of the second stage polymer is reached the grafting reaction becomes less probable due to the reduced availability of PB. In Figure 8.6c-e (thick shells) and Table 8.6 (DG and N) it is seen that the thick shell has no influence on the grafting efficiency, which remains constant up to very high conversions.

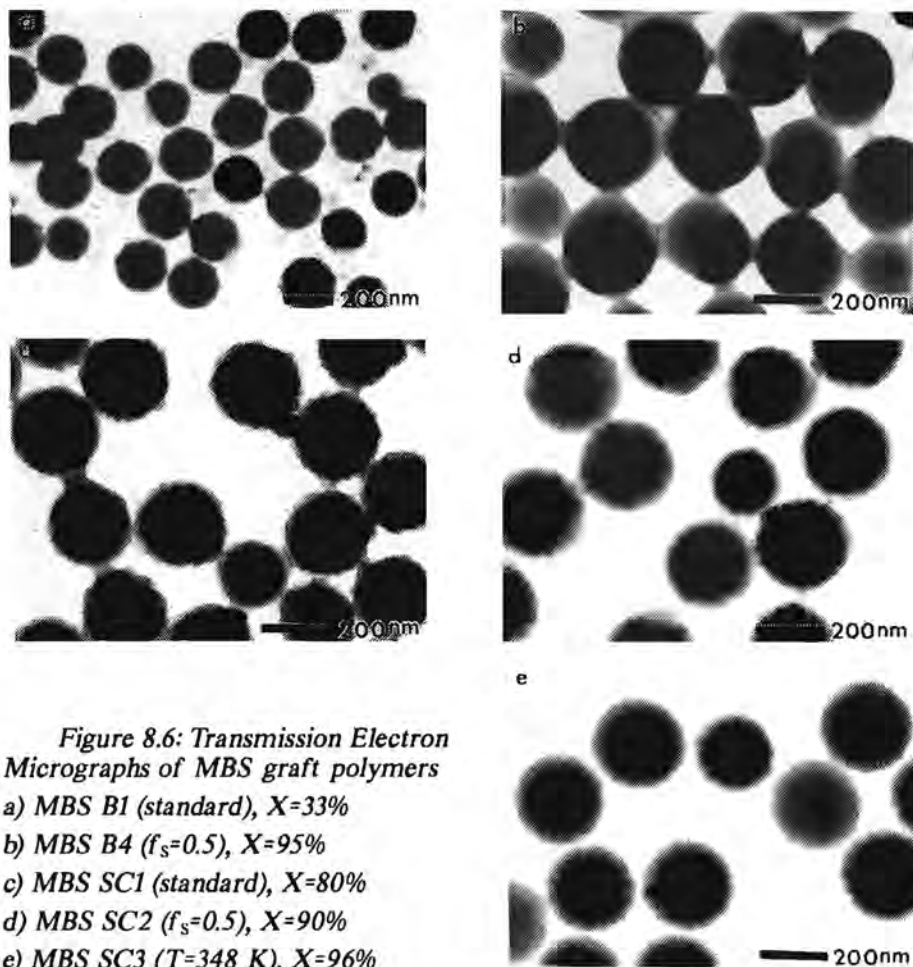
### 8.3.3 Comparison of the morphology of the batch and semi-continuous graft copolymers

It is evident that the semi-continuous operations yield more graft sites but at the same time leads to lower average molecular weights. Also, the mechanism of grafting causes an enhanced composition drift. The radicals entering the particles from the aqueous phase are highly liable to graft. Therefore, the semi-continuous experiments do not lead to the expected homogeneous graft copolymers. Another important difference between the batch and semi-continuous polymers is the particle morphology. Particle morphology is not only important in the interpretation of kinetic results, but also strongly determines the mechanical properties of the products. In Figure 8.6 the transmission electron micrographs are shown of the products of some batch and semicontinuous experiments.

Control of particle morphology in emulsion graft (co)polymerization processes is important for optimizing the properties of a latex system and those of the resulting polymer products in a given application. A large number of factors can affect the morphology of composite latex particles. Some of these



are inherent to the choice of the monomers and others arise from the way in which the synthesis was conducted. The final morphology in polymer microparticles involves the movement of at least two molecular species under the influence of driving forces towards the creation of new interfaces (a change of the free energy), leading to rearrangement through phase separation. This means that the interfacial tensions play an important role, and these can be affected by temperature, type, amount and mode of monomer addition, and depend on the initiator, the emulsifier, and the presence of chain transfer agents. Many of these factors affecting the structure of the multi-stage composite particles are still poorly understood.



The morphology of composite latex particles of acrylonitrile/butadiene/styrene is known to show combinations of different morphologies within the same particle, such as occlusions, core-shell, hemispheres, or raspberry-like structures.

Figure 8.6 shows the various morphologies of the present MBS graft polymers resulting from different processes and process conditions. Figure 7.5c MBS B1(standard) is showing a lot of occlusions and a very thin shell. Shifting the polarity of the systems by changing the feed ratio to more styrene, leads to a large increase in hemispheric structure (see Figure 8.6b).

The products of the semicontinuous process SC1 shown in Figure 8.6c, gives a very distinct core-shell structure. It seems that also occlusions exists. On increasing the fraction of styrene in the monomer feed and at higher reaction temperatures, the semi-continuous MBS morphologies show only small differences. A tendency towards hemispheric structures can be observed (see Figure 8.6d and e, respectively).

Occlusions are expected to arise from free polymer formation under flooded conditions. As a consequence, these occlusions will not be formed at the end of the batch polymerization<sup>9</sup>, but already at the beginning of the reaction, as can be observed very clearly in Figure 8.6a for experiment B1(standard) at 33% of conversion (cf. Figure 7.5c).

#### 8.4 Conclusions

The semi-continuous experiments give much higher graft efficiencies and also larger degrees of grafting than the batch processes when grafting styrene and MMA onto PB. Other important differences are observed in the particle morphology, the number of graft sites, the average molecular weight and the microstructure of the copolymers. The chemical composition distribution of the semi-continuous graft copolymer is even broader than that of the batch graft copolymer. It can be concluded that the desired properties will strongly depend on how the process is performed. In this case comparison of the mechanical properties of the different MBS polymers is extremely difficult due

to the change in more than one polymer characteristic at the same time. Furthermore, the results of this chapter show that the present information, clearly exceeding the information available (*i.e.* DG and GE), provides far more insight into the relevant process (characteristics).

## References

1. Dinges K., Schuster H., *Makromol. Chem.*, 101, 209, 1967.
2. Locatelli J.L., Riess G., *Angew. Makromol. Chem.*, 27, 201, 1972 and 28, 161, 1973.
3. Chauvel B., Daniel J.C., *ACS Polym. Preprints*, 15, 329, 1974.
4. Rosen S.L., *J. Appl. Polym. Sci.*, 17, 1805, 1973.
5. Brydon A., Burnett G.M., Cameron G.G., *J. Polym. Sci. Polym. Chem. Ed.*, 11, 3255, 1973.
6. Brydon A., Burnett G.M., Cameron G.G., *J. Polym. Sci. Polym. Chem. Ed.*, 12, 1011, 1974.
7. Sundberg D.C., Arndt J. Tang M.-Y., *J. Dispers. Sci. Techn.*, 5, 433, 1984.
8. This thesis; Chapter 7.
9. Daniels E.S., Dimonie V.L., El Aasser M.S., Vanderhoff J.W., *J. Polym. Sci. Polym. Chem. Ed.*, 41, 2463, 1990.
10. Doremaele v. G.H.J., Schoonbrood H.A.S., Kurja J., German A.L., *J. Appl. Polym. Sci.*, 45, 957, 1992.
11. Chapter 6: this thesis
12. Merkel M.P., Dimonie V.L., El-Aasser M.S., Vanderhoff J.W., *J. Polym. Sci. Polym. Chem. Ed.*, 25, 1219, 1987.
13. Merkel M.P., Dimonie V.L., El-Aasser M.S., Vanderhoff J.W., *J. Polym. Sci. Polym. Chem. Ed.*, 25, 1755, 1987.

## Epilogue

The primary aim of this study was to obtain insight in the industrially most important, but scientifically highly neglected area of graft copolymerization on rubbery seed particles. The present investigation was started in an attempt to provide answers to a number of basic questions with respect to these systems.

The main initial questions were:

(1) Do graft and free copolymer chains differ in microstructure (e.g. average composition, CCD, length), and can we develop or improve analytical methods to detect those possible differences?

(2) If so, how can these differences between graft and free copolymer be explained?

(3) Can we indicate, at least qualitatively, the main factors controlling the extent of grafting versus free copolymer formation, and can we control the grafts in number, length and composition(al distribution)?

What are the effects on particle morphology?

On the grounds of the results obtained during this investigation, the answers to the above questions can now be given and briefly summarized as follows:

ad(1) A distinct difference was found between grafted and free copolymer in terms of average composition, compositional distribution and chain length.

Among the many analytical methods used, the development of suitable NMR techniques played a crucial role since reliable peak assignments turned out not

to be available in literature. An extensive NMR investigation on SMMA copolymers has led to the indispensable, new and unambiguous peak assignments.

Other extremely helpful techniques like ozonolysis, GPC, HPLC, GLC, TEM, have been made to fit the needs of the present study and have contributed to establish and confirm the differences found between grafted and free copolymer.

ad(2) As the explanation of the different chemical composition distributions, differences in monomer feed ratio between the (PB) network and the copolymer domains inside the latex particles had to be rejected on the grounds of the monomer partitioning study performed. Also it is highly unlikely that in the present system the monomer reactivity ratios would significantly depend on the reaction medium.

Therefore, the present investigation necessarily leads to the conclusion that aqueous phase processes play an important role in graft formation. In other words, the graft copolymer characteristics will be determined by the conditions in the aqueous phase as well as by those in the particle phase.

The latter concept explains *i.a.* why graft copolymer is mainly formed at higher conversions in batch, why it is richer in (M)MA, why it has a broad compositional distribution, and why it is preferentially formed in semi-continuous operation under monomer starved conditions. The importance of the aqueous phase processes is amplified by the higher reactivity of the more water soluble (M)MA (oligomeric) radicals.

As for the free copolymer: the collected evidence indicates that free copolymer formation is mainly determined by the intraparticle conditions, and as such is strongly favoured by the high monomer concentrations occurring in the polymer particles at lower conversions (in batch).

A complicating factor is that initially formed free copolymer may become grafted to the polymer network at higher conversions, especially because the (M)MA units in the free copolymer are quite susceptible to radical attack.

This leads to the observed compositional peak broadening.

ad(3) The present study, comprising batch as well as semicontinuous processes, the microstructural characterization of graft and free copolymer, and the elucidation of particle morphologies, has yielded important handles on controlling graft copolymerization products and thus product properties.

For example:

- The amount of free copolymer formed is strongly increased under monomer flooded conditions, *i.e.* at low conversion during batch processes.

This strategy leads to particle morphologies showing large occlusions.

- On the other hand, graft copolymer formation is favoured at low monomer concentrations, *i.e.* at high conversion during batch processes and under monomer starved conditions in semi-continuous operation.

This mode of operation yield particle morphologies typically showing a copolymer shell and very small occlusions (if any).

- Semi-continuous processes under starved conditions yield (graft and free) copolymer with an even broader(!) chemical composition distribution than batch processes.

- The present insights allow the selection of reaction conditions that can optimize *e.g.* the number and length of the copolymer grafts, and to a limited extent also their compositional distribution.





## Summary

High impact resistant polymers like ABS (acrylonitrile/butadiene/styrene) and MBS (methyl methacrylate/butadiene/styrene) are widely used as commercial products and find many applications in coatings, elastomers, adhesives and impact modifiers. The graft-copolymerizations onto polymer (rubber) seed particles in emulsion is an extremely complicated process, which comprises a heterogeneous reaction system consisting of three distinct phases: aqueous phase, polymer particles, and monomer droplets. In order to obtain better control of the product properties, it is necessary to understand the relations between the process conditions and the microstructure of the graft copolymers.

This thesis provides improved basic insight in some of the main problems involved in microstructural control and characterization of grafted and free SMMA (styrene/methyl methacrylate) copolymers in MBS products.

First of all, the intramolecular microstructure of SMMA copolymers in terms of sequence distributions and tacticity was determined by means of proton and carbon NMR. Because literature assignments of the methoxy protons of the statistical copolymers were inconsistent with experimental results, these proton NMR signals have been reassigned for several MMA-centered sequence resonances. This is described in Chapter 3. Also the carbon NMR signals of MMA-centered and styrene-centered carbon atoms in statistical and alternating copolymers have been reassigned. Chapter 4 first describes the reassignment of the  $\alpha$ -methyl proton and carbon NMR resonances of the alternating copolymer, and subsequently the  $\alpha$ -methyl carbon and also the aromatic C1 resonance of the statistical SMMA copolymers. This new assignment is of crucial importance for the analysis of MMA-centered and S-centered sequences in statistical copolymers.

Another source of confusion in literature is the large number of models proposed for SMMA copolymerization kinetics. Based on the new carbon NMR assignments (Chapter 4) it could now be shown in Chapter 5 that the NMR signal areas obtained for all copolymers of different composition, described in terms of triad sequences, were adequately predicted by the terminal model utilizing reactivity ratios calculated from non-linear last squares fitted to the copolymer compositional data as determined by proton NMR.

In Chapter 5 it is also shown that the non-terminal model behaviour of the kinetics of the rate of polymerization can not only be successfully modelled by the 'restricted' penultimate model, but also by various 'bootstrap' or monomer-polymer complex models.

Beside the analytical and kinetic problems, there is also the important issue of the thermodynamics of the monomer partitioning in the emulsion system of polybutadiene, styrene and MMA. It is shown in Chapter 6 that the behaviour of monomer partitioning in the absence of monomer droplets is independent of polymer type, polymer cross-linking and latex particle diameter. The results of the saturation monomer partitioning experiments showed a good agreement with a simplified thermodynamic theory. The polymer type does not affect the ratio of the two monomers (styrene and MMA) in the polymer particles versus the droplet phase, *i.e.* the configurational entropy of mixing is the determining thermodynamic contribution. This important result, however, does not explain the difference in copolymer microstructure observed between the free and grafted SMMA copolymer, as described in Chapter 7 and 8.

In Chapter 7 and 8 the MBS graft polymerizations are described, carried out in emulsifier free batch and semi-continuous emulsion processes, using an oil-soluble initiator. As a result high degrees of grafting were achieved. The degree of grafting, the grafting efficiency and the average copolymer composition were measured by means of NMR. After ozonolysis of the polybutadiene network carrying the grafted copolymer, the molecular weight distributions (MMD) and the chemical composition distribution (CCD) of the isolated "grafted" SMMA copolymer could be determined. The results show that the chemical composition distribution of the grafted SMMA copolymer is

very broad as compared with the free SMMA copolymer in the batch polymerizations (Chapter 7), and even broader in the semi-continuous polymerizations (Chapter 8). The differences between grafted and free copolymer in terms of CCD, MMD and the average copolymer composition have been shown to arise from the fact that during the grafting process the grafted copolymer and the free copolymer are preferentially formed during different time (conversion) intervals and in different domains of these heterogeneous systems. Furthermore, not only differences in composition drift are observed between batch and semi-continuous processes, but also differences in molecular weight and morphology (Chapter 8).

The results presented in this thesis provide strongly improved insight into the formation of the microstructure of the graft copolymers. As a consequence, the (mechanical) properties of the products can now be more closely related to the process conditions.

## Samenvatting

Slagvaste polymeren zoals ABS (acrylonitril/butadien/styreen) en MBS (methylmethacrylaat/butadien/styreen) vinden hun toepassing in commerciële producten zoals coatings, elastomeren, hechtverbetersaars en slagvastheidsverbetersaars. De entcopolymerisatie op polymere (rubber) deeltjes in emulsie is een uiterst gecompliceerd proces. Dit heterogene reactiesysteem bestaat uit drie afzonderlijke fasen: de waterfase, polymeerdeeltjes en de monomeerfase. Om een betere controle te krijgen over de producteigenschappen, is het noodzakelijk inzicht te krijgen in de invloed van de procescondities op de microstructuur van de entpolymeren.

Dit proefschrift beoogt een verbeterd inzicht te verkrijgen in enkele belangrijke basisproblemen die betrekking hebben op het microstructureel onderzoek aan geënte en vrije SMMA (styreen/methylmethacrylaat) copolymeren in de MBS producten.

Ten eerste werden aspecten van de intramoleculaire microstructuur (sequenties en tacticiteit) van de SMMA copolymeren bepaald met behulp van proton en koolstof NMR. Omdat de in de literatuur vermelde toekenningen van de methoxy protonen van statistische copolymeren in tegenspraak waren met de experimentele resultaten, was het noodzakelijk deze proton NMR-signalen opnieuw toe te kennen voor enkele MMA-gecentreerde sequentie-resonanties. Dit is beschreven in Hoofdstuk 3. Ook de koolstof NMR-signalen van MMA-gecentreerde en styreen-gecentreerde koolstofatomen in statistische en alternerende copolymeren zijn opnieuw toegekend. Hoofdstuk 4 beschrijft eerst de vernieuwde toekenning van de  $\alpha$ -methyl-proton- en koolstof-resonanties van het alternerende copolymeer, en vervolgens de  $\alpha$ -methyl en de aromatische C1 resonanties van de statistische SMMA copolymeren. Deze nieuwe toekenning is van cruciaal belang om de MMA-gecentreerde en de

styreen-gecentreerde sequenties in statistische copolymeren te bepalen.

Een andere bron van verwarring in de literatuur is het grote aantal voorgestelde modellen met betrekking tot de kinetiek van de SMMA copolymerisatie. Gebaseerd op de nieuwe koolstof-NMR toekenning, beschreven in Hoofdstuk 4, blijkt in Hoofdstuk 5 dat de verkregen NMR-piekoppervlakken (in termen van triadesequenties) van de copolymeren met verschillende samenstelling, voorspeld kunnen worden door het 'ultimate' model. Hiervoor zijn de reactiviteitsverhoudingen berekend met de kleinste kwadraten-methode gefit aan de data van de copolymeersamenstellingen gemeten met proton-NMR.

In Hoofdstuk 5 is niet alleen aangetoond dat het 'non-ultimate' model van de polymerisatiesnelheid succesvol gemodelleerd kan worden met het 'restricted penultimate' model, maar ook met enkele 'bootstrap' of monomeer-polymeer complex modellen.

Naast de analytische en kinetische problemen, is er ook het belangrijke aspect van de thermodynamische monomeerverdeling in het emulsie-systeem van polybutadien, styreen en MMA. Hoofdstuk 6 laat zien dat het monomerverdelingsgedrag in afwezigheid van een aparte monomeerfase onafhankelijk is van zowel het type polymeer, de mate van crosslinking van het polymeer, alsook de latexdeeltjesgrootte. De resultaten van de monomeerverdelingsexperimenten onder verzaadiging lieten een goede overeenkomst zien met een vereenvoudigde thermodynamische theorie. Het type polymeer heeft geen invloed op de verhouding van de twee monomeren (styreen en MMA) in de latexdeeltjes en de monomeer fase, dit wil zeggen dat de configurationele mengentropie de bepalende thermodynamische factor is. Dit belangrijke resultaat verklaart echter niet de verschillen in copolymeersamenstelling tussen het geënte en het vrije SMMA copolymeer in Hoofdstuk 7 en 8.

In Hoofdstuk 7 en 8 worden de MBS entpolymerisaties beschreven, uitgevoerd in zeepvrije batch en semi-continue processen en met een olie-oplosbare initiator. Aan de hand van deze processen werden hoge entgraden bereikt. Met behulp van NMR werden de entgraad en de entefficiëntie bepaald alsmede de gemiddelde copolymeersamenstelling. Na ozonolyse van het polybutadieennetwerk, met daaraan de entcopolymeren, konden de

molecuulgewichtsverdelingen (MMD) en de chemische samenstellingsverdelingen (CCD) bepaald worden van de 'geënte' SMMA copolymeren. Uit de resultaten blijkt dat de chemische samenstellingsverdelingen van de geënte copolymeren gepolymeriseerd in batch (Hoofdstuk 7), erg breed zijn vergeleken met de vrije SMMA-copolymeren. De semi-continue processen (Hoofdstuk 8) leveren chemische samenstellingsverdelingen op die nog breder zijn. De verschillen tussen geënte en vrije SMMA copolymeren in termen van CCD, MMD en gemiddelde copolymeersamenstelling worden veroorzaakt doordat gedurende het entproces het entcopolymeer en het vrije copolymeer voornamelijk gevormd worden in verschillende tijds- (conversie-) intervallen en in verschillende domeinen van het heterogene systeem. Bovendien is er niet alleen een verschil in 'composition drift' tussen de batch en semi-continue processen maar zijn er ook verschillen in molecuulgewichten en de morfologie (Hoofdstuk 8).

De resultaten in dit proefschrift geven een beter inzicht in de microstructuur van de entcopolymeren, met als gevolg dat de (mechanische) eigenschappen van de producten nu beter gerelateerd kunnen worden aan de procescondities.

## Dankwoord

Hierbij wil ik iedereen bedanken die heeft bijgedragen op experimenteel en wetenschappelijk gebied aan het onderzoek beschreven in dit proefschrift, en anderen voor de getoonde belangstelling. In het bijzonder wil ik de afstudeerders en stagiaires, alle (ex) collega's en (ex) medewerkers van de Technische Universiteit Eindhoven niet alleen van TPK maar ook van andere vakgroepen, met name TIA en TOC, en de medewerkers van de werkplaats bedanken voor hun hulp en voor de goede sfeer, waardoor ik met veel plezier en enthousiasme heb kunnen werken aan mijn promotieonderzoek. Zeker niet in de laatste plaats wil ik de medewerkers van General Electric Plastics in Villers-Saint-Sépulcre, Bergen op Zoom en Schenectady bedanken voor de goede samenwerking.

## Curriculum Vitae

De schrijfster van dit proefschrift werd geboren op 8 november 1964 te Venlo. Zij behaalde in 1983 het Atheneum-B diploma aan het Collegium Marianum te Venlo.

In datzelfde jaar begon zij haar studie in de Scheikundige Technologie aan de Technische Universiteit Eindhoven. Het propadeuse examen werd in augustus 1985 afgelegd en het doctoraal examen in juni 1988 na een afstudeerproject op het gebied van koolstof-13 vaste stof NMR aan polymere blends onder leiding van prof.dr.ir. C.A.M.G. Cramers en dr.ir. J.W. de Haan in samenwerking met dr. H.H.T.M. Ketels (TPK) en dr. G.P.M. van der Velden (DSM).

In augustus 1988 is zij begonnen met een tweejarige onderzoekersopleiding aan de Technische Universiteit Eindhoven in de vakgroep Polymeerchemie en Kunststofftechnologie onder leiding van prof.dr.ir. A.L. German. Deze opleiding werd afgerond in december 1990. Daarna verrichtte zij in het kader van de samenwerking tussen General Electric Plastics BV en de vakgroep Polymeerchemie en Kunststofftechnologie het in dit proefschrift beschreven onderzoek.



**STELLINGEN**  
**behorende bij het proefschrift**

**MICROSTRUCTURE OF**  
**STYRENE METHYL METHACRYLATE COPOLYMERS**  
**GRAFTED ONTO POLYBUTADIENE SEEDS**

1

Mathey *et al.* concluderen ten onrechte dat "composition drift" veroorzaakt wordt door het verschil in zwelbaarheid van de polybutadienen met styreen en acrylonitril afzonderlijk. Deze conclusie gaat namelijk volledig voorbij aan het feit dat styreen en acrylonitril altijd als comonomieermengsel worden gebruikt en dat gedurende de reactie copolymeer gevormd wordt.

*Mathey P., Guillot J., Polymer, 32(5), 934, 1991*

2

De toepassing van Bernouilli- en 1<sup>ste</sup>-orde-Markov-statistiek bij de sequentie-verdeling van hoge-conversie-SAN- copolymeren in emulsie door Doskocilova *et al.*, wijst op onvoldoende kennis bij de auteurs en referenten op het gebied van de copolymerisatie kinetiek.

*Doskocilova D., Terlemezyan L., Gantchev B., Michailov M., Acta Polymerica, 32(12), 746, 1981*

3

Er moet meer gevit worden op het "fitten" van experimentele data met behulp van mathematische modellen, als een volledig fysisch bewijs nog ontbreekt.

*Hoofdstuk 5 uit dit proefschrift.*

4

Het modelleren van entpolymerisaties in emulsie is uitermate complex door het grote aantal procesparameters en het ontbreken van perfecte "core-shell" structuren, waardoor een eenduidig entingsmodel nog steeds ontbreekt.

5

Het is weinig realistisch om aan te nemen dat chemische verschuivingen in NMR-spectra voor enkele koolstofresonanties van statistische copolymeren alleen worden veroorzaakt door een verschil in tacticiteit, als reeds vijftien jaar geleden onomstotelijk is aangetoond dat de chemische sequenties zeker óók een rol spelen in dezelfde en aanverwante systemen.

*San Roman J., Vazquez B., Valero M., Martín Guzmán G., Macromolecules, 24, 6089, 1991*

*Gerken T.A., Ritchey W.M., J. Appl. Polym. Sci. Appl. Polym. Symp., 34, 17, 1978*

## 6

Hirai *et al.* constateren dat elkaar tegensprekende NMR-toekenningen aan MMA-gecentreerde en S-gecentreerde triadesequenties in statistische styreen(S) - methyl methacrylaat(MMA) copolymeren in de literatuur beschreven worden. Er zijn echter geen pogingen ondernomen om deze toekenningen te herzien voor dit belangrijke systeem. Dit getuigt van de complexiteit van het probleem, maar heeft slechts geleid tot de continuering van het gebruik van foutieve toekenningen.

*Hirai H., Koinuma H., Tansbe T., Takeuchi K., J. Polym. Sci. Polym. Chem. Ed., 17, 1339, 1979*  
 Hoofdstuk 4 uit dit proefschrift

## 7

Bij het schrijven van "reviews" worden referenties veelal passief aangehaald en beschreven, waardoor één van de belangrijkste doelen van "reviews", namelijk een kritische evaluatie van elkaar tegensprekende publikaties, in ernstige mate wordt verwaarloosd.

## 8

In een milieubewuste wereld dienen hogere accijnzen geheven te worden op vuurwerk.

*Onderzoek TNO gepubliceerd in verschillende Dagbladen in Nederland d.d. 23-12-1992*

## 9

De algemene veronderstelling dat trappers tijdens het fietsen niet los gaan door de linkertrapper met linksgesneden schroefdraad en de rechtertrapper met rechtsgesneden schroefdraad uit te voeren, is onjuist.

*Richards H., "fietsreparaties". Ned. ed., Uitgeverij Elmar b.v., Rijswijk, 1983*

## 10

De zwarte neushoorn is tijdelijk door toedoen van de mens zijn naam niet waardig.

*Panda (WWF), oktober 1992*

## 11

"Gezonde Voeding" is niet altijd voor iedereen gezonde voeding.